UNIVERSITY OF CALIFORNIA
RIVERSIDE

Integrated Geochronologic, Geochemical, and Sedimentological Investigation of Proterozoic-Early Paleozoic Strata: From Northern India to Global Perspectives.

A Dissertation submitted in partial satisfaction
of the requirements for the degree of

Doctor of Philosophy

in

Geological Sciences

by

Neil Ryan McKenzie

December 2012

Dissertation Committee:
Dr. Nigel C. Hughes, Chairperson
Dr. Peter M. Sadler
Dr. Timothy W. Lyons

The Dissertation of Neil Ryan McKenzie is approved:

_____

_____

_____
Committee Chairperson

University of California, Riverside

ABSTRACT OF THE DISSERTATION

Integrated Geochronologic, Geochemical, and Sedimentological Investigation of Proterozoic-Early Paleozoic Strata: From Northern India to Global Perspectives

by

Neil Ryan McKenzie

Doctor of Philosophy, Graduate Program in Geological Sciences
University of California, Riverside, December 2012
Dr. Nigel C. Hughes, Chairperson

Research presented here focuses on the tectonic–sedimentary evolution of the north Indian margin and explores the influence of plate tectonics on climate change and metazoan biodiversification during a critical interval of Earth history. The first part of the dissertation focuses on the Himalaya, Vindhyan, and Aravalli sectors of northern India. This project establishes new age constraints for poorly dated Proterozoic sedimentary successions, explores the relationship of these successions across northern India, and tests predeformational models for the Himalayan margin through an integrative study that utilizes aspects of sedimentology, detrital zircon geochronology, sedimentary geochemistry, and paleontology. The second focus of the dissertation uses a global compilation of detrital zircon age data to demonstrate an intrinsic link between spatial and temporal variation in continental arc volcanism – a key source of atmospheric CO_2 – with climate change and metazoan evolution across the Neoproterozoic-Early Paleozoic transition.

TABLE OF CONTENTS

LIST OF FIGURES

LIST OF TABLES

INTRODUCTION

Sedimentary rocks are the archive of earth history and integrative methods are required to interpret their recordings. My research has utilized multidisciplinary approaches to investigate the Proterozoic-early Paleozoic stratigraphic record in order to gain insight into deep-time questions in Earth history. Research presented here has a primary focus on the tectonic-sedimentary evolution of the north Indian margin, both in a regional and global context. This project was based in the north Indian Himalaya and expanded into cratonic regions of the Indian sub-continent, and into a global investigation of tectonism and environmental change during a critical interval of Earth history.

The first chapter of this dissertation focuses on establishing age constraints on Proterozoic strata of the Lesser Himalaya and testing models for the pre-deformational configuration of the north Indian margin. Recently, Ediacaran-Cambrian ages were suggested for the Deoban Group of the Indian Lesser Himalaya based on putative microfossils (Tiwari et al., 2000; Azmi and Paul, 2004; Tiwari and Pant, 2009). These ages are much younger age than previous Mesoproterozoic 'Riphean' age assignments (e.g., Valdyia 1971; Valdyia 1980; Richards et al., 2005). If corroborated, these younger depositional ages raise a number of questions regarding both the pre-deformational configuration of the north Indian margin and our understanding of the uplift and exhumation of the Himalayan orogenic system. A common view in Himalayan geology is that the lithotectonic zones of the system

can be distinguished from each other based on "isotopic signatures", specifically U-Pb age data from detrital zircons and neodymium isotopic compositions of siliciclastic rocks (Parish and Hodges, 1996). Following on this suggestion, these so-called "isotopic signatures" have been used to infer tectonic boundaries along the orogen (Argels et al., 2003; Richards et al., 2005; Celerier et al., 2009) and to time the exhumation of these zones via the introduction of their various "signatures" into the Himalayan foreland basin (e.g., DeCelles, 2004; Najman et al., 2006). In addition these supposed signatures were used to argue the origin of two of the major lithotectonic zones as exotic terranes accreted during an early Paleozoic tectonic event (DeCelles et al., 2000). However, the utility of these signatures for lithotectonic zone distinction and the accreted terrane model was brought into question by comparing Cambrian-aged strata from the three zones, all of which yielded similar isotopic signatures (Myrow et al., 2003). Those authors concluded that the "isotopic signatures" were a function of depositional age and not unique to any particular lithotectonic zone. However, strata of the Deoban Group are part of a succession with isotopic compositions that are distinct from those of Cambrian-aged strata reported by Myrow et al., (2003) (Ahmad et al., 2000; Richards et al., 2005). Therefore if the recently suggested Ediacaran-Cambrian ages hold for this unit, the issue remains unresolved.

Additional Ediacaran carbonate and Cambrian siliciclastic successions exist in the Indian Lesser Himalaya, which are known as the Krol and Tal groups, respectively. The chemo- and lithostratigraphy of the Krol Group has been well

documented and supports an Ediacaran age for these strata (Jiang et al., 2002, 2003; Kaufman et al., 2006). A Cambrian age for the overlying Tal Group is well supported by both micro- and macrofossils (e.g., Bhatt, 1991; Hughes et al., 2005). Given the proximity of the Krol-Tal successions to the Deoban Group within the Lesser Himalayan lithotectonic zone and the lithologic similarity of the two units, an Ediacaran-Cambrian age for the Deoban Group seemed plausible. However, preliminary detrital zircon and carbon isotopic data were inconsistent with the suggested Ediacaran-Cambrian ages and a need to establish firm age constraints on these controversial units was apparent.

Unique phosphatic stromatolites are present in the Gangolihat dolomite that are lithologically identical to deposits reported from the well dated ~1.6 Ga carbonate rocks of the Vindhyan supergroup (Bengtson et al., 2009), which are located ~400 km south of the Himalayan frontal thrust in north-central cratonic India. Given the uniqueness of these deposits, they served as a potential tie-point between these two widely separated successions. Therefore, sedimentological, geochemical and geochronologic investigations were expanded into cratonic regions of India, which include the Ganga, Vindhyan, and Marwar supergroups. Combined results from this project allowed for both the establishment of new age constraints for multiple sedimentary units and correlation between various Proterozoic-early Paleozoic successions across the north Indian margin. Furthermore, the newly established age constraints and correlations allowed me to test the utility of isotopic characterization of Himalayan lithotectonic zones.

The second chapter of my dissertation largely follows on ideas presented in the conclusions of the first chapter and expands on the detrital zircon record of the northern India. Essentially, the research conduced for this chapter aimed to test correlations between the eastern Vindhyan and western Vindhyan strata, and furthermore their potential correlation with strata of the Aravalli-Delhi supergroups of the Aravalli Delhi Orogenic Belt (ADOB) of western India. A long-standing concept in Indian geology is that the modern limits of outcrop patterns and variation in tectonic deformation somehow result from rock units originating in discrete isolated basins, which are often referred to as the "Purana (ancient) Basins" (e.g., Valdiya, 1995). Therefore, all packages of sedimentary rocks that are separated by modern physiographic features or are distinguishable by variation in tectonic deformation are often referred to as 'basins' (e.g., the Vindhyan Basin, the Aravalli Basin, the Himalaya Basins, etc.). One overarching aspect this work is to test sediment-source continuity between these regions and the validity of 'basin' isolation across northern India. Age constraints for strata in the Aravalli-Delhi supergroups are generally lacking. The Aravalli Supergroup is considered to have a depositional age of ~2.1 Ga with the Lomagundi isotope excursion suggested to be preserved in this unit (Sreenivas et al., 2001; Maheshwari et al., 2005; Papineau et al., 2009). Although data to support this mid-Paleoproterozoic age are sparse, these rocks have received much recent attention due to their potential to preserve important geochemical data regarding the early oxygenation of Earth's atmosphere (e.g., Papineau et al., 2009, 2010). The Delhi Supergroup is believed to be ~1.7-1.9

Ga. The only detrital zircon age data generated from the ADOB were from granulite-facies metasediments of the Banded Gneiss Complex-II (Buick et al., 2006) and a single sedimentary unit in the "northern Delhi belt" (Biju-Sekar et al., 2003; Kaur et al., 2011). Results from both of those studies yielded large populations of ~1.7 Ga zircons. Similarly, volcanics in the Hindoli rocks, which are considered part of a 'separate basin' despite their physical proximity to the Aravalli Supergroup, yielded ages of ~1.8 Ga (Deb et al., 2002). These various age data contrast the ~2.1 Ga ages suggested for the Aravalli Supergroup, and thus further investigation is needed.

Based on these age data and reported phosphatic stromatolites of the Jhamarkotra Formation that were allegedly similar to the phosphatic stromatolites of the ~1.6 Ga Vindhyan Supergroup (Banerjee, 1986), I postulated that strata of the Aravalli-Delhi supergroups were correlative to the adjacent Vindhyan successions. To test this hypothesis I collected sandstone samples from major stratigraphic units for detrital zircon analysis, and the phosphatic horizons were investigated. Data generated in this study provide new age constraints for these strata, which contradict the long-standing depositional age assignments and illustrate major problems regarding current correlations between successions within these regions.

The third chapter of the dissertation focuses on the late Neoproterozoic-early Paleozoic transition. This interval witnesses one the most dramatic climatic events in Earth history, namely the Cryogenian "Snowball Earth" events (Kirschvink, 1992; Hoffman et al., 1998). This was closely followed by an Early Paleozoic interval with the highest pCO_2 of the Phanerozoic (e.g., Berner 1990, 2006). The transition

between the Neoproterozoic-early Paleozoic also witnessed the appearance and diversification of animals in the fossil record, with origins dating back to at least the Cryogenian (Love et al., 2009) and major diversification events during the Ediacaran and Cambrian (e.g., Valentine, 2002; Marshall, 2006). Newly derived U-Pb age data from detrital zircons are combined with a compilation of published literature from strata with well-constrained depositional ages that span the Cryogenian 'glacial interval' to end-Devonian. These data are used to qualitatively evaluate the spatiotemporal variation of tectonically active margins, specifically continental arc volcanism. These data are integrated with published geochemical and geochronologic data to better evaluate the relationship between global variation in paleotectonism and major climatic transitions during this interval. In order to better understand these ancient tectonic transitions, they are considered with the more geologically recent Cenozoic Himalayan orogeny and its effects on ocean-atmosphere system as an analogy. Furthermore, I propose a direct link between these tectonic and climatic transitions with trends observed in early animal biodiversification.

References

Ahmad, T., Harris, N., Bickle, M., Chapman, H., Bunbury, J., Prince, C., 2000. Isotopic constraints on the structural relationships between the Lesser Himalayan Series and the High Himalaya Crystalline Series, Garhwal Himalaya. Geological Society of America Bulletin 112, 467-477.

Argles, T., Foster, G., Whittington, A., Harris, N., George, M., 2003. Isotopic studies reveal a complete Himalayan section in the Nanga Parbat syntaxis. Geology 31, 1109-1112.

Azmi, R.J., Paul, S.K., 2004. Discovery of Precambrian-Cambrian boundary protoconodonts from the Gangolihat Dolomite of Inner Kumaun Lesser Himalaya: Implications on age and correlation. Current Science 86, 1653-1659.

Banerjee, D.M., Schidlowski, M., Arneth, J.D., 1986. Genesis of upper Proterozoic-Cambrian phosphorite deposits of India: isotopic inferences from carbonate fluorapatite, carbonate and organic carbon. Precambrian Research 33, 239-253.

Bengtson, S., Belivanova, V., Rasmussen, B., Whitehouse, M., 2009. The controversial "Cambrian" fossils of the Vindhyan are real but more than a billion years older. Proceedings of the National Academy of Sciences 106, 7729-7734.

Berner, R.A., 1990. Atmospheric Carbon-Dioxide Levels over Phanerozoic Time. Science 249, 1382-1386.

Berner, R.A., 2006. GEOCARBSULF: A combined model for Phanerozoic atmospheric O-2 and CO2. Geochimica Et Cosmochimica Acta 70, 5653-5664.

Bhatt, D.K., 1991. The Precambrian-Cambrian transition interval in Himalaya with special reference to small shelly fossils - a review of current status of work. Journal of the Palaeontological Society of India 36, 109-120.

Biju-Sekhar, S., Yokoyama, K., Pandit, M.K., Okudaira, T., Yoshida, M., Santosh, M., 2003. Late Paleoproterozoic magmatism in Delhi Fold Belt, NW India and its implication: evidence from EPMA chemical ages of zircons. Journal of Asian Earth Sciences 22, 189-207.

Buick, I.S., Allen, C., Pandit, M., Rubatto, D., Hermann, J., 2006. The Proterozoic magmatic and metamorphic history of the Banded Gneiss Complex, central Rajasthan, India: LA-ICP-MS U–Pb zircon constraints. Precambrian Research 151, 119-142.

Célérier, J., Harrison, T.M., Webb, A.A., Yin, A., 2009. The Kumaun and Garwhal Lesser Himalaya, India. Part 1: Structure and stratigraphy. Geological Society of America Bulletin 121, 1262-1280.

Deb, M., Thorpe, R., Krstic, D., 2002. Hindoli group of rocks in the eastern fringe of the Aravalli-Delhi orogenic belt-Archean secondary greenstone belt or Proterozoic supracrustals? Gondwana Research 5, 879-883.

DeCelles, P.G., Gehrels, G.E., Najman, Y., Martin, A.J., Carter A., Garzanti, E., 2004. Detrital geochronology and geochemistry of Cretaceous–Early Miocene strata of Nepal: implications for timing and diachroneity of initial Himalayan orogenesis. Earth and Planetary Science Letters 227, 313-330.

DeCelles, P.G., Gehrels, G.E., Quade, J., LaReau, B., Spurlin, M., 2000. Tectonic implications of U-Pb zircon ages of the Himalayan orogenic belt in Nepal. Science 288, 497-499.

Hoffman, P.F., Kaufman, A.J., Halverson, G.P., Schrag, D.P., 1998. A Neoproterozoic snowball earth. Science 281, 1342-1346.

Hughes, N.C., Peng, S.-C., Bhargava, O.N., Ahulwalia, A.D., Walia, S., Myrow, P.M., Parcha, S.K., 2005. The Cambrian biostratigraphy of the Tal Group, Lesser Himalaya, India, and early Tsanglangpuan (late early Cambrian) trilobites from the Nigali Dhar syncline. Geological Magazine 142, 57-80.

Jiang, G., Christie-Blick, N., Kaufman, A.J., Banerjee, D.M., Rai, V., 2002. Sequence stratigraphy of the Neoproterozoic Infra Krol Formation and Krol Group, Lesser Himalaya, India. Journal of Sedimentary Research 72, 524-542.

Jiang, G., Sohl, L.E., Christie-Blick, N., 2003. Neoproterozoic stratigraphic comparison of the Lesser Himalaya (India) and Yangtze Black (South China): paleogeographic implications. Geology 31, 917-920.

Kaufman, A.J., Jiang, G., Christie-Blick, N., Banerjee, D.M., Rai, V., 2006. Stable isotope record of the terminal Neoproterozoic Krol platform in the Lesser Himalayas of northern India. Precambrian Research 147, 156-185.

Kaur, P., Zeh, A., Chaudri, N., Gerdes, A., Okrusch, M., 2011. Archaean to Palaeoproterozoic crustal evolution of the Aravalli mountain range, NW India, and its hinterland: The U–Pb and Hf isotope record of detrital zircon. Precambrian Research 187, 155-164.

Kirschvink, J.L., 1992. Late Proterozoic low-lattitude global glaciation: the snowball Earth, in: Schopf, J.W., Klein, C. (Eds.), The Proterozoic Biosphere: A Multidisciplinary Study. Cambridge University Press, New York, pp. 51-52.

Love, G.D., Grosjean, E., Stalvies, C., Fike, D.A., Grotzinger, J.P., Bradley, A.S., Kelly, A.E., Bhatia, M., Meredith, W., Snape, C.E., Bowring, S.A., Condon, D.J., Summons, R.E., 2009. Fossil steroids record the appearance of Demospongiae during the Cryogenian period. Nature 457, 718-U715.

Maheshwari, A., Sial, A.N., Guhey, R., Ferreira, V.P., 2005. C-isotope Composition of Carbonates from Indravati Basin, India: Implications for Regional Stratigraphic Correlation. Gondwana Research 8, 603-610.

Marshall, C.R., 2006. Explaining the Cambrian "explosion" of animals. Annual Review of Earth and Planetary Sciences 34, 355-384.

Myrow, P.M., Hughes, N.C., Paulsen, T.S., Williams, I.S., Parcha, S.K., Thompson, K.R., Bowring, S.A., Peng, S.-C., Ahluwalia, A.D., 2003. Integrated tectonostratigraphic reconstruction of the Himalaya and implications for its tectonic reconstruction. Earth and Planetary Science Letters 212, 433-441.

Najman, Y., 2006. The detrital record of orogenesis: a review of approaches and techniques used in Himalayan sedimentary basins. Earth-Science Reviews 74, 1-72.

Papineau, D., 2010. Global biogeochemical changes at both ends of the Proterozoic: Insights from phosphorites. Astrobiology 10, 165-181.

Papineau, D., Purohit, R., Goldberg, T., Pi, D., Shields, G.A., Bhu, H., Steele, A., Fogel, M.L., 2009. High primary productivity and nitrogen cycling after the Paleoproterozoic phosphogenic event in the Aravalli Supergroup, India. Precambrian Research 171, 37-56.

Parrish, R.R., Hodges, K.V., 1996. Isotopic constraints on the age and provenance of the Lesser and Greater Himalayan sequences, Nepalese Himalaya. Geological Society of America Bulletin 108, 904-911.

Richards, A., Argles, T., Harris, N., Parrish, R., Ahmad, T., Darbyshire, F., Draganits, E., 2005. Himalayan architecture constrained by isotopic markers from clastic sediments. Earth and Planetary Science Letters 236, 773-796.

Sreenivas, B., Das Sharma, S., Kumar, B., Patil, D.J., Roy, A.B., Srinivasan, R., 2001. Positive d13C excursion in carbonate and organic fractions from the Paleoproterozoic Aravalli Supergroup, Northwestern India. Precambrian Research 106, 277-290.

Tiwari, M., Pant, C.C., Tewari, V.C., 2000. Neoprotoerzoic sponge spicules from the Gangolihat Dolomite , Lesser Himalaya, India. Current Science 79, 651-654.

Tiwari, M., Pant, I., 2009. Microfossils from the Neoproterozoic Gangolihat Formation, Kumaun Lesser Himalaya: Their stratigraphci and evolutionary significance. Journal of Asian Earth Sciences 35, 137-149.

Valdiya, K.S., 1995. Proterozoic sedimentation and pan-African geodynamic development in the Himalaya. Precambrian Research 74, 35-55.

Valentine, J.W., 2002. Prelude to the Cambrian explosion. Annual Review of Earth and Planetary Sciences 30, 285-306.

CHAPTER 1

Correlation of Precambrian–Cambrian sedimentary successions across northern India and the utility of isotopic signatures of Himalayan lithotectonic zones

Abstract

A common view in Himalayan geology is that differences in detrital zircon age distributions and whole-rock neodymium isotopic compositions (εNd) distinguish lithotectonic zones within the system. Such differences are used to map these zones and to locate their modern boundaries, as well as to infer ancient terrane boundaries. I test the utility of this approach using integrated geochemical, geochronological, and sedimentological data from the Himalayan successions of northern India and relatively undeformed, age-equivalent successions of the Indian craton. U-Pb geochronology of detrital zircons from cratonic successions of the Vindhyan, Ganga, and Marwar supergroups and the "inner" and "outer" Lesser Himalaya lithotectonic zones show that rocks of similar depositional age bear strikingly similar detrital zircon age distributions throughout the entire region. A sharp change in εNd occurs within the "inner" Lesser Himalaya and correlates with a regional unconformity recognized on the craton, here constrained to span a period of ~500 million years. Results demonstrate that isotopic differences among the

lithotectonic zones relate primarily to differences in the depositional ages of their constituent rocks, and that all parts of the Himalaya were in sediment-source continuity with the Indian craton from the late Paleoproterozoic to the early Cambrian. Isotopic "signatures" may vary as much within individual Himalayan lithotectonic zones as between such zones and no lithotectonic zone can be characterized by such data alone.

Introduction

Reconstruction of the pre-orogenic configuration of the north Indian margin requires a detailed understanding of the stratigraphic architecture of the Himalaya (Yin, 2006). Current convention in Himalayan geology is to divide the system into lithotectonic zones separated by major fault systems, which are from north to south, the Tethyan Himalaya (TH), Greater Himalaya (GH), Lesser Himalaya (LH), and the uplifted foreland basin deposits of the Sub-Himalaya (SH) (Fig. 1.1a). Thick successions of Precambrian bedrock are exposed in the TH, GH and, to a greater extent, in the LH, and these lack common fossils required for accurate biostratigraphic dating. This, coupled with sparse volcanic material suitable for geochronology, has led to over a decade of research centered primarily on whole-rock neodymium isotopic analysis and U-Pb dating of detrital zircons (e.g., Parrish and Hodges 1996; Ahmad et al., 2000; DeCelles et al., 2000; Robinson et al., 2001; Myrow et al., 2003; Martin et al., 2005; Richards et al., 2005; McQuarrie et al., 2008;

Myrow et al., 2010; Tobgay et al., 2010; Long et al., 2011). Many studies have argued that the LH can be distinguished from the TH and GH independently of structural criteria, by profound geochemical and geochronological differences, with the LH yielding relatively more negative εNd values and containing no detrital zircons younger than 1.6 Ga, whereas strata of both the GH and TH contain abundant younger zircons (1.0 and 0.5 Ga) and relatively less negative εNd (e.g., Parrish and Hodges, 1996; DeCelles et al., 2000, 2004; Martin et al., 2005) (Fig. 1.2a, b).

The notion that unique isotopic signatures characterize these zones has been used as a method for determining structural architecture from isotopic mapping (e.g., Richards et al., 2005; Celerier et al., 2009a) and for correlating these zones over great distances (e.g., Argles et al., 2003). Furthermore, these isotopic differences have been used to argue that the GH and TH were part of an exotic terrane accreted to northern India during an early Paleozoic tectonic event (DeCelles et al., 2000; Yoshida and Upreti, 2006; Spencer et al., 2011). The accreted terrane model was challenged by comparison of Cambrian strata from LH and TH, both of which yielded similar detrital zircon age distributions and εNd supporting deposition of these strata along a continuous margin and casting doubt on the utility of isotopic characterization of the lithotectonic zones (Myrow et al., 2003, 2010). However, recent models suggest that the Cambrian-bearing strata of the LH sampled by Myrow et al. (2003, 2010) are part of a klippe that shared the same original decollement with the either the GH or the TH during early stages of Himalayan deformation (Celerier et al., 2009a,b; Webb et al., 2011). If either of these models is

correct, then the Cambrian-bearing LH strata in northern India may be of TH or GH affinity, leaving the issue unresolved.

This study takes an integrated geochemical, geochronological, and sedimentological approach to explore the predeformational configuration of the north Indian margin. The combination of stratigraphic correlation and detrital zircon geochronology establishes a new chronostratigraphic framework for LH strata. This provides the basis for correlating LH strata with age-equivalent Proterozoic and Cambrian successions of the Indian craton, situated up to ~400 km south of the Himalayan frontal thrust (Fig 1.1). The results are then used to test the hypothesis that fundamental differences in εNd values and detrital zircons age distributions exist between Himalayan lithotectonic zones.

Regional geology and background

The lithotectonic zone approach has been used to characterize regions *en masse,* thus avoiding complications associated with the highly localized stratigraphy of the Himalaya, particularly within the Lesser Himalaya. However, as stratigraphic correlation is essential for evaluating the utility of the lithotectonic zone concept, I used current geochronological constraints, in combination with new data, to establish regional stratigraphic correlations for a variety of Precambrian to lower Paleozoic units (Table 1.1). In the following section I present a summary of those

geochronological constraints that are consider to be firmly established, and which formed the basis for new, targeted analyses presented in the following section.

Northern India is blanketed by thick sedimentary successions of Precambrian and early Paleozoic rocks, often referred to as the "Purana (meaning ancient) Basins" (e.g., Valdyia, 1995). These successions can be broadly categorized into four sectors based on their geographic and tectonic position: 1) The Himalayan margin, comprised of strata uplifted during Cenozoic collision between the Austral-Indian and Eurasian plates; 2) the Indo-Gangetic Basin (IGB), consisting of the sedimentary bedrock underlying the Himalayan foreland basin; 3) cratonic strata west of the Great Boundary Fault, referred here as the Aravalli successions; and 4) the Vindhyan supergroup of the Bundelkhand craton, which are east of the Great Boundary Fault (Fig. 1.1a). The geological relationships between strata within these sectors have long been debated. Although possible geological connections between these regions has been suggested (e.g., Singh, 1985; Tewari, 1989; Valdiya, 1995), the generally excepted view is that these present-day physiographically defined regions equate to ancient sedimentary basins that were isolated from one another at the time of deposition (e.g., Auden, 1934; Bose et al., 2001; Prasad and Asher, 2001; Chakraborty, 2006; Bhargava et al., 2010).

Himalayan margin

The Himalaya consists of the southward vergent fold-thrust belt south of the suture with Tibet that was uplifted as the result of the ongoing continent–continent collision. The orogen is conventionally divided into the lithotectonic zones detailed above (Fig. 1a). In the Kumoan and Tons Valley regions of the north Indian Himalaya, the general structural scheme of Le Fort, (1996) is applicable (Yin, 2006; Webb et al., 2007 Celerier et al., 2009a), where the TH consists primarily of sedimentary rocks in the hanging wall of the South Tibetan Fault System (SFTS), the GH consists mostly of high-grade metamorphic rocks in the hanging wall of the Main Central Thrust (MCT), and the LH primarily consists of sedimentary rocks in the hanging wall of the Main Boundary Thrust (MBT). The Sub Himalaya consists of uplifted foreland deposits in the hanging wall of the Frontal thrust (FT), which marks the southern limit of the Himalaya. While valid in the region of study here, this structural scheme is complicated by along strike variation in deformation, particularly the in the western Himalaya where the MCT and STFS merge and the LH is in direct contact with the TH and the reader is referred to Yin (2006) and Webb et al., (2007) for detailed discussions. In northern India the LH is subdivided by the Tons Thrust (TT), with the "inner" LH zone (iLH) situated north of the Tons Thrust and the "outer" LH zone (oLH) situated to the south (Valdiya, 1980; Ahmad et al., 2000; Richards et al., 2005; Celerier et al., 2009a,b) (Fig. 1.1b). The iLH has produced the isotopic signatures that are considered to characterize the LH

lithotectonic zone (Richards et al., 2005), whereas the oLH has produced isotopic signatures considered characteristic of the GH and TH (Ahmad et al., 2000) (Fig. 1.2c, d).

Stratigraphic nomenclature within the LH is complicated, but here I use a simplified stratigraphic scheme with the iLH consisting of, in ascending order, the Berinag, Damtha, and Deoban groups, and the oLH consisting of the Jaunsar (equivalent to the Simla), Baliana, Krol, and Tal groups (Table 1). Age constraints for strata of the oLH are well established. The Jaunsar Group is considered to be early Neoproterozoic based in part on its stratigraphic position below the Marinoan-aged (ca. 635 Ma) diamictite and cap-carbonate of the Baliana Group (Jiang et al., 2002, 2003a,b), and presence of ~0.8 Ga detrital zircons (Celerier et al., 2009a). The lithostratigraphy, biostratigraphy, and chemostratigraphy of the Krol–Tal succession unequivocally demonstrate Ediacaran–Cambrian depositional ages for these strata (e.g., Jiang et al., 2002, 2003a,b; Hughes et al., 2005, Kaufman et al., 2006, Maithy and Kumar, 2007).

In contrast to the oLH, age constraints in the iLH are sparse, which has limited understanding of the relationships among its component lithostratigraphic units. The Berinag Group is dated by interbedded ca. 1.8 Ga metabasalt flows (Miller et al., 2000), whereas suggested ages for the overlying Damtha and Deoban groups are disparate. The Deoban Group consists of the lower Deoban Formation of the Tons Valley and its suggested equivalent, the Gangolihat Dolomite of Kumaon, which are overlain by the mixed siliciclastic-carbonate Mandhali Formation. The Deoban

Group has been traditionally viewed as Mesoproterozoic based on "Riphean" stromatolite biostratigraphy (e.g., Valdyia 1969, 1980; Rupke, 1974; Bhattacharya, 1983), but recent revised estimates for its age range from Ediacaran–Cambrian (based on putative microfossils; Azmi and Paul, 2004; Tiwari and Pant, 2009, and refs therein) to early Neoproterozoic (Richards et al., 2005), or as spanning the entire Mesoproterozoic (Tewari and Sial, 2007).

Indo-Gangetic Basin

The Ganga supergroup underlies the Cenozoic deposits of the Indo-Gangetic Himalayan foreland basin, and is known from a series of drill cores. It is divided into two units, the Bahraich Group and the overlying Madhubani Group. Age estimates for these stratigraphic successions have spanned from the Paleoproterozoic through the Cambrian (e.g., Fuloria, 1996). More recently, Prasad and Asher (2001) reassigned the Bahraich Group to the Mesoproterozoic based on the presence of the acritarch *Tappania plana* and *Spiromorpha segmentata* (=*Navifusa segmentatus*). These distinctive taxa have been reported from the lower Vindhyan Kheinjua Group in central India (Prasad et al., 2005), the late Mesoproterozoic Ruyang Group in North China (Xiao et al., 1997; Yin et al., 2005), and the Mesoproterozoic Kamo Group of the Central Angara Basin, Siberian Craton (Nagovitsin, 2009), and *Tappania plana* is also known from the ~1.5 Ga Roper Group in northern Australia (Javaux et al., 2001). Thus, an early Mesoproterozoic age estimate for the upper

Bahraich Group is robust. The Bahraich Group is unconformably overlain by the Madhubani Group, which contains purported basal Cambrian to upper Silurian acritarchs (Prasad and Asher, 2001). However, based on inspection of Prasad and Asher's (2001) figured material and independent extraction of leiospheric forms from the Madhubani Group core, all organic walled microfossils identified belong to taxa that range from the Neoproterozoic to the early Paleozoic. Hence, the age determination of the Madhubani Group remains loosely constrained. The absence of bioturbation in any of the heterolithic marine sandstone/mudstone beds that make up much of the Madhubani Group was noted during inspection of the original cores. This would be surprising for rocks of Paleozoic age, but is consistent with a Neoproterozoic age.

Aravalli Successions

The Aravalli cratonic region of northwestern India is associated with three major sedimentary successions, the Aravalli, Delhi, and Marwar supergroups, and various Precambrian igneous rocks. It is bounded to the east by the Great Boundary Fault, which separates it from the Bundelkhand craton and Vindhyan supergroup (Pradhan et al., 2009). The structural and stratigraphic nomenclature applied to the Aravalli cratonic region complicated and problematic, and here the Aravalli Supergroup is considered to consist of sedimentary successions with depositional ages bracketed between 1.8 and 1.5 Ga (Deb et al., 1989, 1990, 2002; Pradhan et al.,

2010), and the Delhi Supergroup to consist of 1.0 to 0.8 Ga sedimentary successions (Deb et al., 2001; Pradhan et al., 2010).

The Aravalli–Delhi successions are overlain by volcanic rocks of the ca. 770 Ma Malani Igneous province (Rathore et al., 1999; Torsvik et al., 2001; Gregory et al., 2009), which are in turn overlain by the relatively undeformed Neoproterozoic–Cambrian Marwar Supergroup (Pandit et al., 2001; Malone et al., 2008; Gregory et al., 2009). The Marwar Supergroup is subdivided into the Jodhpur, Bilara, and Nagaur groups (in ascending order). The siliciclastic Jodhpur Group sits depositionally above the Malani Igneous suite and contains detrital zircons that produce a peak at 850 Ma (Malone et al., 2008), and has produced macroscopic fossils, including possible constituents of the Ediacaran biota (Kumar and Pandey, 2009). The carbonate-dominated Bilara Group has been assigned as Ediacaran to earliest Cambrian based on fossil, lithological, and chemostratigraphic data (Pandit et al., 2001; Mazumdar and Strauss, 2006; Pandey and Bahadur, 2009), and the overlying Nagaur Group contains arthropod trace fossils (Kumar and Pandey, 2008, 2010) including the unequivocal early Cambrian arthropod trace fossil *Cruziana nabatacica (fidé* Seilacher 2010).

Vindhyan supergroup

The relatively unmetamorphosed Vindhyan supergroup crops out in a large syncline situated immediately south of the Indo-Gangetic basin on the Indian craton

(Fig. 1.1). A major angular unconformity divides the Vindhyan supergroup into "upper" and "lower" successions. The lower Vindhyan succession consists of the Semri Group and the upper Vindhyan succession consists of, in ascending order, the Kaimur, Rewa, and Bhander groups (Table 1). The age of the Vindhyan supergroup has long been controversial. Recent debate was driven by reports of putative Cambrian microfossils and trace fossils from the lower Semri Group (Azmi, 1998; Seilacher, 1998) that contrasted with established isotopic ages (Ray, 2006, refs therein). However, over a decade of geochronological studies on the lower Vindhyan strata have confirmed late Paleoproterozoic ages (Ray et al., 2002; Rasmussen et al., 2002; Sarangi et al., 2004). These age assignments have been supported by a more comprehensive paleontological and geochronological study by Bengtson et al. (2009) that confirmed isotopic ages for the upper Semri Group of ~1.6 Ga, and discounted these younger age claims (Table 1.1).

The base of the Kaimur Group is cut by the Majhgawan Kimberlite, which recently has been dated at 1073.5 ± 13.7 Ma (Gregory et al., 2006), consistent with previous suggested ages (e.g., Crawford and Compston, 1969; Kumar et al., 1993). This provides a minimum depositional age for the Kaimur Group. The Rewa and Bhander groups have structures reported to be trace fossils (Chakrabarti, 1990) and putative Ediacaran-type fossils (De, 2003, 2006), although these are all poorly preserved and their affinities are debatable. Seawater $^{87}Sr/^{86}Sr$ values lower than 0.7065 are not known in rocks younger than ~0.8 Ga (Halverson et al., 2007) and reported $^{87}Sr/^{86}Sr$ values of 0.70678, 0.70599, and 0.70605 from the Bhander Group

(Ray et al., 2002) thus provide an upper age constraint for the Bhander Group rocks. However, the $^{87}Sr/^{86}Sr$ data cannot be used to rule out older depositional ages, as similar low values are present throughout older Proterozoic and Archean successions (Shields and Veizer, 2002). Malone et al. (2008) showed that paleomagnetic poles of the Bhander Group are similar to those of the Kaimur Group (minimum depositional age 1.1 Ga based on the cutting relationship of the Majhgawan Kimberlite), and that all upper Vindhyan paleomagnetic poles differ significantly from paleomagnetic poles from the 770 Ma Malani Igneous province of the Aravalli region (Torsvik et al., 2001; Gregory et al., 2009). Therefore, these data suggest that the upper Vindhyan strata span a relatively narrow range of depositional ages. The Bhander Group of Rajasthan and the lower Marwar Supergroup of the neighboring Aravalli region yielded different detrital zircon age distributions, with the Marwar Supergroup distribution containing a high concentration of Neoproterozoic grains (~850 Ma), the Bhander Group lacking grains younger than 1.0 Ga (Fig. 1.4). From these data, Malone et al. (2008) suggest that depositional ages of the Bhander Group are likely not much younger 1.0 Ga, an interpretation consistent with an earlier estimate (Gregory et al., 2006).

Accordingly, existing data suggest that there are broad similarities in the depositional ages of rocks within all regions mentioned above, and permitted the targeted collection of new samples in order to provide addition depositional age constraints on various units, refine correlations, and assess sediment source relationships among rocks of similar depositional age. This has helped to

understand stratigraphic relationships among these regions, test lateral continuity between the craton and Himalayan margin, and ultimately review the utility of isotopic mapping of Himalayan lithotectonic zones.

Methods

The approach taken here has been to focus on distinctive stratigraphic units that are strong candidates for correlation between the craton and the Himalaya. Criteria for comparison include specific lithological and paleobiological features (e.g. the phosphate-capped stromatolites, or age diagnostic trace fossils discussed below), and also geochronological and geochemical properties.

Sandstone samples were collected for individual grain U-Pb dating of detrital zircons from cratonic successions with independent depositional age control, specifically the major units of the Vindhyan supergroup from sections of the Son Valley and the Nagaur Group of the Marwar Supergroup, and the major units of the iLH (Berinag, Damtha, and Deoban groups) and the lower oLH (Jaunsar Group and Blaini Formation) in the Tons Valley and Kumaon region of the Himalaya (Fig. 1.1, Table 1.2). These data were combined with preexisting data of the upper oLH Tal Group (Myrow et al., 2003, 2010) to produce a more complete spectral profile of the north Indian LH. The Nagaur Group sample from Nagaur quarry was analyzed using a SHRIMP ion microprobe at the Research School of Earth Sciences, Australian National University (analytical procedures follow those described in Myrow et al,

[2010]). All other samples were analyzed at the University of Arizona LaserChron Center using laser ablation multicollector inductively coupled plasma mass spectrometry (LA-MC-ICPMS) (procedural details available in Supporting Material SM1.1). Fine-grained siliciclastic material was collected from selected iLH and oLH strata for whole rock Sm-Nd isotopic analysis via Thermal Ion Mass Spectrometry (TIMS) at the Massachusetts Institute of Technology (procedure details follow those described in Schone et al. [2009]). Detrital zircon data tables are available as online supplements.

Results and Discussion

Phosphatic stromatolites of the iLH and Indian craton

The phosphorite-bearing stromatolitic carbonate of the Gangolihat Dolomite forms a distinctive deposit in the Kumaon iLH. It consists of branching columnar stromatolite bioherms belonging to the form genus *Baicalia*, with early diagenetic black phosphatic crusts formed around the stromatolite columns and intraclastic phosphatic grainstone filling the intercolumnar spaces. This suite of specific features is found within the Tirhoan Dolomite (Rohtas Formation) of the Semri Group from the Vindhyan supergroup (Fig. 1.3). The Tirohan Dolomite sits depositionally above dated 1.6 Ga volcanic deposits in the upper Semri Group (Rasmussen et al., 2002; Ray et al., 2002; Bengtson et al., 2009), and a 1602 ± 11 Ma

Pb-Pb isochron was produced directly from phosphatic intraclasts from one sample (Bengtson et al., 2009). A variety of microbial textured clasts with gas bubbles and organic walled microfossils have been described from acid residues of the intercolumnar material (Bengtson et al., 2009) and material identical in these respects has been reported from the Gangolihat Dolomite (McKenzie et al., 2010). Lithologically similar deposits of phosphatic branching columnar stromatolites have also been described from the Aravalli Supergroup (Banerjee et al., 1971; Raha and Sastry, 1982) in late Paleoproterozoic and early Mesoproterozoic rocks, coarsely bracketed between ~1.8 and ~1.5 Ga (Deb et al., 1989; Deb et al., 2001).

The specific similarities listed above, and the fact that these characteristics are only known to occur together at a single horizon in both the Vindhyan Basin and the Himalaya, suggests that the ~1.6 Ga Rohtas Formation is correlative with the Gangolihat Dolomite of iLH, and both were part of a continuous late Paleoproterozoic carbonate platform covering the northern Indian margin.

Detrital zircon geochronology

Detrital zircon geochronology has become an important tool in characterization of strata in the Himalaya (e.g., DeCelles et al., 2000; Myrow et al., 2003, 2010; Martin et al., 2005; McQuarrie et al., 2008; Webb et al., 2011). Here results are first presented from age-controlled cratonic successions, which are essential for interpretation of the results of the Himalayan samples. These results provide

approximate ages of peaks produced by various grain populations, which are rounded to the nearest 10 Ma. All detrital zircon age distributions are presented in Figure 1.4.

The Chorhat Sandstone of the upper Semri Group (lower Vindhyan) is interbedded with 1.6 Ga volcanic rocks and, as expected, yielded no grains younger than 1.6 Ga, with the age distribution dominated by two populations with peaks at 1650 Ma and 1730 Ma (Fig. 1.4). This unit is stratigraphically below the phosphorite-bearing Rohtas Formation.

A sample from the overlying Kaimur Group yielded an age distribution with the youngest grains producing a peak at 1170 Ma and older peaks of 1730, 1850, and 2500 Ma. The depositional age of the Kaimur Group is here constrained to the late Mesoproterozoic (1.1 Ga), older than the 1073.5 ± 13.7 Ma Majhgawan Kimberlite that intrudes it (Gregory et al., 2006) but younger than the 1170 Ma zircon population it contains. The Rewa Group and upper Bhander Group yielded similar age distributions with youngest zircons around 1000 Ma and older peaks at 1600, and 1750 Ma. These are similar to a published distribution from the Bhander Group in Rajasthan (Malone et al., 2008) (Fig. 1.4), supporting correlation between these rocks. Malone et al. (2008) used paleomagnetic data to argue that the upper Vindhyan succession was deposited within a relative short interval, and data presented here are consistent with this hypothesis. Specifically, Kaimur Group deposition occurred during the late Mesoproterozoic (1.1 Ga), and Bhander Group deposition took place during the terminal Mesoproterozoic to earliest

Neoproterozoic (1.0 Ga). Furthermore, a depositional age of 1.1 Ga for the Kaimur Group, compared to that of the upper Semri Group (~1.6 Ga), implies that the regional unconformity between these groups spans a gap of time of approximately 500 million years.

Within the IGB a drill core sample from the lower Madhubani Group (SPNACC14) of the Ganga Supergroup produced an age distribution with a broad population of zircons between 1.6 and 1.8 Ga, and a youngest population of 1.2 Ga grains (Fig. 1.4). The overall distribution of Madhubani Group grain ages is similar to the age distribution from the Kaimur Group (Fig. 1.4), and as biostratigraphic arguments for a Paleozoic depositional age for the lower Madhubani Group are unfounded, an age equivalent to that of the Kaimur Group (1.1 Ga) (see above) is most likely, and these units may be correlative. A published detrital zircon age distribution from uplifted bedrock that underlies the foreland basin of eastern India (the Shillong Group of the Shillong Plateau [Yin et al., 2010b]) is similar to the upper Vindhyan and Madhubani Group distributions (Fig. 1.4).

Two samples were analyzed from the Marwar Supergroup of the Aravalli succession. One sandstone sample was collected from the Nagaur Group at Nagaur Quarry, which may represent latest Neoproterozoic–earliest Cambrian deposition, and another sandstone sample collected from the Nagaur Group sandstone at Dulmera Quarry contains unequivocal arthropod trace fossils indicative of a trilobitic early Cambrian depositional age. The Nagaur Quarry sample contains a large concentration of grains between 700 Ma and 1000 Ma grains, and a smaller

population with a peak at 2500 Ma. The trace fossil-bearing Nagaur Group from Dulmera Quarry sample yielded an array of age populations with peaks 770, 980, 1600, 1720, 1880, and 2500 Ma, with a small population of grains with a peak of 540 Ma, consistent with the Cambrian depositional age indicated by the ichnology.

Age distributions from two samples of the Berinag Group in Kumaon showed a large population of grains with a peak of 1880 Ma (data combined in Fig. 1.4), consistent with a depositional age of ~1.8 Ga for the Berinag–Rampur groups (Miller et al., 2000; Richards et al., 2005; Kohn et al., 2010). A sample from the lower Damtha Group (DGAD) yielded an age distribution with a large peak 1870 Ma and no grains younger than 1800 Ma (Fig. 1.4). If the Gangolihat Dolomite were part of a continuous contemporaneous carbonate platform with the Rohtas Formation of the lower Vindhyan succession, then associated siliciclastic strata should yield similar detrital zircon age distributions. A sandstone sample analyzed from the upper Damtha Group (RTG3), which underlies the phosphatic section of the Gangolihat Dolomite in the Kumaon Himalaya, sample yielded no grains younger than a small population of 1600 Ma grains, with older peaks at 1750, 1880, and 2500 Ma (Fig. 1.4). The distribution from the upper Damtha sample was similar to the lower Vindhyan distribution (CSV-1-25) and further supports correlation between the Gangolihat Dolomite (iLH) and the Rohtas Formation.

A sample from a mixed siliciclastic succession of gray shale with thin–bedded fine to medium grained sandstone of the Mandhali Formation (TV-16-MD), which unconformably overlies the Deoban Formation in the Tons Valley, yielded an age

distribution with a youngest peak at 950 Ma and older peaks at 1560, 1750, and 2500 Ma. This latter population of grains is slightly younger than strata of the upper Vindhyan sequence, but lacks the abundant younger material (≤850 Ma) seen in Cryogenian and younger successions both in the Himalayan margin and on the craton (Fig. 1.4). Based on this, and the similarity between the Mandhali Formation peak distribution and those of upper Vindhyan distributions, a pre-Cryogenian, earliest Neoproterozoic depositional age for the Mandhali Formation is suggested, which is approximately equivalent to that of the upper Bhander Group. Importantly, the change in distributions from the upper Damtha Group to the Mandhali Formation mirror those seen across the unconformity in the Vindhyan supergroup, which implies that the same unconformity exists in the Himalayan margin. This unconformity has been recognized by other studies as the boundary between the "upper" and "lower" Lesser Himalaya (e.g., McQuarrie et al., 2008; Kohn et al., 2010; Long et al., 2011) and, in earlier reports, it was speculated to span an interval of ~1 billion years or greater. Based on the correlation to the Vindhyan successions and the new age conatraints presented here, the unconformity represents a gap in time not greater than ~500 million years. Importantly, the unconformity is here identified to occur *within* the iLH, and the terms "upper" and "lower" Lesser Himalaya thus refer to units of different stratigraphic age, and thus are not synonymous with "inner" and "outer" LH, which refer to fault-bounded structural units.

Within the oLH, analysis of poorly sorted pebble conglomerate from the Jaunsar Group (SJM), collected immediately north of the Main Boundary Thrust in the Tons Valley, yielded a detrital zircon distribution dominated by 850 Ma grains, and nothing younger (Fig 1.4). A sample of diamictite from the Cryogenian-aged Baliana Group (NBLD-1) was collected immediately below a pink dolostone cap carbonate in the Nainital syncline, and yielded youngest grains with a 770 Ma age peak, and an array of older populations of approximately 850, 1100, 1600, 1880, and 2500 Ma. Published data from lower Cambrian strata of the Tal Group have populations similar to those of the Blaini diamictite, whereas an age distribution from Cambrian rocks stratigraphically higher in the Tal Group contained high concentrations of Cambrian and Neoproterozoic age grains, yet lacked more ancient Paleoproterozoic and Mesoproterozoic material (Myrow et al., 2010).

As a whole, strata of Cryogenian to early Cambrian ages of both the oLH and the Marwar Supergroup possess the same young Neoproterozoic to Cambrian zircons, and additionally these strata possess the same general Paleoproterozoic and Mesoproterozoic age zircon populations as the depositionally older iLH and Vindhyan successions. This suggests that similar zircon sources persisted across various parts of the northern Indian margin from the Paleoproterozoic to the Cambrian.

Neodymium geochemistry of the iLH and oLH

Differences in εNd have been noted between the lithotectonic units of the Himalaya (e.g., Parrish and Hodges, 1996; DeCelles et al., 2000; Robinson et al., 2001; Argles et al., 2003; Martin et al., 2005), as well as within the LH, where values for iLH rocks are more negative than those of oLH rocks (Ahmad et al., 2000; Richards et al., 2005). In order to integrate εNd with independent geochronological constraints, four fine-grained siliciclastic samples were analyzed for Nd isotopes, two from oLH strata and two from iLH strata (Table 1.3). A sample of shale collected from below the phosphorite-bearing horizon in the suggested ~1.6 Ga Gangolihat Dolomite (GNG), which sits depositionally above the upper Damtha Group, has an εNd(0) value of -22 and a εNd(500) value of -16. A Mandhali Formation sample (TV-MD) was collected directly above the unconformable contact with the Deoban Formation in the Tons Valley (same outcrop as the Mandhali Formation detrital zircon sample TV-16-MD: see Fig. 1.4), which yielded an εNd(0) value of -16 and εNd(500) value of -11. A Jaunsar Group sample (TVBS) collected from the Tons Valley from black shale, above the stratigraphic level of the detrital zircon sample, yielded an εNd(0) value of -17 and εNd(500) of -12. Finally, a shale sample collected from the Blaini Formation, taken below the Blaini diamictite, yielded an εNd(0) value of -16 and εNd(500) of -11.

The εNd values for the Gangolihat Dolomite are similar to reported εNd values from known late Paleoproterozoic strata of the lower Nawakot unit in the Nepalese

Himalaya (Robinson et al., 2001; Martin et al., 2005), which is consistent with the depositional age of ~1.6 Ga for the Gangolihat Dolomite suggested here. The εNd values from the Mandhali Formation overlap with the values from the Cryogenian Jaunsar and Baliana groups. Interestingly, these values are considered characteristic of GH and oLH, and not of the iLH, (e.g., Ahmad et al., 2000; Richards et al., 2005) (Fig. 1.2), although the Mandhali Formation sample comes from strata north of the Tons thrust and is unequivocally part of the iLH. This supports that the Mandhali Formation and Jaunsar–Baliana successions are much closer in depositional age than the Mandhali Formation is to other lower iLH strata (i.e., the Berinag-Rautgara-Gangolihat succession). Most importantly, the similarity of εNd compositions and depositional ages of strata both in the iLH and oLH refutes the idea of a fundamental isotopic difference between these tectonically distinguished zones. Richards et al. (2005) suggested that an ~850 Ma rifting event marked the transition from "iLH-type" isotopic signatures to "GH-type" (i.e., oLH-type) signatures, but data presented here imply this isotopic shift likely took place prior to deposition of the upper Vindhyan and Mandhali Formations (>1.0 Ga).

Correlation, chronostratigraphy, and continuity of cratonic and Himalayan successions

The work described above leads to a revised chronostratigraphic correlation between north Indian sedimentary units (Table 1.4). If the terms "lower" and

"upper" succession are to be applied to the Lesser Himalaya, then the lower succession consists of late Paleoproterozoic to earliest Mesoproterozoic strata, which includes the Berinag-Damtha-Gangolihat units, and the upper succession consists of the late Mesoproterozoic–early Neoproterozoic to Cambrian Mandhali-Jaunsar-Baliana-Krol-Tal units. The Berinag Group has been dated at 1.8 Ga (Miller et al., 2000) and detrital zircon data presented here are in agreement with this age. The depositional ages of the Damtha Group and Gangolihat Dolomite have been problematic, but they can now be correlated with dated 1.6 Ga strata of the Semri Group of the lower Vindhyan succession. Furthermore, detrital zircon age distributions and εNd values of the Berinag-Damtha Groups are similar to the lower Nawakot unit of Nepal and the Shumar Formation of Bhutan, which are also considered to be Paleoproterozoic (DeCelles et al., 2004; Martin et al., 2005; Richards et al., 2006; McQuarrie et al., 2008; Long et al., 2011; Martin et al., 2011). While it is suggested here that the Damtha-Gangolihat successions are correlative to the Semri Group, there is no presently known Vindhyan unit correlative with the Berinag Group. The Semri Group sits unconformably on the 2.5 Ga Bundelkhand granitic basement, and the best current age constraint on the depositional age of the lower Semri Group is a 1729 ± 110 Ma Pb-Pb errorchron from the Kajrahat Limestone (Sarangi et al., 2004). The siliciclastic Deoland Formation is the lowermost unit of the Vindhyan supergroup (stratigraphically below the Kajrahat Limestone), and is a possible equivalent of the Berinag Group.

The Kaimur Group (upper Vindhyan succession) is here constrained to an approximate depositional age of 1.1 Ga, and data presented here are in agreement with the previously suggested 1.0 Ga depositional age for the upper Bhander Group (Malone et al., 2008). The Mandhali Formation (iLH) is correlated with the uppermost Bhander Group, with a depositional age of terminal Mesoproterozoic to earliest Neoproterozoic. The age of the Deoban Formation of the Tons Valley iLH remains poorly constrained. While it is traditionally correlated with the Gangolihat Dolomite of the Kumaon iLH, the two units are not laterally continuous in map view and are regarded to display different characteristic facies (Valdyia, 1980; Thakur, 1992). A Pb model age of ~970 Ma was reported from samples of galena within the Jammu Limestone which is a putative equivalent of the Tons Valley Deoban Formation, but the accuracy of this method remains questionable (Raha et al., 1978). Age distributions of detrital zircons from the upper Vindhyan are similar to distributions from the bedrock that underlies the Himalayan foreland basin of the Madhubani Group of the IGB and the Shillong Group of the Shillong Plateau (Yin et al., 2010b), as well as distributions from the Lesser Himalaya of Bhutan (McQuarrie et al., 2008) and Arunachal Pradesh (Yin et al., 2006). The Cryogenian through Cambrian deposits of the Jaunsar-Baliana-Krol-Tal succession are here correlated with the late Neoproterozoic–early Cambrian Marwar Supergroup from the Aravalli craton. The overall temporal variation of age distributions of detrital zircons in the cratonic successions mirrors that of the Lesser Himalaya. Variation can be observed in the relative abundance of zircon age populations, especially for those peaks that

represent periods of tectonism during which local sources flooded the samples (e.g., the Berinag Quartzite is flooded with ~1.8 Ga grains, derived during late Paleoproterozoic tectonism [see Kohn et al., 2010]). Nonetheless, in both craton and Himalaya, similar grain age populations are maintained from their initial introduction into the sedimentary system in the Paleoproterozoic through until at least the Cambrian. The Paleoproterozoic grain peaks that characterize the lower successions (i.e., roughly 1600, 1750, 1880, and 2500 Ma) are robust throughout the cratonic late Mesoproterozoic upper Vindhyan succession and in the iLH Mandhali Formation, as well as in the oLH Cryogenian Blaini Formation**,** the early Cambrian Tal Group of the Himalaya, and in the early Cambrian Marwar Supergroup of the craton. Furthermore, the younger strata of the cratonic successions, iLH, and oLH all share similar younger late Mesoproterozoic to Cambrian zircon populations (e.g., roughly 1000, 850, 770, and 500 Ma). The similarity of these age peaks strongly suggests shared sources of detritus between these regions, derived from a combination of continuous erosion of regionally prominent igneous bodies, and a long shared history of reworking of siliciclastic sedimentary material. Hence, even if the oLH is a klippe of either GH or TH affinity the fact that the Cryogenian Jaunsar Group and Blaini Formations share similar age distributions with both the iLH and cratonic successions ~400 km south of the Himalayan front, as well as εNd values with upper iLH strata, supports deposition as part of a continuous north Indian margin (Myrow et al., 2003, 2010).

The similarity of zircon age distributions from the cratonic successions and across the length of the Himalaya demonstrates the striking sediment-source continuity between these regions (*cf*. Myrow et al. 2010)**.** The three broad age ranges that are suggested to characterize pre-Ordovician strata in eastern India (late Paleoproterozoic, late Mesoproterozoic to early Neoproterozoic, and late Neoproterozoic to Cambrian [Yin et al., 2010a]) mirror those seen in rocks from the north Indian Himalaya and the central and western craton (i.e., Vindhyan and Aravalli successions), which demonstrates that the entire north Indian margin was subjected to a long history of similar controls on sediment transport and deposition. Hence, putatively characteristic detrital zircon age distributions of the various Himalayan lithotectonic units are all present in the cratonic successions, and variation in isotopic signatures can be related directly to the depositional age of the strata. While notable differences in isotopic signatures can be used to identify structural boundaries, as major faults typically juxtapose rocks of substantially different age against each other, these signatures cannot define any structural block over long distances. The greatest utility of these "signatures" is that they provide a first order approximation of the depositional age of the exposed unit.

The similarity between the Vindhyan and Himalayan detrital zircon age distributions suggests that these two sectors received detritus from similar sources. This calls into question current models that argue the Vindhyan supergroup was deposited in an isolated intracratonic basin (Bose et al., 2001; Prasad and Asher, 2001; Chakraborty 2006; Malone et al., 2008; Pradhan et al. 2010). Alternatively,

Vindhyan strata may represent the proximal portion of the northward facing epicontinental sea, with coeval Himalayan strata representing more distal equivalents. This model is consistent with Vindhyan paleocurrent directions dominantly oriented to the northwest (e.g., Bose et al., 2001). The lack of <1.0 Ga strata may be related to "closure" of the basin (Malone et al., 2008), or perhaps due to the docking of either Antarctica or Australian along the east Indian margin during Rodinia amalgamation in the late Mesoproterozoic to early Neoproterozoic (e.g., Torsvik et al., 2001; Kelley et al., 2002; Pradhan et al., 2010; Yin et al, 2010b), which may have caused local uplift the Vindhyan region. Such uplift may have prevented deposition or preservation of the younger strata observed in the adjacent Aravalli, Himalayan, and eastern Shillong regions.

Conclusions

1) The Gangolihat Dolomite of the inner Lesser Himalaya is correlative with the Rohtas Formation the Semri Group, and has an approximate depositional age of 1.6 Ga. This constrains the depositional age of the Berinag-Damtha-Gangolihat succession of the iLH to late Paleoproterozoic (bracketed ages between 1.8 and 1.6 Ga).

2) The unconformity between the upper and lower Vindhyan sequences spans a duration of approximately 500 million years (i.e., from 1.6 to 1.1 Ga). This

unconformity is identifiable within the iLH, and whereas the terms “upper” and “lower” Lesser Himalaya signify this break, these terms are not synonymous with “inner” and “outer” Lesser Himalaya**.** The latter terms refer to fault-bound blocks, the constituents of which are not uniformly represented by particular depositional ages.

3) All detrital zircon age populations previously suggested to be characteristic of individual Himalayan lithotectonic blocks are also present in samples from Indian cratonic successions. Variations in age distributions are directly related to depositional age, and cannot define Himalayan lithotectonic zones.

4) Strata with similar depositional ages in both the iLH and oLH yielded similar εNd values, which refute the suggestion that these zones contain diagnostically distinct geochemical signatures.

5) Detrital zircon age distributions from cratonic successions are remarkably similar to distributions from depositionally coeval rocks of the Lesser Himalaya, suggesting that both regions shared similar detrital sources, and were not likely isolated. If so, then the Vindhyan basin represents the proximal part of a northward deepening epicontinental platform, with the current Himalayan margin situated along the distally deepening continental margin.

Acknowledgements

I thank N. Hughes, P. Myrow, S. Xiao, and M. Sharma for assistance in the planning and execution of this project and helpful critical discussions throughout. S. Bowring and F. Dudas at the Massachusetts Institute of Technology, G. Gehrels, M. Pecha, and M. Ibanez-Mejia at the Arizona LaserChron Center and M. Fanning at the Australian National University are thanked for analytical assistance. S. Kumar, V. Mathur, B. Singh, A. Bhattacharya, G. Kumar, A. Seilacher, N. Planavsky, and C. Reinhard are thanked for assistance in multiple aspects of this project. ONGC access was kindly facilitated by B. Prasad. This project was partially funded by NSF-EAR053868 and 1124303 to N. Hughes, EAR 1124518 to P. Myrow, EAR 1124062 to S. Xiao, and graduate student research grants to N.R. McKenzie from the Geological Society of America, the Paleontological Society (the Allison R. "Pete" Palmer Award), American Association of Petroleum Geologists (the J. Funkhouser Memorial Grant and F. Sutton Memorial Grant), and the Institute for Cambrian Studies, with additional support provided by the IGCP-512. NSF-EAR 0732436 supports the Arizona LaserChron Center.

References

Auden, J.B., 1934. Geology of the Krol Belt, Simla Himalaya. Records of the Geological Survey of India 67.

Ahmad, T., Harris, N., Bickle, M., Chapman, H., Bunbury, J., Prince, C., 2000. Isotopic constraints on the structural relationships between the Lesser Himalayan Series and the High Himalaya Crystalline Series, Garhwal Himalaya. Geological Society of America Bulletin 112, 467-477.

Argles, T., Foster, G., Whittington, A., Harris, N., George, M., 2003. Isotopic studies reveal a complete Himalayan section in the Nanga Parbat syntaxis. Geology 31, 1109-1112.

Azmi, R.J., 1998. Discovery of Lower Cambrian small shelly fossils and brachiopods from the Lower Vindhyan of Son Valley, Central India. Journal of the Geological Society of India 52, 381-389.

Azmi, R.J., Paul, S.K., 2004. Discovery of Precambrian-Cambrian boundary protoconodonts from the Gangolihat Dolomite of Inner Kumaun Lesser Himalaya: Implications on age and correlation. Current Science 86, 1653-1659.

Banerjee, D.M., 1971. Precambrian Stromatolitic Phosphorites of Udaipur, Rajasthan, India. Geological Society of America Bulletin 82, 2319-&.

Bengtson, S., Belivanova, V., Rasmussen, B., Whitehouse, M., 2009. The controversial "Cambrian" fossils of the Vindhyan are real but more than a billion years older. Proceedings of the National Academy of Sciences 106, 7729-7734.

Bhargava, O.N., Frank, W., Bertle, R., 2011. Late Cambrian deformation in the Lesser Himalaya. Journal of Asian Earth Sciences 40, 201-212.

Bhattacharya, A.R., 1983. Record of stromatolite *Plicatina* from India. Geological Magazine 160, 543-548.

Bose, P.K., Sarkar, S., Chakrabarty, S., Banerjee, S., 2001. Overview of the Meso- to Neoproterozoic evolution of the Vindhyan basin, central India. Sedimentary Geology 141, 395-419.

Brookfield, M.E., 1993. The Himalayan passive margin from Precambrian to Cretaceous times. Sedimentary Geology 84, 1-35.

Cawood, P.A., Johnson, M.R.W., Nemchin, A.A., 2007. Early Palaeozoic orogenesis along the Indian margin of Gondwana: Tectonic response to Gondwana assembly. Earth and Planetary Science Letters 255, 70-84.

Celerier, J., Harrison, T.M., Beyssac, O., Herman, F., Dunlap, W.J., Webb, A.A.G., 2009. The Kumaun and Garwhal Lesser Himalaya, India: Part 2. Thermal and deformation histories. Geological Society of America Bulletin 121, 1281-1297.

Celerier, J., Harrison, T.M., Webb, A.A.G., Yin, A., 2009. The Kumaun and Garwhal Lesser Himalaya, India: Part 1. Structure and stratigraphy. Geological Society of America Bulletin 121, 1262-1280.

Chakrabarti, A., 1990. Traces and dubiotraces: examples from the so-called Late Proterozoic
siliciclastic rocks of the Vindhyan Supergroup around Maihar, India. Precambrian Research 47, 141-153.

Chakraborty, C., 2006. Proterozoic intracontinental basin: The Vindhyan example. Journal of Earth System Science 115, 3-22.

Crawford, A.R., Compston, W., 1969. The age of the Vindhyan System of Peninsular India. Quarterly Journal of the Geological Society 125, 351-371.

De, C., 2003. Possible organisms similar to Ediacaran forms from the Bhander Group, Vindhyan Supergroup, Late Neoproterozoic of India. Journal of Asian Earth Sciences 21, 387-395.

De, C., 2006. Ediacara fossil assemblage in the upper Vindhyans of Central India and its significance. Journal of Asian Earth Sciences 27, 660-683.

Deb, M., Thorpe, R., Krstic, D., 2002. Hindoli group of rocks in the eastern fringe of the Aravalli-Delhi orogenic belt-Archean secondary greenstone belt or Proterozoic supracrustals? Gondwana Research 5, 879-883.

Deb, M., Thorpe, R.I., Cumming, G.L., Wagner, P.A., 1989. Age, Source and Stratigraphic Implications of Pb Isotope Data for Conformable, Sediment-Hosted, Base-Metal Deposits in the Proterozoic Aravalli-Delhi Orogenic Belt, Northwestern India. Precambrian Research 43, 1-22.

Deb, M., Thorpe, R.I., Krstic, D., Corfu, F., Davis, D.W., 2001. Zircon U-Pb and galena Pb isotope evidence for an approximate 1.0 Ga terrane constituting the western margin of the Aravalli-Delhi orogenic belt, northwestern India. Precambrian Research 108, 195-213.

DeCelles, P.G., Gehrels, G.E., Najman, Y., Martin, A.J., Carter A., Garzanti, E., 2004. Detrital geochronology and geochemistry of Cretaceous–Early Miocene strata of Nepal: implications for timing and diachroneity of initial Himalayan orogenesis. Earth and Planetary Science Letters 227, 313-330.

DeCelles, P.G., Gehrels, G.E., Quade, J., LaReau, B., Spurlin, M., 2000. Tectonic implications of U-Pb zircon ages of the Himalayan orogenic belt in Nepal. Science 288, 497-499.

Fuloria, R.C., 1996. Geology and hydrocarbon prospects of the Vindhyan sediments in Ganga valley. Geological Society of India Memoir 36, 235-256.

Gregory, L.C., Meert, J.G., Bingen, B., Pandit, M.K., Torsvik, T.H., 2009. Paleomagnetism and geochronology of the Malani Igneous Suite, Northwest India: Implications for the configuration of Rodinia and the assembly of Gondwana. Precambrian Research 170, 13-26.

Gregory, L.C., Meert, J.G., Pradhan, V., Pandit, M.K., Tamrat, E., Malone, S.J., 2006. A paleomagnetic and geochronologic study of the Majhgawan kimberlite, India: Implications for the age of the Upper Vindhyan Supergroup. Precambrian Research 149, 65-75.

Halverson, G.P., Dudas, F.O., Maloof, A.C., Bowring, S.A., 2007. Evolution of the Sr-87/Sr-86 composition of Neoproterozoic seawater. Palaeogeography Palaeoclimatology Palaeoecology 256, 103-129.

Hughes, N.C., Peng, S.-C., Bhargava, O.N., Ahulwalia, A.D., Walia, S., Myrow, P.M., Parcha, S.K., 2005. The Cambrian biostratigraphy of the Tal Group, Lesser Himalaya, India, and early Tsanglangpuan (late early Cambrian) trilobites from the Nigali Dhar syncline. Geological Magazine 142, 57-80.

Javaux, E.J., Knoll, A.H., Walter, M.R., 2001. Morphological and ecological complexity in early eukaryotic ecosystems. Nature 412, 66-69.

Jiang, G., Christie-Blick, N., Kaufman, A.J., Banerjee, D.M., Rai, V., 2002. Sequence stratigraphy of the Neoproterozoic Infra Krol Formation and Krol Group, Lesser Himalaya, India. Journal of Sedimentary Research 72, 524-542.

Jiang, G., Christie-Blick, N., Kaufman, A.J., Banerjee, D.M., Rai, V., 2003. Carbonate platform growth and cyclicity at a terminal Proterozoic passive margin, Infra Krol Formation and Krol Group, Lesser Himalaya, India. Sedimentology 50, 921-952.

Jiang, G., Sohl, L.E., Christie-Blick, N., 2003. Neoproterozoic stratigraphic comparison of the Lesser Himalaya (India) and Yangtze Black (South China): paleogeographic implications. Geology 31, 917-920.

Kaufman, A.J., Jiang, G., Christie-Blick, N., Banerjee, D.M., Rai, V., 2006. Stable isotope record of the terminal Neoproterozoic Krol platform in the Lesser Himalayas of northern India. Precambrian Research 147, 156-185.

Kelly, N.M., Clarke, G.L., Fanning, C.M., 2002. A two-stage evolution of the Neoproterozoic Rayner Structural Episode: new U-Pb sensitive high resolution ion microprobe constraints from the Oygarden Group, Kemp Land, East Antarctica. Precambrian Research 116, 307-330.

Kohn, M.J., Paul, S.K., Corrie, S.L., 2010. The lower Lesser Himalayan sequence: A Paleoproterozoic arc on the northern margin of the Indian plate. Geological Society of America Bulletin 122, 323-335.

Kumar, A., Kumari, V.M.P., Dayal, A.M., Murthy, D.S.N., Gopalan, K., 1993. Rb-Sr Ages of Proterozoic Kimberlites of India - Evidence for Contemporaneous Emplacement. Precambrian Research 62, 227-237.

Kumar, S., Pandey, S.K., 2008. Discovery of trilobite trace fossils from the Nagaur sandstone, the Marwar Supergroup, Dulmera area, Bikaner district, Raasthan. Current Science 94, 1081-1085.

Kumar, S., Pandey, S.K., 2009. Note on the occurrence of *Arumberia banksi* and associated fossils from the Jodhpur sandstone, Marwar Supergroup, western Rajasthan. Journal of the Palaeontological Society of India 54, 171-178.

Kumar, S., Pandey, S.K., 2010. Trace fossils from the Nagaur Sandstone, Marwar Supergroup, Dulmera area, Bikaner district, Rajasthan, India. Journal of Asian Earth Sciences 38, 77-85.

Long, S., McQuarrie, N., Tobgay, T., Rose, C., Gehrels, G., Grujic, D., 2011. Tectonostratigraphy of the Lesser Himalaya of Bhutan: Implications for the along-strike stratigraphic continuity of the northern Indian margin. Geological Society of America Bulletin doi:10.1130/B30202.1.

Malone, S.J., Meert, J.G., Banerjee, D.M., Pandit, M.K., Tamrat, E., Kamenov, G.D., Pradhan, V.R., Sohl, L.E., 2008. Paleomagnetism and detrital zircon geochronology of the upper Vindhyan sequence, Son Valley and Rajasthan, India: A ca. 1000Ma closure age for the Purana basins? Precambrian Research 164, 137-159.

Martin, A.J., Burgy, K.D., Kaufman, A.J., Gehrels, G.E., 2011. Stratigraphic and tectonic implications of field and isotopic constraints on depositional ages of Proterozoic Lesser Himalayan rocks in central Nepal. Precambrian Research 185, 1-17.

Martin, A.J., DeCelles, P.G., Gehrels, G.E., Patchett, P.J., Isachsen, C., 2005. Isotopic and structural constraints on the location of the Main Central thrust in the Annapurna Range, central Nepal Himalaya. Geological Society of America Bulletin 117, 926-944.

Maithy, P. K. and Kumar, G. 2007. Biota in the Terminal Proterozoic successions on the Indian subcontinent: a review. *In*: Vickers-Rich, P. and Komarower, P. (eds.) *The rise and fall of the Ediacaran Biota*. Geological Society, London, Special Publications 286, 315-330.

Mazumdar, A., Strauss, H., 2006. Sulfur and strontium isotopic compositions of carbonate and evaporite rocks from the late Neoproterozoic-early Cambrian Bilara Group (Nagaur-Ganganagar Basin, India): Constraints on intrabasinal correlation and global sulfur cycle. Precambrian Research 149, 217-230.

McKenzie, N.R., N.C., H., Myrow, P.M., Xiao, S., Jiang, G., 2010. Chronostratigraphic constraints on the inner Lesser Himalayan sedimentary belt of north India and Proterozoic sediment continuity of the north Indian margin, in: Leech, M.L., et al. (Ed.), Proceedings for the 25th Himalaya-Karakoram-Tibet Workshop: U.S. Geological Survey, Open-File Report 2010-1099, 2 p. [http://pubs.usgs.gov/of/2010/1099/mckenzie/], San Francisco.

McQuarrie, N., Robinson, D., Long, S., Tobgay, T., Grujic, D., Gehrels, G., Ducea, M., 2008. Preliminary stratigraphic and structural architecture of Bhutan: Implications for the along strike architecture of the Himalayan system. Earth and Planetary Science Letters 272, 105-117.

Miller, C., Klotzli, U., Frank, W., Thoni, M., Grasemann, B., 2000. Proterozoic crustal evolution in the NW Himalaya (India) as recorded by circa 1.80 Ga mafic and 1.84 Ga granitic magmatism. Precambrian Research 103, 191-206.

Myrow, P.M., Hughes, N.C., Goodge, J.W., Fanning, C.M., Williams, I.S., Peng, S.C., Bhargava, O.N., Parcha, S.K., Pogue, K.R., 2010. Extraordinary transport and mixing of sediment across Himalayan central Gondwana during the Cambrian-Ordovician. Geological Society of America Bulletin 122, 1660-1670.

Myrow, P.M., Hughes, N.C., Paulsen, T.S., Williams, I.S., Parcha, S.K., Thompson, K.R., Bowring, S.A., Peng, S.-C., Ahluwalia, A.D., 2003. Integrated tectonostratigraphic reconstruction of the Himalaya and implications for its tectonic reconstruction. Earth and Planetary Science Letters 212, 433-441.

Myrow, P.M., Hughes, N.C., Searle, M.P., Fanning, C.M., Peng, S.-C., Parcha, S.K., 2009. Stratigraphic correlation of Cambrian-Ordovician deposits along the Himalaya: implications for the age and nature of rocks in the Mt. Everest region. Geological Society of America Bulletin 121, 323-332.

Nagovitsin, K., 2009. *Tappania*-bearing association of the Siberian platform: Biodiversity, stratigraphic position and geochronological constraints. Precambrian Research 173, 137-145.

Pandey, D.K., Bahadur, T., 2009. A review of the stratigraphy of Marwar Supergroup of west-central Rajasthan. Journal of the Geological Society of India 73, 747-758.

Pandit, M.K., Sial, A.N., Jamrani, S.S., Ferreira, V.P., 2001. Carbon isotopic profile across the Bilara Group rocks of trans-Aravalli Marwar Supergroup in western India: Implications for Neoproterozoic-Cambrian transition. Gondwana Research 4, 387-394.

Parrish, R.R., Hodges, K.V., 1996. Isotopic constraints on the age and provenance of the Lesser and Greater Himalayan sequences, Nepalese Himalaya. Geological Society of America Bulletin 108, 904-911.

Pradhan, V.R., Meert, J.G., Pandit, M.K., Kamenov, G., Gregory, L.C., Malone, S.J., 2010. India's changing place in global Proterozoic reconstructions: A review of geochronologic constraints and paleomagnetic poles from the Dharwar, Bundelkhand and Marwar cratons. Journal of Geodynamics 50, 224-242.

Prasad, B., Asher, R., 2001. Acritarch biostratigraphy and lithostratigraphic classification of Proterozoic and lower Paleozoic sediments (Pre-unconformity) of Ganga Basin, India. Geoscience Research Group, Keshava Deva Malaviya Institute of Petroleum Exploration, Oil and Gas Corporation Limited DehraDun 5, 1-153.

Prasad, B., Uniyal, S.N., Asher, R., 2005. Organic-walled microfossils from the Proterozoic Vindhyan Supergroup of Son Valley, Madhya Pradesh, India. Palaeobotanist 54, 13-60.

Raha, P.K., Chandy, K.C., Balasubrahmanyan, M.N., 1978. Geochronlogy of the Jammu Limestone, Udhampur District, Jammu & Kashmir State, India. Journal of the Geological Society of India 18, 221-223.

Raha, P.K., Sastry, M.V.A., 1982. Stromatolites and Precambrian Stratigraphy in India. Precambrian Research 18, 293-318.

Rasmussen, B., Bose, P.K., Sarkar, S., Banerjee, S., Fletcher, I.R., McNaughton, N.J., 2002. 1.6 GaU-Pb zircon age for the Chorhat Sandstone, lower Vindhyan, India: Possible implications for early evolution of animals. Geology 30, 103-106.

Rathore, S.S., Venkatesan, T.R., Srivastava, R.K., 1999. Rb-Sr isotope dating of Neoproterozoic (Malani Group) magmatism from Southwest Rajasthan, India: Evidence of younger Pan-African thermal event by Ar-40-Ar-39 studies. Gondwana Research 2, 271-281.

Ray, J.S., 2006. Age of the Vindhyan Supergroup: A review of recent findings. Journal of Earth Systems Science 115, 149-160.

Ray, J.S., Martin, M.W., Veizer, J., Bowring, S.A., 2002. U-Pb zircon dating and Sr isotope systematics of the Vindhyan Supergroup, India. Geology 30, 131-134.

Ray, J.S., Veizer, J., Davis, W.J., 2003. C, O, Sr and Pb isotope systematics of carbonate sequences of the Vindhyan Supergroup, India: age, diagenesis, correlations and implications for global events. Precambrian Research 121, 103-140.

Richards, A., Argles, T., Harris, N., Parrish, R., Ahmad, T., Darbyshire, F., Draganits, E., 2005. Himalayan architecture constrained by isotopic markers from clastic sediments. Earth and Planetary Science Letters 236, 773-796.

Robinson, D.M., DeCelles, P.G., Patchett, P.J., Garzione, C.N., 2001. The kinematic evolution of the Nepalese Himalaya interpreted from Nd isotopes. Earth and Planetary Science Letters 192, 507-521.

Rupke, J., 1974. Stratigraphic and structural evolution of the Kumaon Lesser Himalaya. Sedimentary Geology 11, 81-256.

Sarangi, S., Gopalan, K., Kumar, S., 2004. Pb-Pb age of earliest megascopic, eukaryotic alga bearing Rohtas Formation, Vindhyan Supergroup, India: implications for Precambrian atmospheric oxygen evolution. Precambrian Research 132, 107-121.

Schoene, B., Dudas, F.O.L., Bowring, S.A., de Wit, M., 2009. Sm-Nd isotopic mapping of lithospheric growth and stabilization in the eastern Kaapvaal craton. Terra Nova 21, 219-228.

Seilacher, A., Bose, P.K., Pflüger, F., 1998. Triploblastic animals more than 1 billion years ago: trace fossil evidence from India. Science 282, 80-83.

Shields, G., Veizer, J., 2002. Precambrian marine carbonate isotope database: Version 1.1. Geochemistry Geophysics Geosystems 3.

Singh, I.B., 1985. Paleogeography of Vindhyan basin and its relationship with other late Proterozoic basins of India. Journal of the Palaeontological Society of India 30, 35-41.

Spencer, C.J., Harris, R.A., Kumar Sachan, H., Saxena, A., 2011. Depositional provenance of the Greater Himalayan Sequence, Garhwal Himalaya, India: Implications for tectonic setting. Journal of Asian Earth Sciences 41, 344-354.

Tewari, V.C., 1989. Upper Proterozoic-Lower Cambrian stromatolites and Indian stratigraphy. Himalayan Geology 13, 143-180.

Tewari, V.C., Sial, A.N., 2007. Neoproterozoic-Early Cambrian isotopic variation and chemostratigraphy of the Lesser Himalaya, India, Eastern Gondwana. Chemical Geology 237, 64-88.

Thakur, V.C., 1992. Geology of Western Himalaya. Pergamon, Oxford.

Tiwari, M., Pant, I., 2009. Microfossils from the Neoproterozoic Gangolihat Formation, Kumaun Lesser Himalaya: Their stratigraphic and evolutionary significance. Journal of Asian Earth Sciences 35, 137-149.

Tobgay, T., Long, S., McQuarrie, N., Ducea, M.N., Gehrels, G., 2010. Using isotopic and chronologic data to fingerprint strata: Challenges and benefits of variable sources to tectonic interpretations, the Paro Formation, Bhutan Himalaya. Tectonics 29, doi:10.1029/2009TC002637

Torsvik, T.H., Carter, L.M., Ashwal, L.D., Bhushan, S.K., Pandit, M.K., Jamtveit, B., 2001. Rodinia refined or obscured: palaeomagnetism of the Malani igneous suite (NW India). Precambrian Research 108, 319-333.

Valdiya, K.S., 1969. Stromatolites of the Lesser Himalayan carbonate formation and the Vindhyans. Journal of the Geological Society of India 10, 1-25.

Valdiya, K.S., 1980. Geology of Kunaun Lesser Himalaya. Wadia Institute of Himalayan Geology, DehraDun.

Valdiya, K.S., 1995. Proterozoic sedimentation and pan-African geodynamic development in the Himalaya. Precambrian Research 74, 35-55.

Webb, A.A.G., Yin, A., Harrison, T.M., Celerier, J., Burgess, W.P., 2007. The leading edge of the Greater Himalayan Crystalline complex revealed in the NW Indian Himalaya: Implications for the evolution of the Himalayan orogen. Geology 35, 955-958.

Webb, A.A.G., Yin, A., Harrison, T.M., Celerier, J., Gehrels, G.E., Manning, C.E., Grove, M., 2011. Cenozoic tectonic history of the Himachal Himalaya (NW India) and its constraints on the formation mechanism of the Himalayan orogen. Geosphere 7, 1013-1061.

Xiao, S., A. H. Knoll, A. J. Kaufman, L. Yin and Y. Zhang, 1997. Neoproterozoic fossils in Mesoproterozoic rocks? Chemostratigraphic resolution of a biostratigraphic conundrum from the North China Platform. Precambrian Research 84, 197-220.

Yin, A., 2006. Cenozoic tectonic evolution of the Himalayan orogen as constrained by along-strike varaition in structural geometry, exhumation history, and foreland sedimentation. Earth Science Reviews 76, 1-131.

Yin, A., Dubey, C.S., Kelty, T.K., Gehrels, G.E., Chou, C.Y., Grove, M., Lovera, O., 2006. Structural evoliution of the Arunachal Himalaya and implications for asymmetric development of the Himalaya orogen. Current Science 90, 195-206.

Yin, A., Dubey, C.S., Kelty, T.K., Webb, A.A.G., Harrison, T.M., Chou, C.Y., Celerier, J., 2010a. Geologic correlation of the Himalayan orogen and Indian craton: Part 2. Structural geology, geochronology, and tectonic evolution of the Eastern Himalaya. Geological Society of America Bulletin 122, 360-395.

Yin, A., Dubey, C.S., Webb, A.A.G., Kelty, T.K., Grove, M., Gehrels, G.E., Burgess, W.P., 2010b. Geologic correlation of the Himalayan orogen and Indian craton: Part 1. Structural geology, U-Pb zircon geochronology, and tectonic evolution of the Shillong Plateau and its neighboring regions in NE India. Geological Society of America Bulletin 122, 336-359.

Yin, L.M., Yuan, X.L., Meng, F.W., Hu, J., 2005. Protists of the Upper Mesoproterozoic Ruyang Group in Shanxi Province, China. Precambrian Research 141, 49-66.

Yoshida, M., Upreti, B.N., 2006. Neoproterozoic India within east Gondwana: constraints from recent geochronological data from Himalaya. Gondwana Research 10, 349-356.

Figures

Figure 1.1. (a) Simplified geological map of northern India. (b) Simplified map of the Tons Valley-Kumaon region of the Lesser Himalaya (modified after Valdiya, [1980]; Celerier et al., [2009a]). Undiff = Undifferentiated.

Figure 1.2. Purported isotopic "signatures" of Himalayan lithotectonic zones. a) Suggested characteristic detrital zircon (DZ) age distributions of the Lesser, Greater, and Tethyan Himalaya (LH, GH, and TH, respectively). b) Comparison of εNd values between GH and undifferentiated LH. c) εNd values from north India with LH differentiated into "inner" and outer zones (iLH and oLH, respectively). d) εNd for iLH, oLH, and GH illustrating similarity between oLH and "GH-type" values.

Figure 1.3. Phosphatic *Baicalia* stromatolites. (a-b) Stromatolites from the Tirohan Dolomite (Rohtas Formation) of the Semri Group, Son Valley Vindhyan succession and (c-f) Stromatolites from the Gangolihat Dolomite, Kumaon section of the "inner" Lesser Himalaya. a) Outcrop of columnar stromatolites with thick black phosphoric crusts. US penny for scale. b) Cut and polished sample of phosphatic stromatolite showing black phosphorite crust and phosphatic intraclasitc grainstone surrounding the column. c) Outcrop of upper stromatolitic bioherm with thick phosphatic crusts. Beds are vertically oriented and picture was taken of upper cliff face without scale. Stromatolites are comparable in size to [e]. d) Polished slab of phosphorite crusted stromatolite. e) Outcrop of stromatolite bioherm stratigraphically below [c]. This section lacks the thick phosphatic crust, but contains similar phosphatic intraclastic grainstone in the intercolumnar space. f) polished slab of stromatolite and phosphatic intraclastic grainstone.

Figure 1.4. Comparison of new and published detrital zircon age distributions of cratonic and Himalayan strata. Distributions are arranged in regional and stratigraphic order, with successions of similar depositional ages placed next to each other for direct comparison. Distributions of Paleoproterozoic and Mesoproterozoic successions of the Vindhyan supergroup are between the "inner" Lesser Himalaya and comparable late Mesoproterozoic distributions from other cratonic regions (i.e., Rajasthan, Aravalli, and Shillong Plateau). The correlative regional unconformity that differentiates the "upper" and "lower" sequences is

indicated by a dashed line. Distributions of Neoproterozoic to Cambrian-aged successions of the Marwar Supergroup are placed next to “outer” Lesser Himalayan distributions. It is important to note the continuous introduction and presence of younger zircon populations while moving up stratigraphically. Shaded reference bars: yellow = 0.9-1.1 Ga and blue = 1.6-1.8 Ga.

Table 1.1. Stratigraphic nomenclature and recent geochronologic constraints.

Table 1.2. Locality information for samples analyzed.

Table 1.3. Epsilon neodymium values.

Table 1.4. Chronostratigraphic correlation of cratonic and Himalayan successions.

Figure 1.1

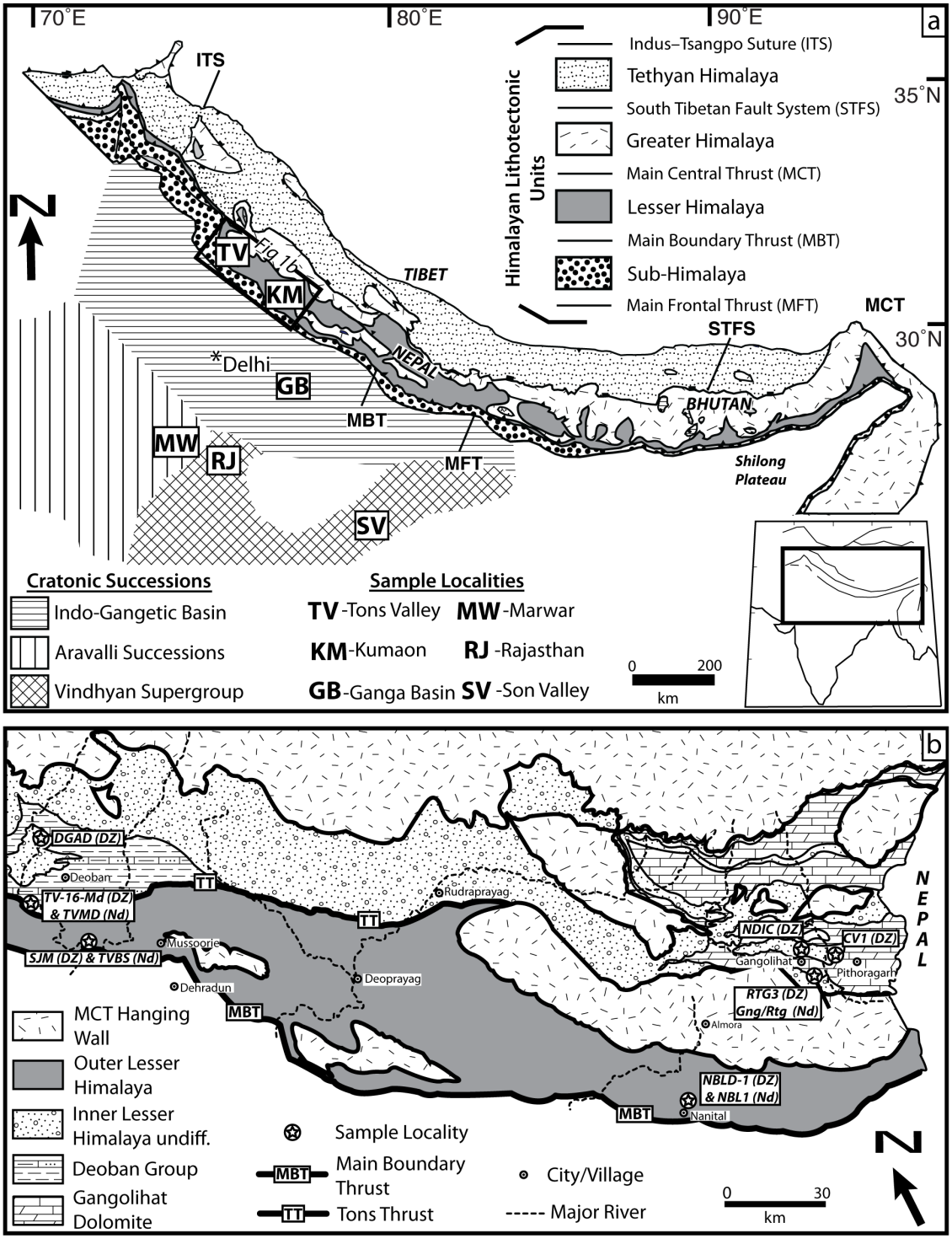
a
70˚E
80˚E
90˚E
35˚N
30˚N
ITS
TV
KM
Fig 1b
TIBET
NEPAL
BHUTAN
Shilong Plateau
*Delhi
GB
MBT
MFT
MW
RJ
SV
STFS
MCT
Himalayan Lithotectonic Units
Indus–Tsangpo Suture (ITS)
Tethyan Himalaya
South Tibetan Fault System (STFS)
Greater Himalaya
Main Central Thrust (MCT)
Lesser Himalaya
Main Boundary Thrust (MBT)
Sub-Himalaya
Main Frontal Thrust (MFT)
Cratonic Successions
Indo-Gangetic Basin
Aravalli Successions
Vindhyan Supergroup
Sample Localities
TV -Tons Valley
MW -Marwar
KM -Kumaon
RJ -Rajasthan
GB -Ganga Basin
SV -Son Valley
0
200
km
b
DGAD (DZ)
Deoban
TT
TV-16-Md (DZ) & TVMD (Nd)
Rudraprayag
SJM (DZ) & TVBS (Nd)
Mussoorie
Dehradun
Deoprayag
MBT
NDIC (DZ)
CV1 (DZ)
Gangolihat
Pithoragarh
RTG3 (DZ) Gng/Rtg (Nd)
Almora
NBLD-1 (DZ) & NBL1 (Nd)
Nanital
NEPAL
MCT Hanging Wall
Outer Lesser Himalaya
Inner Lesser Himalaya undiff.
Deoban Group
Gangolihat Dolomite
Sample Locality
Main Boundary Thrust
Tons Thrust
City/Village
Major River
0
30
km

Figure 1.2

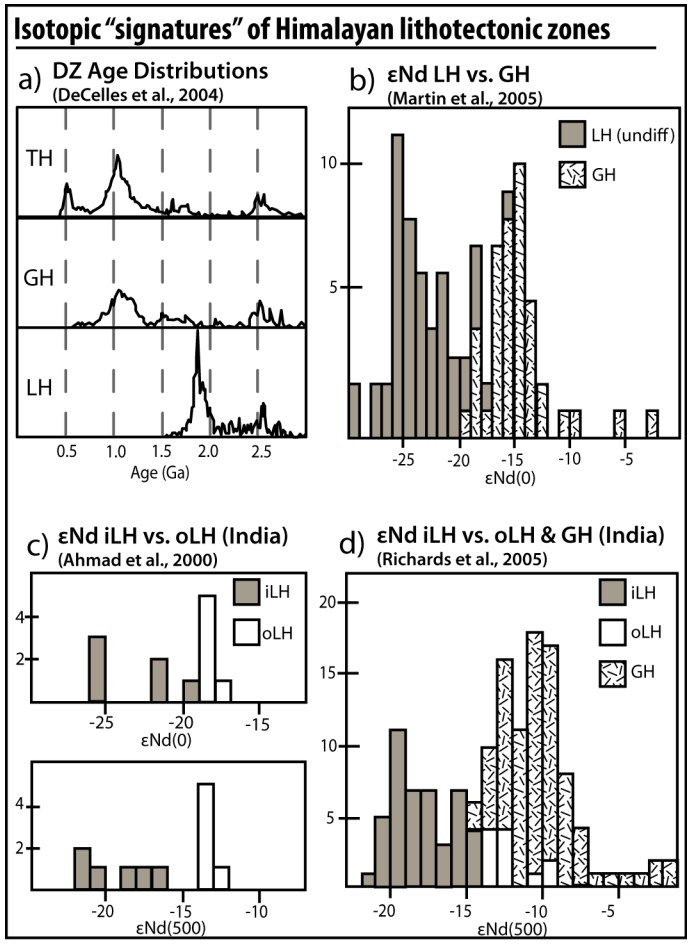
Isotopic "signatures" of Himalayan lithotectonic zones
a) DZ Age Distributions
(DeCelles et al., 2004)
TH
GH
LH
0.5
1.0
1.5
2.0
2.5
Age (Ga)
b) εNd LH vs. GH
(Martin et al., 2005)
LH (undiff)
GH
10
5
-25
-20
-15
-10
-5
εNd(0)
c) εNd iLH vs. oLH (India)
(Ahmad et al., 2000)
iLH
oLH
4
2
-25
-20
-15
εNd(0)
4
2
-20
-15
-10
εNd(500)
d) εNd iLH vs. oLH & GH (India)
(Richards et al., 2005)
iLH
oLH
GH
20
15
10
5
-20
-15
-10
-5
εNd(500)

Figure 1.3

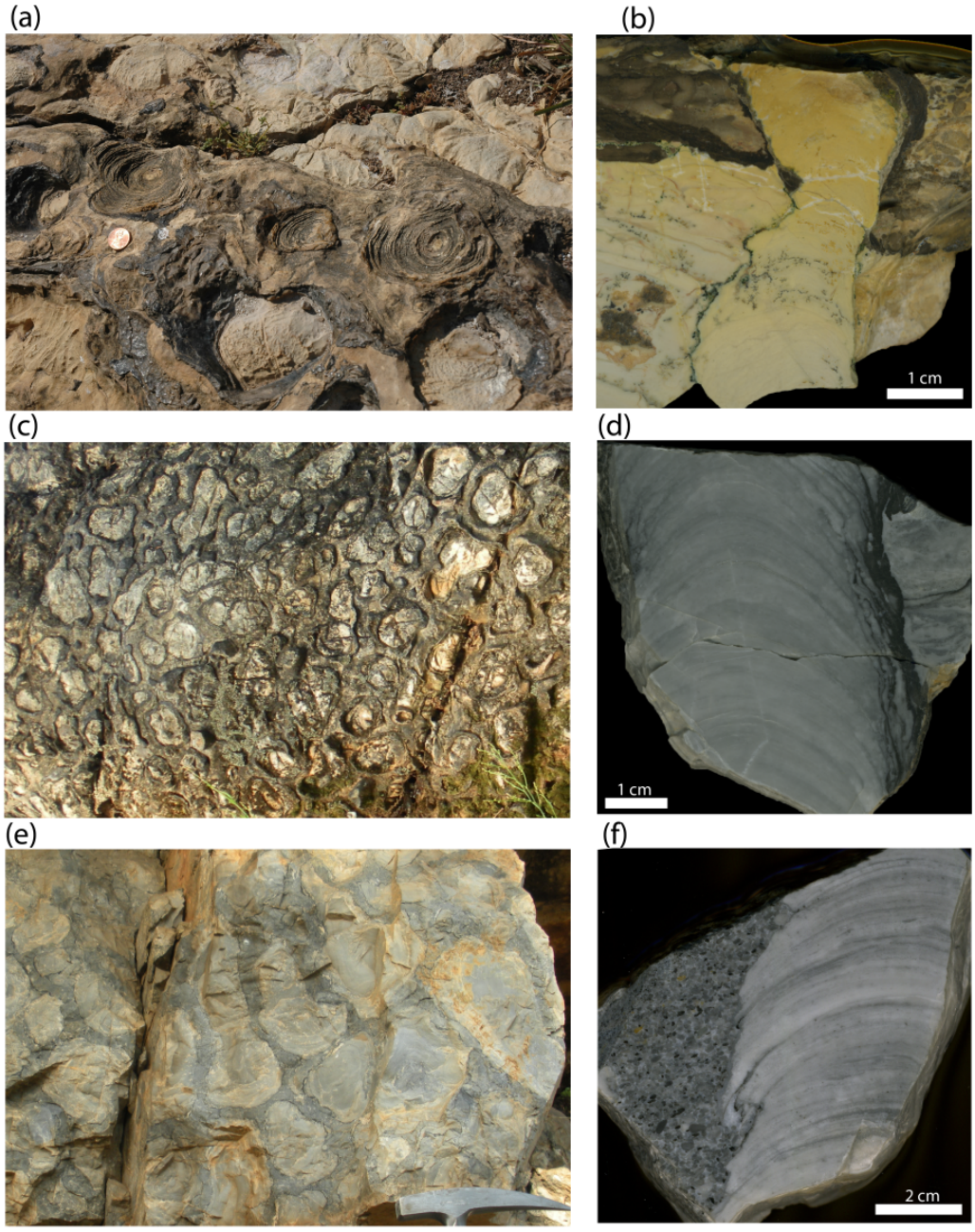

Figure 1.4

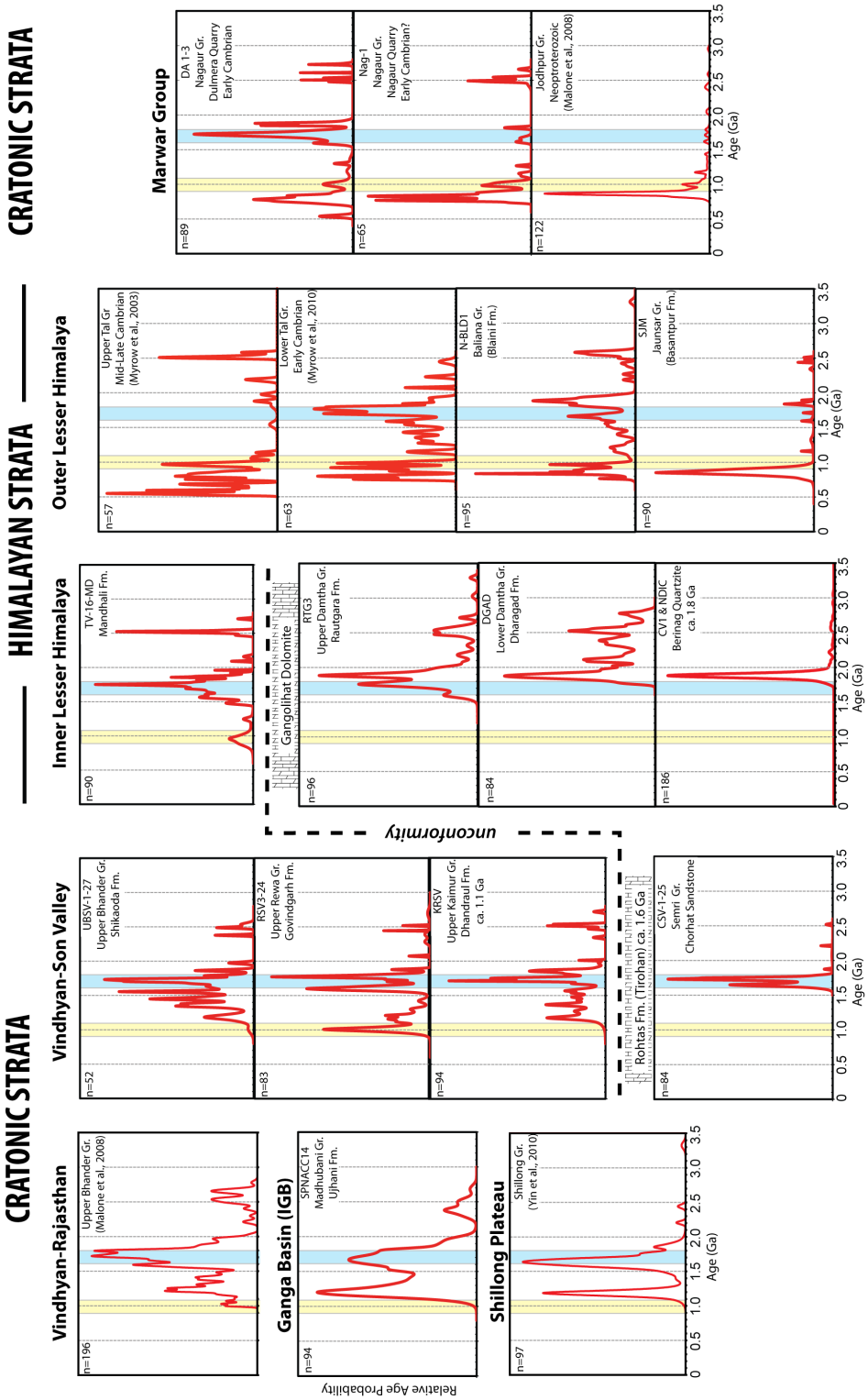
CRATONIC STRATA
HIMALAYAN STRATA
CRATONIC STRATA
Vindhyan-Rajasthan
Upper Bhander Gr. (Malone et al., 2008)
n=196
Ganga Basin (IGB)
SPNACC14
Madhubani Gr.
Ujhani Fm.
n=94
Shillong Plateau
Shillong Gr. (Yin et al., 2010)
n=97
Relative Age Probability
Age (Ga)
Vindhyan-Son Valley
UBSV-1-27
Upper Bhander Gr.
Shikaoda Fm.
n=52
RSV3-24
Upper Rewa Gr.
Govindgarh Fm.
n=83
KRSV
Upper Kaimur Gr.
Dhandraul Fm.
ca. 1.1 Ga
n=94
Rohtas Fm. (Tirohan) ca. 1.6 Ga
CSV-1-25
Semri Gr.
Chorhat Sandstone
n=84
unconformity
Inner Lesser Himalaya
TV-16-MD
Mandhali Fm.
n=90
Gangolihat Dolomite
RTG3
Upper Damtha Gr.
Raurgara Fm.
n=96
DGAD
Lower Damtha Gr.
Dharagad Fm.
n=84
CV1 & NDIC
Berinag Quartzite
ca. 1.8 Ga
n=186
Outer Lesser Himalaya
Upper Tal Gr
Mid-Late Cambrian
(Myrow et al., 2003)
n=57
Lower Tal Gr.
Early Cambrian
(Myrow et al., 2010)
n=63
N-BLD1
Baliana Gr.
(Blaini Fm.)
n=95
SJM
Jaunsar Gr.
(Basantpur Fm.)
n=90
Marwar Group
DA 1-3
Nagaur Gr.
Dulmera Quarry
Early Cambrian
n=89
Nag-1
Nagaur Gr.
Nagaur Quarry
Early Cambrian?
n=65
Jodhpur Gr.
Neoproterozoic
(Malone et al., 2008)
n=122
0 0.5 1.0 1.5 2.0 2.5 3.0 3.5
Age (Ga)

Table 1.1

Table 1. Stratigraphic nomenclature and current age contstraints

	Age constraint	Method	Reference	Data presented here
CRATONIC SUCCESSIONS				
VINDHYAN SUPERGROUP				
Bhander Group				
Shikaoda Sandstone				≤1.0 Ga DZ (LAICPMS)
Bhander Limestone	≥750 Ma	87Sr/86Sr	Ray et al., (2002)	
Bhander (undiff)	≤1.0 Ga	DZ (SHRIMP)	Malone et al., (2008)	
Rewa Group				
Govindgarh Sandstone				≤1.0 Ga DZ (LAICPMS)
Rewa (undiff)				
Kaimur Group				
Dhandraul Quartzite				≤1.1 Ga DZ (LAICPMS)
Kaimur (undiff)	≥1073.5 ± 13 Ma	Ar-Ar kimberlite	Gregory et al., (2006)	
Semri Group				
Rohtas Formation/	1599 ± 48 Ma	Pb-Pb isochron	Sarangi et al., (2004)	
Tirohan Dolomite	1602 ± 11 Ma	Pb-Pb isochron	Bengtson et al., (2009)	
Rampur Fromation	1599 ± 8 Ma	U-Pb zircon (SHRIMP)	Rasmussen et al., (2002)	
Chorhat Sandstone				≤1.6 Ga DZ (LAICPMS)
Deonar/Porcellanite Formation	1630.7 ± 0.4 Ma	U-Pb zircon (TIMS)	Ray et al., (2002)	
Kajrahat Limestone	1721 ± 90 Ma	Pb-Pb errorchron	Sarangi et al., (2004)	
Deoland Formation				
ARAVALLI SUCCESSIONS				
Marwar Supergroup				
Naugar Group	E. Cambrian	Trace fossils	Kumar and Pandey, (2010)	≤540 Ma DZ (LAICPMS)
Bilara Group				
Jodhpur Group	≤850 Ma	DZ (SHRIMP)	Malone et al., (2008)	
Malani Igneous suite	771 ± 5 Ma	U-Pb zircon (SIMS)	Gregory et al., (2009)	
Delhi Supergroup				
Aravalli Supergroup				
GANGA SUPERGROUP				
Madhubani Group				
Karnapur Formation				
Tilhar Formation				
Ujhani Formation				≤1.2 Ga DZ (LAICPMS)
Bahraich Group				
HIMALAYAN SUCCESSIONS				
"outer" LESSER HIMALAYA				
Tal Group	Cambrian	Macrofossils	Hughes et al., (2005)	
Krol Group	Ediacaran	Chemo- & Lithostrat	Kaufman et al., (2006)	
Baliana Group				
Blaini Formation	Cryogenian	Chemo- & Lithostrat	Jiang et al., (2003)	≤770 Ma DZ (LAICPMS)
Jaunsar/Simla Group	≤ 850 Ma	DZ (SHRIMP)	Celerier et al., (2009a)	
Nagthat Formation				
Chandpur Formation				
Basantpur Formation				≤850 Ma DZ (LAICPMS)
"inner" LESSER HIMALAYA				
Deoban Group				
Mandhali Formation				≤950 Ma DZ (LAICPMS)
Deoban Formation				
Gangolihat Dolomite*				
Damtha Group				
Rautgrara Formation				≤1.6 Ga DZ (LAICPMS)
Chakrata/Dharagad Formation				≤1.8 Ga DZ (LAICPMS)
Berinag Group				
Berinag Quartzite				≤1.8 Ga DZ (LAICPMS)
Rampur Formation	1800 ± 13 Ma	Pb-Pb zircon (TIMS)	Miller et al., (2000)	

* Gangolihat Dolomite is here differentiated from the Deoban Fm but not suggested to be stratigraphically below the Deoban Fm.
DZ = Detrital Zircon; LAICPMS = Laser Ablation Inductively Coupled Plasma Mass Spectrometry; SIMS = Secondary Ion Mass Spectrometry;
SHRIMP = Sensitive High Resolution Ion Microprobe; TIMS = Thermal Ion Mass Spectrometry; undiff = undifferentiated

Table 1.2

Sample ID	Locality - unit	Analysis	GPS
	Cratonic Sections		
DA 1-3	MW - Dulmera Quarry - Naguar Gr	DZ	28° 24.351'N; 73° 39.526'E
Nag-1	MW - Nagaur Quarry - Naguar Gr	DZ	27° 12.381'N; 73° 45.262'E
UBSV-1-27	SV - Bhander Gr - Shikaoda SS	DZ	24° 16.905'N; 80° 43.707'E
RSV3-24	SV - Rewa Gr - Govindarh SS	DZ	24° 51.669'N; 82° 08.933'E
KRSV	SV - Kaimur Gr - Dhandrual Fm	DZ	24° 21.161'N; 81° 21.175'E
CSV-1-25	SV - Semri Gr - Chorhat SS	DZ	24° 25.658'N; 81° 40.635'E
SPNACC14	GB- Madhubani Gr - Ujhani Fm	DZ	see Prashad & Asher 2001
	Himalayan Sections		
SJM	TV (oLH) - Jansuar Gr - Basantpur Fm	DZ	30° 32.928'N; 77° 49.118'E
TVBS	TV (oLH) - Jansuar Gr- Basantpur Fm	Nd	30° 32.928'N; 77° 49.118'E
TV-16-MD	TV (iLH) - Deoban Gr - Mandhali Fm	DZ	30° 41.712'N; 77° 45.202'E
TV-MD	TV (iLH) - Deoban Gr - Mandhali Fm	Nd	30° 41.712'N; 77° 45.202'E
DGAD	TV (iLH) - Damtha Gr - Dharagad Fm	DZ	30° 53.159'N; 77° 49.378'E
N-BLD1	KM (oLH) - Baliana Gr - Blaini Fm	DZ	29° 23.339'N; 79° 29.517'E
NBL1	KM (oLH) - Baliana Gr- Blaini Fm	Nd	29° 23.339'N; 79° 29.517'E
NDIC-1	KM (iLH) - Berinag Gr - Berinag Qtz	DZ	29° 39.657'N; 80° 02.394'E
CV-1	KM (iLH) - Berinag Gr - Berinag Qtz	DZ	29° 37.504'N; 80° 10.599'E
RTG3	KM (iLH) - Damtha Gr - Rautgara Fm	DZ	29° 34.610'N; 80° 05.278'E
GNG	KM (iLH) - Gangolihat Dolomite	Nd	29° 34.610'N; 80° 05.278'E

Gr = Group, Fm = Formation, Qtz = Quartzite, SS = Sandstone, DZ = Detrital zircon, Nd = Neodymium

Table 1.3

Sample	143Nd/144Nd (1)	% SE (2)	2-sigma s.e.	147Sm/144Nd	Nd, ppm (3)	Sm, ppm (3)	Epsilon Nd(0)	T, DM (Ma) (4)	Epsilon Nd (500) (5)	143Nd/144Nd at 500 Ma
GNG (iLH)	0.511510	0.0005	0.000006	0.1089±0.0005	36.52 ± 0.09	6.58±0.017	**-22.01**	2234	**-16.41**	0.511153
TV-MD (iLH)	0.511819	0.0008	0.000008	0.1249±0.0005	28.32±0.07	5.85±0.015	**-15.98**	2101	**-11.40**	0.511410
NBL1 (oLH)	0.511816	0.0004	0.000004	0.1148±0.0005	40.31 ± 0.09	7.66±0.019	**-16.04**	1889	**-10.82**	0.511440
TVBS (oLH)	0.511774	0.0008	0.000008	0.1205±0.0005	44.50±0.11	8.87±0.022	**-16.85**	2074	**-12.00**	0.511379

(1) Corrected for fractionation, using 146Nd/144Nd = 0.7219. Measured value of the JNdi-1 standard is 0.512102 ± 0.000009 (2 sigma, N = 25), compared to a recommended value of 0.512115.

(2) Within-run precision of individual analysis.

(3) Nd and Sm concentrations determined by isotope dilution using a 150Nd - 149Sm spike; errors are one sigma.

(4) Calculated using a quadratic model with epsilon(0) = 8.5; uncertainty is approximately 100 Ma.

(5) 143Nd/144Nd (CHUR) at 500 Ma = 0.511994

Table 1.4

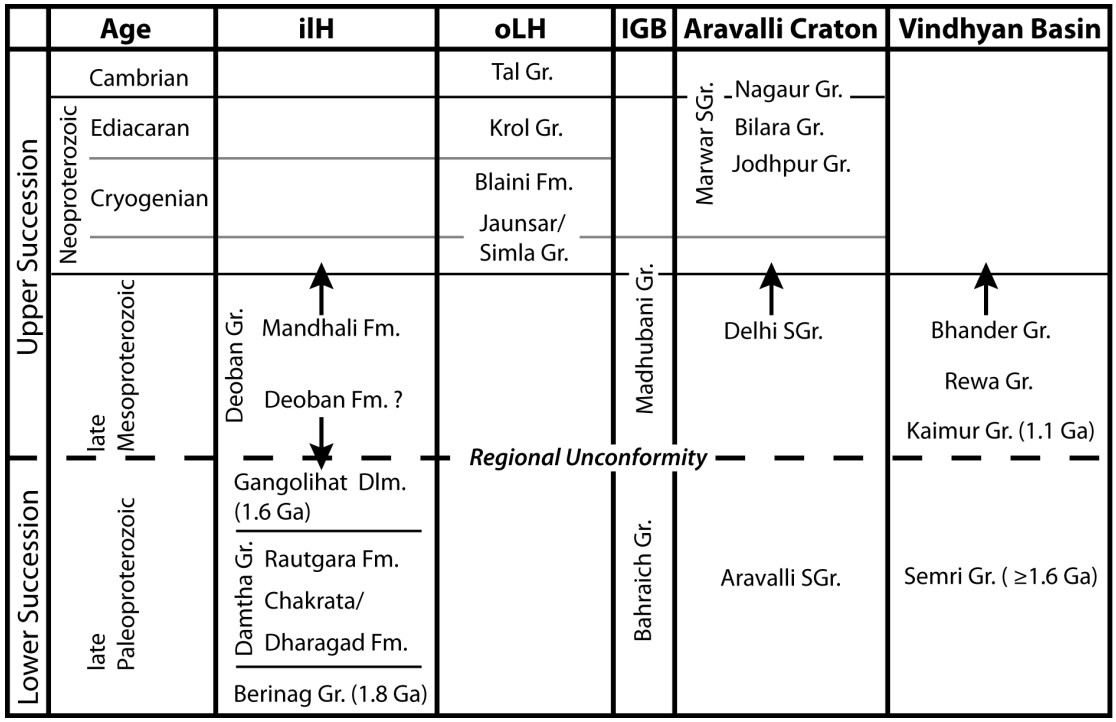
Age
ilH
oLH
IGB
Aravalli Craton
Vindhyan Basin
Upper Succession
Lower Succession
Cambrian
Ediacaran
Cryogenian
Neoproterozoic
late Mesoproterozoic
late Paleoproterozoic
Tal Gr.
Krol Gr.
Blaini Fm.
Jaunsar/ Simla Gr.
Deoban Gr.
Mandhali Fm.
Deoban Fm. ?
Gangolihat Dlm. (1.6 Ga)
Damtha Gr.
Rautgara Fm.
Chakrata/ Dharagad Fm.
Berinag Gr. (1.8 Ga)
Madhubani Gr.
Bahraich Gr.
Marwar SGr.
Nagaur Gr.
Bilara Gr.
Jodhpur Gr.
Delhi SGr.
Aravalli SGr.
Bhander Gr.
Rewa Gr.
Kaimur Gr. (1.1 Ga)
Semri Gr. (≥1.6 Ga)
Regional Unconformity

Supporting Material

SM1.1. Detrital zircon analytical details.

All detrital zircon analyses, except for the Naguar Quarry sample, were conducted at the University Arizona LaserChon Center (see website for additional information https://sites.google.com/a/laserchron.org/laserchron/). Samples were analyzed on multiple visits, the analytical details of which are specified below. All samples were subjected to the same mineral separation methods.

Zircon crystals were extracted from samples by traditional methods of crushing and grinding, followed by separation with a Wilfley table, heavy liquids, and a Frantz magnetic separator. Samples were processed such that all zircons were retained in the final heavy mineral fraction. A large split of these grains (generally 1000-2000 grains) was incorporated into a 1" epoxy mount together with fragments of our Sri Lanka standard zircon. The mounts were sanded down to a depth of ~20 microns, polished, imaged, and cleaned prior to isotopic analysis.

U-Pb geochronology of zircons analyzed from the Berinag, Dharagad, Rautgara, and Blaini samples was conducted by laser ablation multicollector inductively coupled plasma mass spectrometry (LA-MC-ICPMS) at the Arizona LaserChron Center. The analyses involve ablation of zircon with a New Wave/Lambda Physik DUV193 Excimer laser (operating at a wavelength of 193 nm) using a spot diameter of 25-35 microns depending on coarseness of sample. The ablated material is carried in helium into the plasma source of a GVI Isoprobe, which is equipped with a

flight tube of sufficient width that U, Th, and Pb isotopes are measured simultaneously. All measurements are made in static mode, using 10e11 ohm Faraday detectors for 238U, 232Th, 208Pb, and 206Pb, a 10e12 ohm faraday collector for 207Pb, and an ion-counting channel for 204Pb. Ion yields are ~1.0 mv per ppm. Each analysis consists of one 12-second integration on peaks with the laser off (for backgrounds), 12 one-second integrations with the laser firing, and a 30 second delay to purge the previous sample and prepare for the next analysis. The ablation pit is ~12 microns in depth.

For each analysis, the errors in determining 206Pb/ 238U and 206Pb/ 204Pb result in a measurement error of ~1-2% (at 2-sigma level) in the 206Pb/ 238U age. The errors in measurement of 206Pb/ 207Pb and 206Pb/ 204Pb also result in ~1-2% (at 2-sigma level) uncertainty in age for grains that are >1.0 Ga, but are substantially larger for younger grains due to low intensity of the 207Pb signal. For most analyses, the cross-over in precision of 206Pb/ 238U and 206Pb/ 207Pb ages occurs at 0.8-1.0 Ga.

Common Pb correction is accomplished by using the measured 204Pb and assuming an initial Pb composition from Stacey and Kramers (1975) (with uncertainties of 1.0 for 206Pb/ 204Pb and 0.3 for 207Pb/ 204Pb). Our measurement of 204Pb is unaffected by the presence of 204Hg because backgrounds are measured on peaks (thereby subtracting any background 204Hg and 204Pb), and because very little Hg is present in the argon gas.
Inter-element fractionation of Pb/U is generally ~20%, whereas apparent

fractionation of Pb isotopes is generally ~2%. In-run analysis of fragments of a large zircon crystal (generally every fifth measurement) with known age of 564 4 Ma (2-sigma error) is used to correct for this fractionation. The uncertainty resulting from the calibration correction is generally 1-2% (2-sigma) for both 206Pb/ 207Pb and 206Pb/ 238U ages.

The analytical data are reported in Supplementary Datatables. Uncertainties shown in these tables are at the 1- sigma level, and include only measurement errors. Interpreted ages are based on 206Pb/ 238U for <1000 Ma grains and on 206Pb/ 207Pb for >1000 Ma grains. This division at 1000 Ma results from the increasing uncertainty of 206Pb/ 238U ages and the decreasing uncertainty of 206Pb/ 207Pb ages as a function of age. Analyses that are >30% discordant (by comparison of 206Pb/ 238U and 206Pb/ 207Pb ages) or >5% reverse discordant are not considered further.

The resulting interpreted ages are shown on relative age-probability diagrams (from Ludwig, 2003). These diagrams show each age and its uncertainty (for measurement error only) as a normal distribution, and sum all ages from a sample into a single curve.

U-Pb geochronology of zircons from the Mandhali, Jaunsar, Semri, Kaimur, Rewa, Bhander, and Naguar Dulmera Quarry samples was conducted by laser ablation multicollector inductively coupled plasma mass spectrometry (LA-MC-ICPMS) at the Arizona LaserChron Center (Gehrels et al., 2006, 2008). The analyses involve ablation of zircon with a New Wave UP193HE Excimer laser (operating at a

wavelength of 193 nm) using a spot diameter of 25-35 microns depending on coarseness of sample. The ablated material is carried in helium into the plasma source of a Nu HR ICPMS, which is equipped with a flight tube of sufficient width that U, Th, and Pb isotopes are measured simultaneously. All measurements are made in static mode, using Faraday detectors with $3x10^{11}$ ohm resistors for ^{238}U, ^{232}Th, ^{208}Pb-^{206}Pb, and discrete dynode ion counters for ^{204}Pb and ^{202}Hg. Ion yields are ~0.8 mv per ppm. Each analysis consists of one 15-second integration on peaks with the laser off (for backgrounds), 15 one-second integrations with the laser firing, and a 30 second delay to purge the previous sample and prepare for the next analysis. The ablation pit is ~15 microns in depth.

For each analysis, the errors in determining $^{206}Pb/^{238}U$ and $^{206}Pb/^{204}Pb$ result in a measurement error of ~1-2% (at 2-sigma level) in the $^{206}Pb/^{238}U$ age. The errors in measurement of $^{206}Pb/^{207}Pb$ and $^{206}Pb/^{204}Pb$ also result in ~1-2% (at 2-sigma level) uncertainty in age for grains that are >1.0 Ga, but are substantially larger for younger grains due to low intensity of the ^{207}Pb signal. For most analyses, the cross-over in precision of $^{206}Pb/^{238}U$ and $^{206}Pb/^{207}Pb$ ages occurs at ~1.0 Ga. ^{204}Hg interference with ^{204}Pb is accounted for measurement of ^{202}Hg during laser ablation and subtraction of ^{204}Hg according to the natural $^{202}Hg/^{204}Hg$ of 4.35. This Hg is correction is not significant for most analyses because our Hg backgrounds are low (generally ~150 cps at mass 204).

Common Pb correction is accomplished by using the Hg-corrected ^{204}Pb and assuming an initial Pb composition from Stacey and Kramers (1975). Uncertainties

of 1.5 for $^{206}Pb/^{204}Pb$ and 0.3 for $^{207}Pb/^{204}Pb$ are applied to these compositional values based on the variation in Pb isotopic composition in modern crystal rocks.

Inter-element fractionation of Pb/U is generally ~5%, whereas apparent fractionation of Pb isotopes is generally <0.2%. In-run analysis of fragments of a large zircon crystal (generally every fifth measurement) with known age of 563.5 ± 3.2 Ma (2-sigma error) is used to correct for this fractionation. The uncertainty resulting from the calibration correction is generally 1-2% (2-sigma) for both $^{206}Pb/^{207}Pb$ and $^{206}Pb/^{238}U$ ages.

Concentrations of U and Th are calibrated relative to our Sri Lanka zircon, which contains ~518 ppm of U and 68 ppm Th.

The analytical data are reported in datables. Uncertainties shown in these tables are at the 1-sigma level, and include only measurement errors. Analyses that are >20% discordant (by comparison of $^{206}Pb/^{238}U$ and $^{206}Pb/^{207}Pb$ ages) or >5% reverse discordant are not considered further.

The resulting interpreted ages are shown as relative age-probability diagrams using the routines in Isoplot (Ludwig, 2008). The age-probability diagrams show each age and its uncertainty (for measurement error only) as a normal distribution, and sum all ages from a sample into a single curve.

SM1.1 References:

Gehrels, G.E., Valencia, V., Ruiz, J., 2008, Enhanced precision, accuracy, efficiency, and spatial resolution of U-Pb ages by laser ablation–multicollector–inductively coupled plasma–mass spectrometry: Geochemistry, Geophysics, Geosystems, v. 9, Q03017, doi:10.1029/2007GC001805.

Gehrels, G.E., Valencia, V., Pullen, A., 2006, Detrital zircon geochronology by Laser-Ablation Multicollector ICPMS at the Arizona LaserChron Center, in Loszewski, T., and Huff, W., eds., Geochronology: Emerging Opportunities, Paleontology Society Short Course: Paleontology Society Papers, v. 11, 10 p.

Ludwig, K.R., 2003, Isoplot 3.00. Berkeley Geochronology Center, Special Publication No. 4, 70 p.

Ludwig, K.R., 2008, Isoplot 3.60. Berkeley Geochronology Center, Special Publication No. 4, 77 p.

Stacey, J.S., and Kramers, J.D., 1975, Approximation of terrestrial lead isotope evolution by a two-stage model: Earth and Planetary Science Letters, v. 26, p. 207-221.

SM1.2. Detrital zircon data tables are available in online supplementary files.

CHAPTER 2

New detrital zircon age constraints on the Proterozoic Aravalli-Delhi successions of central India and their implications

Abstract

Proterozoic sedimentary successions of India are important archives of the tectonic and sedimentary evolution of the Indian subcontinent, as well as geochemical records that track the evolution of Earth surface system processes. However, the lack of firm age constraints on many of these stratigraphic units limits their current utility. Here we present detrital zircon age data from the Aravalli and Delhi supergroups of the southern Aravalli–Delhi Orogenic Belt (ADOB) that provide significant new depositional age constraints for these units. A sandstone from the Alwar Group of the southern Delhi Supergroup yielded a large population of ~1.2 Ga detrital zircons which refutes the 1.9–1.7 Ga age assertion for this unit. Detrital zircon age distributions from the southern Alwar Group differ strongly from the Alwar Group of the "North Delhi Belt", demonstrating miscorrelation between these two regions. Sandstone from the Jhamarkotra Formation of the Lower Aravalli Group contains a large population of 1.9–1.7 Ga detrital zircons. Therefore, the unit cannot be 2.2–2.0 Ga as traditionally assumed. Age distributions of the Aravalli and Delhi supergroups are similar to those of the lower and upper Vindhyan successions

and we postulate contiguous sediment sources for both regions, with strata of the tectonically deformed ADOB representing the continental margin equivalents of the epicratonic Vindhyan successions. Additionally, a late Paleoproterozoic age for the Jhamarkotra Formation refutes the hypothesis that the markedly positive carbonate $\delta^{13}C$ values in this unit are linked to the 2.2–2.0 Ga Lomugundi positive isotope excursion. The potential for a significant ca. 1.7 Ga positive $\delta^{13}C$ excursion contrasts with the view of a prolonged period of carbonate carbon isotope stasis during the so-called 'boring billion'.

Introduction

The thick Proterozoic sedimentary successions that cover the Indian shield are considered to have been deposited in discrete, isolated basins, which are often referred to as the "Purana (meaning ancient) Basins" (e.g., Holland 1909; Valdiya, 1995). Modern physiographic features or differences in tectonic deformation typically define the boundaries of the "Purana Basins" with basin isolation inferred from their modern relationships. Interbasinal correlation has largely been hindered by a lack of depositional ages constraints on the strata within them. The development of a firm chronostratigraphic framework for these various successions is necessary to further our understanding of the tectonic–sedimentary evolution of the Indian subcontinent. Additionally, they also preserve critical information about Proterozoic evolution of the biosphere (e.g., Bengtson et al., 2009; Papineau 2009,

2010). The Aravalli Supergroup, in particular, contains carbonate rocks with markedly positive carbonate $\delta^{13}C$ values, which have been linked to the mid-Paleoproterozoic Lomagundi carbonate carbon isotope excursion (Sreenivas et al., 2001; Maheshwari et al., 2002, 2010; Purohit et al., 2010). Geochemical data derived from these successions have been used for inferences on biogeochemical cycling following the Great Oxidation Event (GOE) (Papineau et al., 2009, 2010).

In this study we present new U-Pb detrital zircon age data from major stratigraphic units of the southern Aravalli–Delhi supergroups and the Rajasthan Vindhyan successions. The evaluation of detrital zircon age populations provides a maximum depositional age (the rock cannot be older than the youngest zircon) and allows assessment of shared provenance between depositional systems. Furthermore, new age constraints presented here provide a novel view of the significance of carbonate carbon isotope trends from Aravalli strata.

Regional geology and background

The ADOB of western India records major tectonic events during the late Paleoproterozoic (1.9–1.6 Ga) and late Mesoproterozoic–early Neoproterozoic (1.0-0.8 Ga) (Deb et al., 1989, 2001; Buick et al., 2006; Bhowmik et al., 2010). The ADOB is divided into southern and northern "belts" with strata of both the Aravalli and Delhi supergroups recognized in the southern belt, whereas all strata of the northern belt are classified as Delhi Supergroup, thus it is commonly termed the

"North Delhi Belt". The Aravalli Supergroup overlies the ~2.5 Ga Banded Gneiss Complex-I (BGC-I) (Deb et al., 1989; Wiedenbeck et al., 1996; Buick et al. 2006; Pradhan et al., 2010). The Aravalli Supergroup is divided into lower, middle and upper groups. The Lower Aravalli Group consists of the basal Delwara Formation consisting mostly of siliciclastics with interspersed volcanics, and the overlying Jhamarkotra Formation, which is carbonate-dominated with localized phosphorite (Banerjee 1971, Banerjee et al., 1986). The Lower Aravalli Group is weakly constrained between 2.2–1.8 Ga based on a combination of Pb-Pb model ages for galena (Deb and Thorpe, 2004) and the suggested presence of the 2.2–2.0 Ga Lomagundi isotope excursion in the Jhamarkotra Formation (Sreenivas et al., 2001; Maheshwari et al., 2002, 2010; Purohit et al., 2010). The Delhi Supergroup is divided into the lower Alwar and upper Ajabgarh groups with depositional ages traditionally assumed to range between ~1.7–1.5 Ga (Choudhary et al., 1984). However, recent age data for the Delhi Supergroup are conflicting, as the "North Delhi Belt" is constrained to ~1.8–1.7 Ga (Biju-Sekhar et al., 2003; Kaur et al., 2011) and the southern belt is as young as ~1.0 Ga (Deb et al., 2001).

The Great Boundary Fault marks the eastern limits of the ADOB and is the structural boundary with the Vindhyan basin. The Vindhyan basin is regionally divided into the western Rajasthan and eastern Son Valley sections (Fig. 2.1). Vindhyan strata are divided into lower and upper successions by a prominent unconformity, with the lower Vindhyan succession consisting of the Semri Group and the upper Vindhyan succession consisting of the Kaimur, Rewa, and Bhander

groups, in ascending order. The upper part of the Semri Group is well dated at ~1.6 Ga (Ray et al., 2006; Bengtson et al., 2009), and strata of the upper Vindhyan succession are constrained between ~1.2–1.0 Ga (McKenzie et al., 2011).

New age constraints, controversies, and correlation for strata of the ADOB

U-Pb dating of detrital zircons has proven useful for establishing age constraints on siliciclastic strata and resolving correlation issues across the Indian craton (e.g., Malone et al., 2008; McKenzie et al., 2011). In this study, new detrital zircon U-Pb age data were generated from siliciclastic rocks of the Aravalli and Delhi supergroups of the southern ADOB and Vindhyan successions of Rajasthan by means of LA-ICP-MS at the University of Arizona LaserChron Center (data tables available as online supplements). Sandstone samples analyzed from the Aravalli Supergroup include the basal Delwara Formation (RA10), the "Jhamarkotra Sandstone" (RA5), and the Middle Aravalli Group (RA11). A Delhi Supergroup sample was analyzed from the Alwar Group (RD4). Vindhyan samples collected near Chittorgarh include the Semri (RSV1) and Kaimur groups (RVK1). Unfortunately, samples collected from the Upper Aravalli Group and the Ajabgarh Group of the upper Delhi Supergroup did not yield zircon.

The basal Delwara Formation sample contains a range of Archean zircons with only a single zircon younger than ~2.5 Ga, which yielded a $^{206}Pb/^{207}Pb$ age of 1709.3 ± 7.5 Ma that is similar to ages from other Aravalli Group samples (discussed

below). The Delwara sample was collected <10 meters above the depositional contact with the BGC-I basement and the near absence of ~1.7 Ga grains might result from dilution of locally derived detritus. The possibility that this singe grain resulted from contamination during sample processing must also be considered. Therefore, the single ~1.7 Ga grain is problematic and only provides a speculative age constraint for the Delwara Formation.

The Jhamarkotra Sandstone sample contains a large population of 1.9–1.7 Ga detrital zircons, yielding a ~1772 Ma age peak, and the Middle Aravalli Group sample contains a broad population of 1.8–1.6 Ga detrital zircons with abundant ~2.5 Ga grains (Fig. 2.2). These population ages nullify assertions of 2.2–2.0 Ga depositional ages for the Aravalli Supergroup, or at least the Jhamarkotra Formation and all overlying strata. The Aravalli region experienced significant magmatic activity between 1.9–1.7 Ga (Deb et al., 2002; Biju-Sekhar et al., 2003; Buick et al., 2006; Kaur et al., 2007, 2009) with Andean-type subduction postulated (Kaur et al., 2009), and the abundance of 1.9–1.7 Ga zircons in the Jhamarkotra Formation may result from deposition along the tectonically active margin (c.f., Cawood et al., 2012). As the Jhamarkotra sample lacks younger ~1.6 Ga zircons present in younger strata of the ADOB and other Indian cratonic successions (Fig. 2.2), the Jhamarkotra Formation is interpreted to have a depositional age close to the youngest ~1.7 Ga zircons. Furthermore, the prevalence of ~2.5 Ga zircons in the Middle Aravalli Group adds support to the possibility of dilution from BGC-I in the Delwara Formation. It is noteworthy that detrital zircons between 2.5–1.8 Ga are uncommon

in all cratonic sedimentary successions (Fig. 2.2). Therefore, rocks deposited between 2.5–1.8 Ga will be difficult to constrain with detrital zircon age dating.

The Jhamarkotra sample was collected stratigraphically below the phosphatic carbonate in the Jhamarkotra mine, which cannot be older than ~1.7 Ga. This brings into question claims that $\delta^{13}C$ enrichments in the Jhamarkotra Formation ($\delta^{13}C$ up to +11‰) are related to the Lomagundi event (Sreenivas et al., 2001; Maheshwari et al., 2002, 2010; Purohit et al., 2010), which took place between 2.22 and 2.06 Ga (Melezik et al., 2007). The positive values in the Jhamarkotra Formation are likely to record a primary marine signal given that they are reportedly found in a pure, organic-lean carbonate succession (rather than a carbonate-cemented siliciclastic unit) throughout relatively thick stratigraphic intervals (>55 m, $\delta^{13}C$ > +7‰)(Maheshwari et al., 2002, 2010). Typical methanic-zone $\delta^{13}C$ enrichment in carbonates constitutes a relatively minor aspect of sedimentary successions (Irwin et al., 1977). Although the Jhamarkotra Formation has been metamorphosed to greenschist facies (Papineau et al., 2009), it is difficult to imagine a metamorphic origin of the anomalously high positive carbonate $\delta^{13}C$ values. Therefore, based on standing correlation of the Jhamarkotra Formation within the ADOB and our new age constraints, it is possible that the Jhamarkotra Formation hosts a previously unidentified late Paleoproterozoic positive $\delta^{13}C$ excursion (Fig 2.3).

The prevailing view is that the mid-Precambrian (1.8 to 0.8 Ga) was characterized by carbonate isotope stasis, which has given rise to the moniker the 'boring billon'. The potential implications of a billion years of carbon isotope stasis

have been far reaching. For example, this framework has shaped models of eukaryotic diversification (e.g. Anbar and Knoll, 2002), as well as played a central role in models of environmental change and carbon isotope chemistry bracketing the Proterozoic (e.g., Swanson Hysell et al., 2010; Bekker and Holland, 2012). If both the age and primary nature of this isotope excursion are corroborated, and it does reflect global-scale marine processes, the presence of a significant late Paleoproterozoic positive carbon isotope excursion would affect views of the evolution of the carbon cycle during the Precambrian. Additionally, the ~1.7 Ga maximum depositional age for the Jhamarkotra Formation both nullifies the relevance of the unit to the suggested ~2.0 Ga global phosphogenic event and diminishes the significance of data derived from the unit to the 2.4–2.3 Ga Great Oxidation Event (GOE) (Papineau et al., 2009, 2010).

A sample from the so-called Alwar Group of the southern Delhi Supergroup possesses a large population of ~1.2 Ga detrital zircons. Therefore, the southern Delhi Supergroup cannot be 1.9–1.7 Ga as previously asserted. This ~1.2 Ga depositional age together with reports of 987 ± 6.4 and 986 ± 2.4 Ma rhyolites associated with the uppermost part of the Delhi Supergroup (Deb et al., 2001) brackets the depositional ages of the Delhi Supergroup between 1.2–1.0 Ga. The age distribution from the southern sample differs from published age data from the Alwar Group of the North Delhi Belt (Kaur et al., 2011) as the northern sample contains a large population of ~1.7 Ga zircons with nothing younger (Fig. 2.4). A potential age discrepancy between the northern and southern Delhi groups has

been previously recognized (Biju-Sekhar et al., 2003), although this discrepancy was attributed to differences in tectonic history of each "basin". Based on data presented here, we suggest that the discrepancy results from a longstanding miscorrelation of strata between the two regions. The northern Alwar Group age distribution is similar to the Jhamarkotra Sandstone. Therefore, strata of the so-called "North Delhi Belt" likely represent the northern equivalents of the Aravalli Supergroup.

Forty-eight of the fifty zircons analyzed from the Semri Group sample yielded $^{206}Pb/^{207}Pb$ ages between 2514.5 ± 3.6 and 2588.2 ± 40.9 Ma and the two other grains yielded ages of 1877.4 ± 7.2 and 1885 ± 17.2 Ma. This sample was acquired from coarse-grained feldspathic sandstone and the abundance of ~2.5 Ga zircons likely results from derivation of detritus almost exclusively from a proximal ~2.5 felsic igneous source. The two ~1.8 Ga grains are close in age to the 1854 ± 7 Ma volcanic Hindoli rocks located ~150 km northeast of the Semri Group locality (Deb et al., 2002). The Semri Group age distribution from Rajasthan is substantially different from a Semri Group age distribution from the Son Valley (Fig. 2.2) and correlation between these regions is not possible based on data presented here. Kaimur Group sandstone contains large populations of ~1.2 Ga and ~1.6 Ga zircons. This is similar to a published age distribution from the Son Valley Kaimur Group, as are age distributions from both the Rajasthan and Son Valley Bhander groups (McKenzie et al., 2011). Together, these similarities support correlation of upper Vindhyan successions between Rajasthan and Son Valley sections.

While the concentration of grains within each distribution is variable, the Kaimur Group distributions are similar to the age distribution of the southern Delhi Group. McKenzie et al. (2011) suggested correlation between the Aravalli Supergroup and coeval ~1.6 Ga Himalayan and Vindhyan successions based partially on the presence of phosphatic stromatolites in all regions. However, differences observed in the Jhamarkotra phosphorites from the Himalayan–Vindhyan deposits weaken direct correlation between the phosphatic horizons (see Supporting Material SM2.1 for discussion). Nonetheless, strata of the ADOB have similar age-relationships to lower and upper Vindhyan successions and we suggest that the Aravalli–Delhi supergroups represent the tectonically deformed equivalents of the Vindhyan successions with the Aravalli–Delhi supergroups separated by the same ~500 million year unconformity present in Vindhyan successions (Fig. 2.2). The similarity of detrital zircon age distributions in the Vindhyan successions and strata of the ADOB likely result from shared sediment sources, and thus these strata were likely deposited as part of contiguous margin with Vindhyan strata deposited in epicontinental settings and the Aravalli deposited along the continental margin, rather than in discrete isolated basins.

Conclusions

1) The Aravalli Supergroup is constrained to be late Paleoproterozoic in age. The Jhamarkotra Formation has a maximum depositional age of ~1.7 Ga, therefore the

positive carbonate $\delta^{13}C$ values in this unit are not linked to the 2.2-2.0 Ga Lomugundi event. These revised ages present the possibility of an unrecognized late Paleoproterozoic positive $\delta^{13}C$ excursion that may call into question the idea of mid-Precambrian carbon isotope stasis.

2) The Delhi Supergroup has a depositional age of 1.2–1.0 Ga. The Delhi Supergroup of the southern ADOB is not correlative with the supposed Delhi Supergroup of the North Delhi Belt. Strata of the northern belt are likely correlative with the Aravalli Supergroup.

3) Age relationships of the Aravalli–Delhi supergroups reflect those of the lower–upper Vindhyan successions and similar age distributions of detrital zircons from all regions are used to suggest that these strata were deposited across a contiguous margin, with Vindhyan strata representing epicontinental deposits and strata of the ADOB representing the continental margin equivalents.

Acknowledgements

I thank N. Hughes, P. Myrow, D. Banerjee, M. Deb, and N. Planavsky for assitance in the planning and execution of this project, and helpful discussions throughout. I thank Dr. N.K. Chauhan for local support in Udaipur, G. Gehrels, M. Pecha, and N. Giesler for analytical assistance at the Arizona LaserChron Center, J.S. Lackey for

providing facilities and assistance for sample processing, and C. Lee for analytical assistance. This work was supported by National Science Foundation grants EAR-1124303 to N. Hughes and EAR-1124518 to P. Myrow. The Arizona LaserChron Center is supported by NSF-EAR0732436.

References

Anbar, A.D., Knoll, A.H., 2002. Proterozoic ocean chemistry and evolution: A bioinorganic bridge? Science 297, 1137-1142.

Banerjee, D.M., 1971. Precambrian Stromatolitic Phosphorites of Udaipur, Rajasthan, India. Geological Society of America Bulletin 82, 2319-&.

Banerjee, D.M., Schidlowski, M., Arneth, J.D., 1986. Genesis of upper Proterozoic-Cambrian phosphorite deposits of India: isotopic inferences from carbonate fluorapatite, carbonate and organic carbon. Precambrian Research 33, 239-253.

Bekker, A., Holland, H.D., 2012. Oxygen overshoot and recovery during the early Paleoproterozoic. Earth and Planetary Science Letters 317, 295-304.

Bekker, A., Holland, H.D., Wang, P.L., Rumble, D., Stein, H.J., Hannah, J.L., Coetzee, L.L., Beukes, N.J., 2004. Dating the rise of atmospheric oxygen. Nature 427, 117-120.

Bengtson, S., Belivanova, V., Rasmussen, B., Whitehouse, M., 2009. The controversial "Cambrian" fossils of the Vindhyan are real but more than a billion years older. Proceedings of the National Academy of Sciences 106, 7729-7734.

Bhowmik, S.K., Bernhardt, H.-J., Dasgupta, S., 2010. Grenvillian age high-pressure upper amphibolite-granulite metamorphism in the Aravalli-Delhi Mobile Belt, Northwestern India: New evidence from monazite chemical age and its implication. Precambrian Research 178, 168-184.

Biju-Sekhar, S., Yokoyama, K., Pandit, M.K., Okudaira, T., Yoshida, M., Santosh, M., 2003. Late Paleoproterozoic magmatism in Delhi Fold Belt, NW India and its implication: evidence from EPMA chemical ages of zircons. Journal of Asian Earth Sciences 22, 189-207.

Buick, I.S., Allen, C., Pandit, M., Rubatto, D., Hermann, J., 2006. The Proterozoic magmatic and metamorphic history of the Banded Gneiss Complex, central Rajasthan, India: LA-ICP-

MS U–Pb zircon constraints. Precambrian Research 151, 119-142.

Cawood, P.A., Hawkesworth, C.J., Dhuime, B., 2012. Detrital zircon record and tectonic setting. Geology 40, 875-878.

Choudhary, A.K., Gopalan, K., Sastry, C.A., 1984. Present status of the geochronology of the Precambrian rocks of Rajasthan. Tectonophysics 105, 131-140.

Deb, M., Sarkar, S.C., 1990. Proterozoic Tectonic Evolution and Metallogenesis in the Aravalli Delhi Orogenic Complex, Northwestern India. Precambrian Research 46, 115-137.

Deb, M., Thorpe, R., Krstic, D., 2002. Hindoli group of rocks in the eastern fringe of the Aravalli-Delhi orogenic belt-Archean secondary greenstone belt or Proterozoic supracrustals? Gondwana Research 5, 879-883.

Deb, M., Thorpe, R.I., 2004. Geochronological Constraints in the Precambrian Geology of Rajasthan and their Metallogenic Implications, in: Deb, M., Goodfellow, W.D. (Eds.), Sediment-hosted Lead-Zinc Sulphide Deposits. Narosa Publishing House, New Delhi, pp. 246-263.

Deb, M., Thorpe, R.I., Cumming, G.L., Wagner, P.A., 1989. Age, Source and Stratigraphic Implications of Pb Isotope Data for Conformable, Sediment-Hosted, Base-Metal Deposits in the Proterozoic Aravalli-Delhi Orogenic Belt, Northwestern India. Precambrian Research 43, 1-22.

Deb, M., Thorpe, R.I., Krstic, D., Corfu, F., Davis, D.W., 2001. Zircon U-Pb and galena Pb isotope evidence for an approximate 1.0 Ga terrane constituting the western margin of the Aravalli-Delhi orogenic belt, northwestern India. Precambrian Research 108, 195-213.
Irwin, H., Curtis, C., Coleman, M., 1977. Isotopic Evidence for Source of Diagenetic Carbonates Formed during Burial of Organic-Rich Sediments. Nature 269, 209-213.

Holland, T.H., 1909. Classification of the Indian Strata. Transactions, Mining, Geological and Metallurgical Institute of India, (Imperial Gazetteer of India) 1, 50-103.

Kaur, P., Chaudhri, N., Raczek, I., Kroner, A., Hofmann, A.W., 2007. Geochemistry, zircon ages and whole-rock Nd isotopic systematics for Palaeoproterozoic A-type granitoids in the northern part of the Delhi belt, Rajasthan, NW India: implications for late Palaeoproterozoic crustal evolution of the Aravalli craton. Geological Magazine 144, 361-378.

Kaur, P., Chaudhri, N., Raczek, I., Kroner, A., Hofmann, A.W., 2009. Record of 1.82 Ga Andean-type continental arc magmatism in NE Rajasthan, India: Insights from zircon and Sm-Nd ages, combined with Nd-Sr isotope geochemistry. Gondwana Research 16, 56-71.

Kaur, P., Zeh, A., Chaudri, N., Gerdes, A., Okrusch, M., 2011. Archaean to Palaeoproterozoic crustal evolution of the Aravalli mountain range, NW India, and its hinterland: The U–Pb and Hf isotope record of detrital zircon. Precambrian Research 187, 155-164.

Maheshwari, A., Sial, A.N., Chittora, V.K., Bhu, H., 2002. A positive delta C-13 carb anomaly in Paleoproterozoic carbonates of the Aravalli Craton, Western India: support for a global isotopic excursion. Journal of Asian Earth Sciences 21, 59-67.

Maheshwari, A., Sial, A.N., Gaucher, C., Bossi, J., Bekker, A., Ferreira, V.P., Romano, A.W., 2010. Global nature of the Paleoproterozoic Lomagundi carbon isotope excursion A review of occurrences in Brazil, India, and Uruguay. Precambrian Research 182, 274-299.

Malone, S.J., Meert, J.G., Banerjee, D.M., Pandit, M.K., Tamrat, E., Kamenov, G.D., Pradhan, V.R., Sohl, L.E., 2008. Paleomagnetism and detrital zircon geochronology of the upper Vindhyan sequence, Son Valley and Rajasthan, India: A ca. 1000Ma closure age for the Purana basins? Precambrian Research 164, 137-159.

McKenzie, N.R., N.C., H., Myrow, P.M., Sharma, M., 2011. Correlation of Precambrian–Cambrian sedimentary successions across northern India and the utility of isotopic signatures of Himalayan lithotectonic zones. Earth and Planetary Science Letters 312, 471-483.

Melezhik, V.A., Huhma, H., Condon, D.J., Fallick, A.E., Whitehouse, M.J., 2007. Temporal constraints on the Paleoproterozoic Lomagundi-Jatuli carbon isotopic event. Geology 35, 655-658.

Papineau, D., 2010. Global biogeochemical changes at both ends of the Proterozoic: Insights from phosphorites. Astrobiology 10, 165-181.

Papineau, D., Purohit, R., Goldberg, T., Pi, D., Shields, G.A., Bhu, H., Steele, A., Fogel, M.L., 2009. High primary productivity and nitrogen cycling after the Paleoproterozoic phosphogenic event in the Aravalli Supergroup, India. Precambrian Research 171, 37-56.

Pradhan, V.R., Meert, J.G., Pandit, M.K., Kamenov, G., Gregory, L.C., Malone, S.J., 2010. India's changing place in global Proterozoic reconstructions: A review of geochronologic constraints and paleomagnetic poles from the Dharwar, Bundelkhand and Marwar cratons. Journal of Geodynamics 50, 224-242.

Sreenivas, B., Das Sharma, S., Kumar, B., Patil, D.J., Roy, A.B., Srinivasan, R., 2001. Positive d13C excursion in carbonate and organic fractions from the Paleoproterozoic Aravalli Supergroup, Northwestern India. Precambrian Research 106, 277-290.

Swanson-Hysell, N.L., Rose, C.V., Calmet, C.C., Halverson, G.P., Hurtgen, M.T., Maloof, A.C., 2010. Cryogenian Glaciation and the Onset of Carbon-Isotope Decoupling. Science 328, 608-611.

Valdiya, K.S., 1995. Proterozoic sedimentation and Pan-African geodynamic development in the Himalaya. Precambrian Research 74, 35-55.

Wiedenbeck, M., Goswami, J.N., Roy, A.B., 1996. Stabilization of the Aravalli Craton of northwestern India at 2.5 Ga: An ion microprobe zircon study. Chemical Geology 129, 325-340.

Figures

Figure 2.1. Simplified Geologic map of Vindhyan and Aravalli Successions (modified after Buick et al., 2006; Malone et al., 2008) with small-scale location map insert (ADOB = Aravalli-Delhi Orogenic Belt; RV = Rajasthan Vindhyan; SV = Son Valley Vindhyan). Published data: NAQ = Northern Alwar Quartzite (Kaur et al., 2011); RVB = Rajasthan Vindhyan Bhander Group (Malone et al., 2008); SVS, SVK, SVR, and SVB = Son Valley Semri, Kaimur, Rewa, and Bhander groups, respectively (McKenzie et al., 2011). GPS coordinates for sample localities: RSV1 = 24° 50.513'N, 74° 35.458'E; RSK1 = 24° 53.750'N, 74° 38.586'E; RA05 = 24° 27.492'N, 73° 52.372'E; RA10 = 24° 49.971'N, 73° 46.029'E; RA11 = 24° 36.002'N, 73° 40.688'E; RD4 = 24° 45.173'N, 73° 21.510'E.

Figure 2.2. Detrital zircon age distributions and suggested correlation of strata from the southern Aravalli-Delhi Orogenic Belt the Vindhyan successions.

Figure 2.3. A generalized carbonate carbon isotope curve through time (upper) and a revised curve assuming a ~1.7 Ga rather than a ~2.1 Ga for the Jhamarkotra Formation based on a new maximum age constraints presented here (lower).

Figure 2.4. Comparison of detrital zircon age distributions from the so-called Alwar Group from the northern and southern ADOB.

Figure 2.1

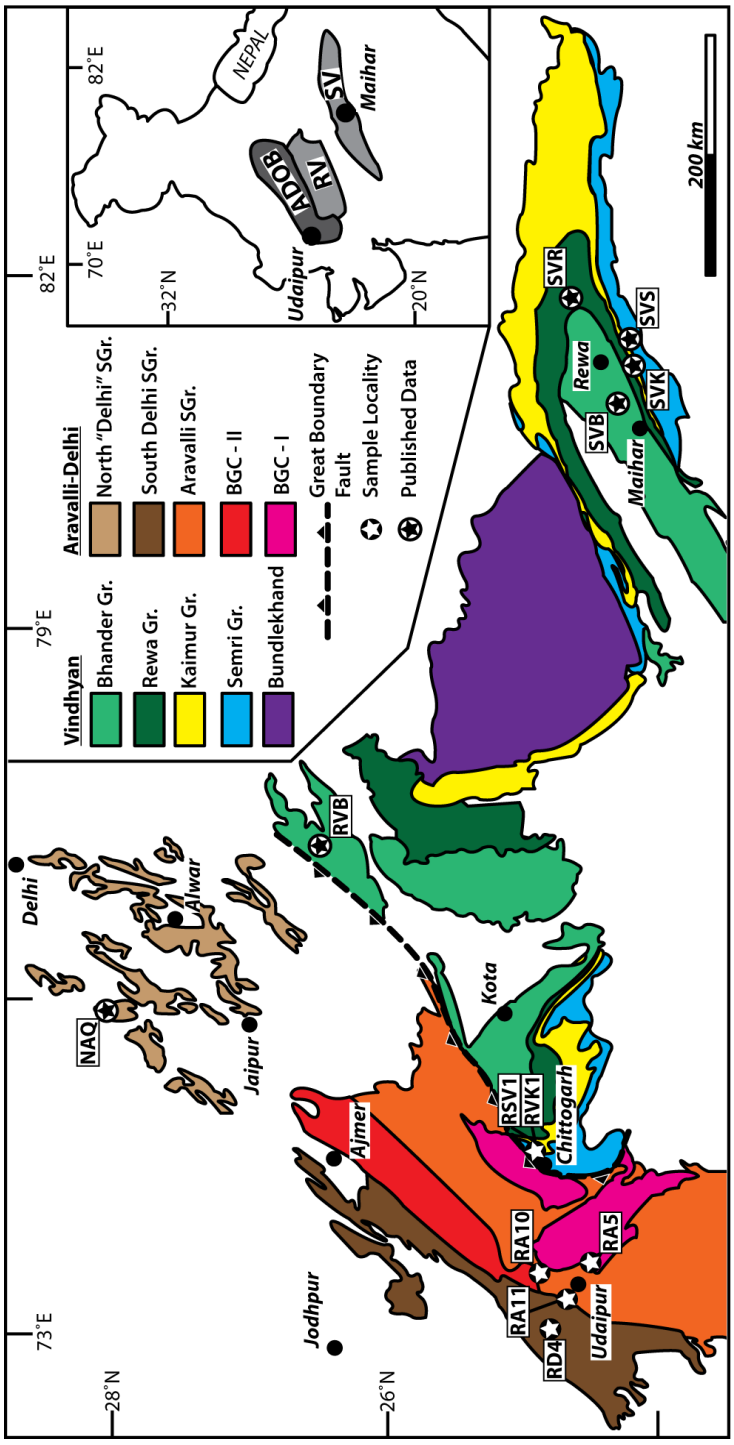
Vindhyan
Bhander Gr.
Rewa Gr.
Kaimur Gr.
Semri Gr.
Bundlekhand
Aravalli-Delhi
North "Delhi" SGr.
South Delhi SGr.
Aravalli SGr.
BGC - II
BGC - I
Great Boundary Fault
Sample Locality
Published Data
NEPAL
ADOB
RV
SV
Maihar
Udaipur
70°E
82°E
32°N
20°N
Delhi
Alwar
Jaipur
NAQ
RVB
Kota
Ajmer
Jodhpur
RSV1
RVK1
Chittogarh
RA10
RA5
RA11
RD4
Udaipur
SVR
Rewa
SVB
SVK
SVS
Maihar
73°E
79°E
82°E
28°N
26°N
200 km

Figure 2.2

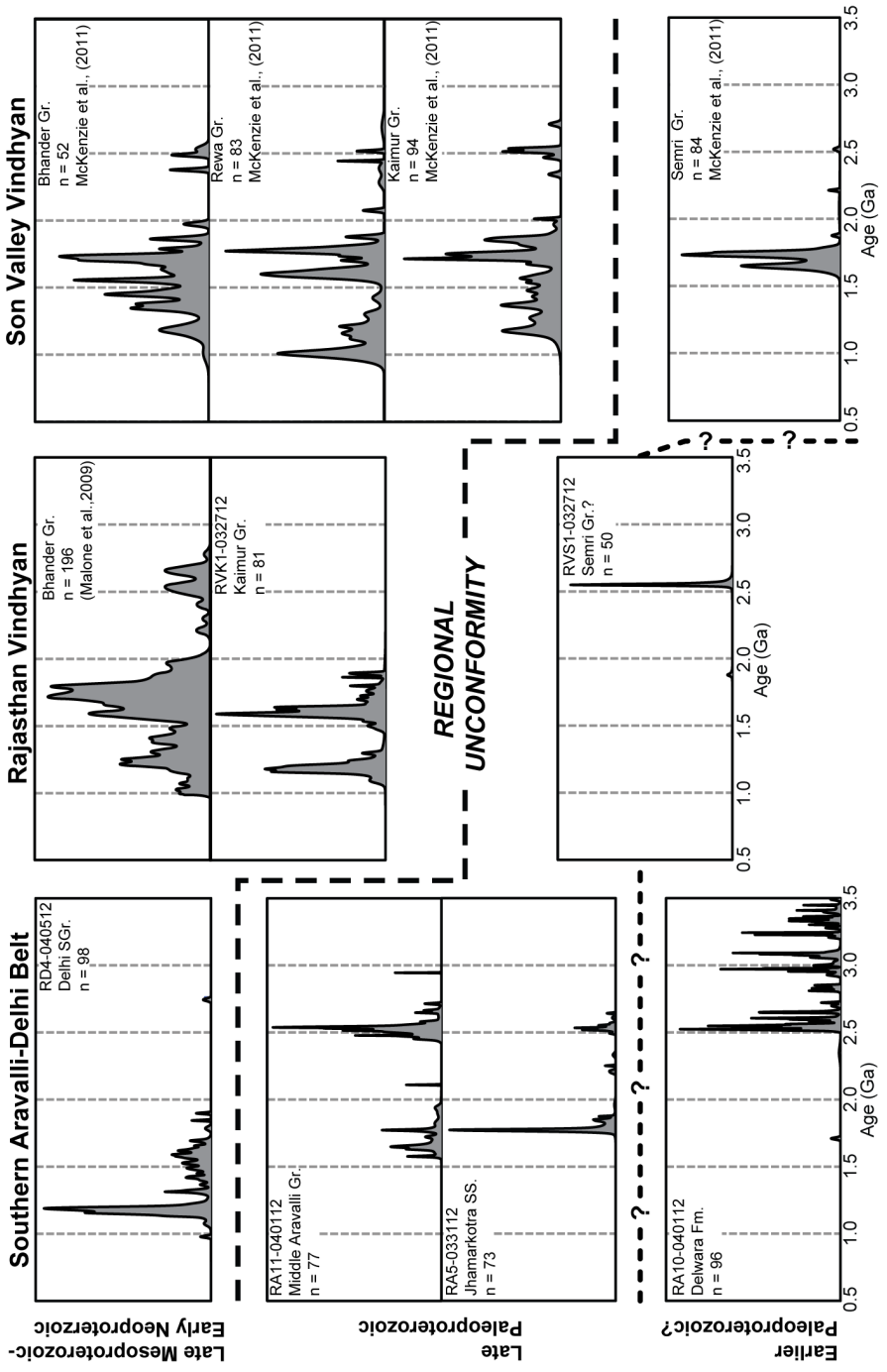
Southern Aravalli-Delhi Belt
Rajasthan Vindhyan
Son Valley Vindhyan
REGIONAL UNCONFORMITY
Late Mesoproterozoic-Early Neoproterozoic
Late Paleoproterozoic
Earlier Paleoproterozoic?
RD4-040512
Delhi SGr.
n = 98
Bhander Gr.
n = 196
(Malone et al.,2009)
RVK1-032712
Kaimur Gr.
n = 81
Bhander Gr.
n = 52
McKenzie et al., (2011)
Rewa Gr.
n = 83
McKenzie et al., (2011)
Kaimur Gr.
n = 94
McKenzie et al., (2011)
RA11-040112
Middle Aravalli Gr.
n = 77
RA5-033112
Jhamarkotra SS.
n = 73
RVS1-032712
Semri Gr.?
n = 50
Semri Gr.
n = 84
McKenzie et al., (2011)
RA10-040112
Delwara Fm.
n = 96
0.5
1.0
1.5
2.0
2.5
3.0
3.5
Age (Ga)
?

Figure 2.3

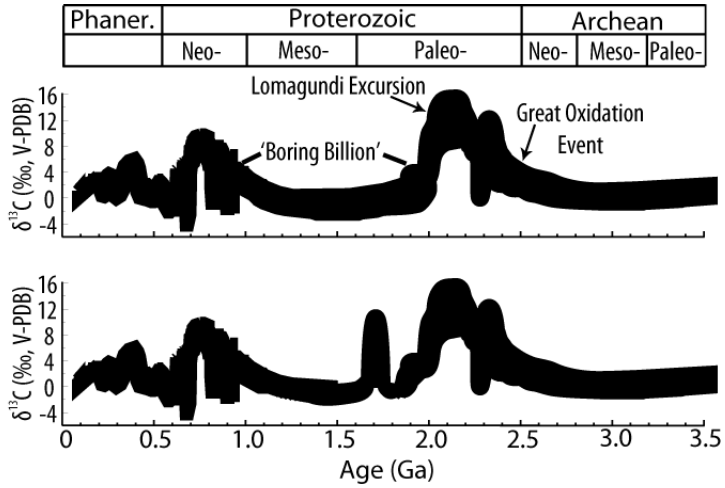
Phaner.
Proterozoic
Archean
Neo-
Meso-
Paleo-
Neo-
Meso-
Paleo-
Lomagundi Excursion
'Boring Billion'
Great Oxidation Event
δ13C (‰, V-PDB)
16
12
8
4
0
-4
0
0.5
1.0
1.5
2.0
2.5
3.0
3.5
Age (Ga)

Figure 2.4

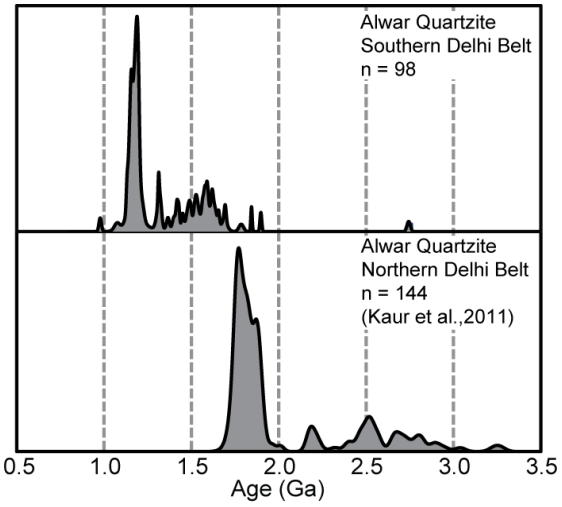
Alwar Quartzite
Southern Delhi Belt
n = 98
Alwar Quartzite
Northern Delhi Belt
n = 144
(Kaur et al.,2011)
0.5
1.0
1.5
2.0
2.5
3.0
3.5
Age (Ga)

Supporting Material

SM2.1. Phosphatic stromatolites of the Jhamarkotra Formation.

McKenzie et al. (2011) suggested a possible correlation between the phosphatic stromatolites of the Jhamarkotra Formation and the coeval ~1.6 Ga phosphatic stromatolites in the Lesser Himalaya (Gangolihat Dolomite) and the lower Vindhyan succession of the Son Valley (Rohtas Formation). However, both the Himalayan and Vindhyan phosphatic deposits differ significantly from the Aravalli phosphorite. The Himalayan-Vindhyan phosphatic deposits consist of branching columnar stromatolitic bioherms (form genus *Baicalia*) with columns exceeding 10 cm in diameter. The phosphatic horizons in these deposits are restricted to only a few meters of the bioherm with the phosphate occurring in the inter-columnar spaces as phosphatic grainstone, as coatings on terrigenous material, and as crusts on the stromatolite columns, whereas the stromatolite build-ups themselves are dolostone (Banerjee et al., 1986; Bengtson et al., 2009; McKenzie et al., 2011). In contrast, the phosphate-bearing Jhamarkotra stromatolitic bioherms are on the scale of 10's of meters in thickness (e.g., Banerjee, 1971) and are dominated by single columnar stromatolites that are only a few centimeters in diameter and rarely branch (Fig. SM2.1). In the Jhamarkotra deposits it is the stromatolitic column itself that is phosphatic with the intercolumnar space consisting primarily of massive dolostone. The replacement and preservation of delicate structures such as organic-walled mircofossils and putative gas bubbles in microbial mats in the lower Vindhyan

succession requires rapid phosphatization during very early diagenesis (Bengtson et al., 2009). In both the Vindhyan and Himalayan deposits the phosphate does not occur throughout the stromatolitic lamina and the phosphatic crusts around the individual columns appear to pinch-out along the stromatolitic heads in a discrete interval of the bioherms (McKenzie et al., 2011). Therefore it is inferred that phosphogenesis in both regions occurred contemporaneously during a relatively short distinct interval, which may have been associated with increased upwelling or primary productivity, and some aspect of these stromatolite bioherms created a local environment that favored phosphatization. On the other hand, as the Jhamarkotra stromatolites are almost exclusively phosphatized throughout the majority of the bioherm, phosphatization likely occurred in a manner that is unrelated to phosphatization of the Himalayan-Vindhyan phosphatic stromatolites. While both Himalayan-Vindhyan and Aravalli phosphorites share similar late Paleoproterozoic depositional ages, the suggested correlation based on the presence of phosphatic stromatolites made by McKenzie et al., (2011) is not necessarily valid.

SM2.1 References:

Banerjee, D.M., 1971, Precambrian Stromatolitic Phosphorites of Udaipur, Rajasthan, India: Geological Society of America Bulletin, v. 82, p. 2319-2329.

Banerjee, D.M., Schidlowski, M., and Arneth, J.D., 1986, Genesis of upper Proterozoic-Cambrian phosphorite deposits of India: isotopic inferences from carbonate fluorapatite, carbonate and organic carbon: Precambrian Research, v. 33, p. 239-253.

Bengtson, S., Belivanova, V., Rasmussen, B., and Whitehouse, M., 2009, The controversial

"Cambrian" fossils of the Vindhyan are real but more than a billion years older: Proceedings of the National Academy of Sciences, v. 106, p. 7729-7734.

McKenzie, N.R., N.C., H., Myrow, P.M., and Sharma, M., 2011, Correlation of Precambrian–Cambrian sedimentary successions across northern India and the utility of isotopic signatures of Himalayan lithotectonic zones: Earth and Planetary Science Letters, v. 312, p. 471-483.

Figure SM2.1. Phosphatic stromatolites of the Jhamarkotra Formation from the Jhamarkotra mine. a) Out-place-block with cross-sectional view of stromatolites. Arrow points in “up” direction based on stromatolitic laminae. b) Polished cross-section of stromatolites. Note white phosphatic stromatolite and dark gray dolostone filling intercolumnar space. c) Quasi-planar view of stromatolitic bioherm. d) Polished quasi-planar section of stromatolite. Scale bars = 2 cm.

Figure SM2.1

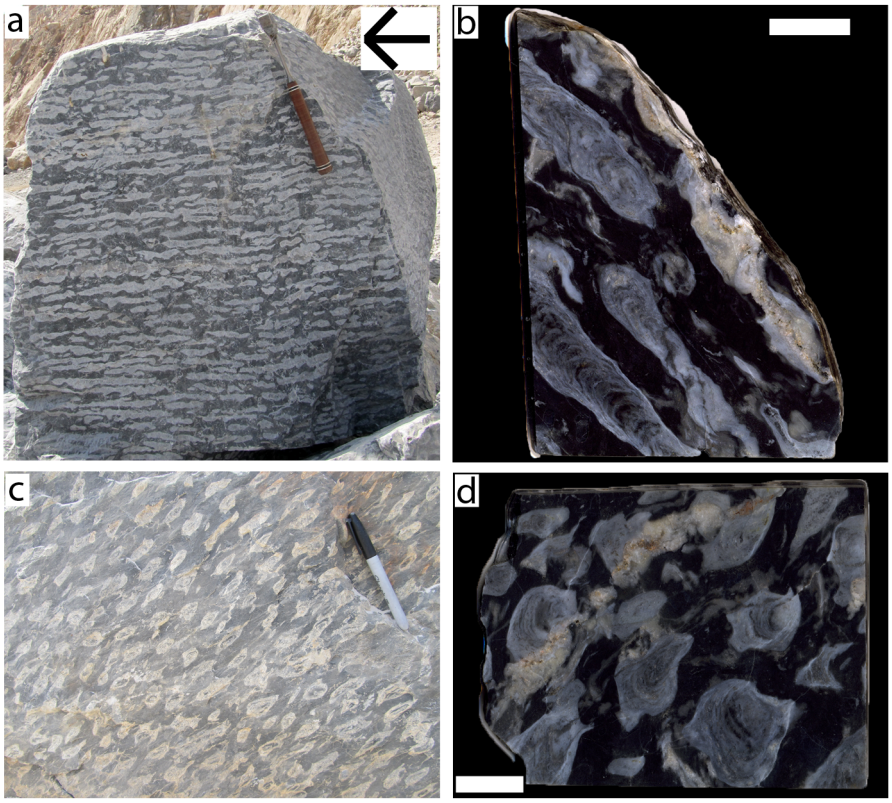

SM2.2. Detrital zircon data tables are available in online supplementary files.

CHAPTER 3

Plate-tectonic influences on Neoproterozoic-early Paleozoic climate and metazoan biodiversity

Abstract

Tracking Earth processes that are major controllers of atmospheric CO_2 is essential to understanding past and future climatic changes. Here we present a detrital zircon age data set acquired from globally distributed siliciclastic rocks to reconstruct spatial and temporal variation in continental arc volcanism — a major source for atmospheric CO_2 — during the dynamic Neoproterozoic to Cambrian times. The scarcity of zircons with ages around the onset of Cryogenian glaciation indicates a global low in arc-volcanism and associated CO_2 outgassing. In contrast Ediacaran–Cambrian age zircons are globally abundant pointing to widespread arc-volcanism. The subsequent rise in pCO_2 associated with this volcanism would have served as a mechanism to bring Earth out of the Cryogenian "snowball" climates. Large populations of Cambrian age zircons occur in lower Paleozoic strata indicating one of the most spatially extensive periods of arc-volcanism in the Phanerozoic. This extensive volcanism led to the high pCO_2 Cambrian "hothouse" resulting in widespread oceanic oxygen deficiency, which drove the high extinction rates observed during the later half of Cambrian. Cessation of volcanism across

Gondwana during the Ordovician coincided with global cooling and the Great Ordovician Biodiversification Event.

Introduction

Some of the most dramatic changes in Earth system history occurred during the Neoproterozoic-early Paleozoic transition. This interval includes the climatic shift from the Cryogenian "icehouse" (e.g., Hoffman et al., 1998) to the Cambrian "hothouse" which had the highest pCO_2 of the Phanerozoic (Berner et al., 1983; Berner, 1990, 2006; Montanez et al., 2000; Royer et al., 2004, 2007). This climatic shift event coincides with the initial diversification and proliferation of animals in the fossil record (e.g. Maloof et al., 2010).

At least two major glaciations of global magnitude occurred during the latter half of the Cryogenian period (850-635 Ma) during which ice sheets reached equatorial regions (e.g., Hoffman et al., 1998; Evans 2000; Pierrehumbert, 2011). The oldest definitive evidence for metazoan life comes from molecular fossils extracted from rocks situated between deposits of these glaciations (716 to 635 Ma) (Love et al., 2009) and body fossils first appear in strata of Ediacaran age (635-542 Ma) (e.g., Xiao et al., 1998; Droser et al., 2006). The subsequent Cambrian 'explosion' is characterized by the rapid appearance of most major metazoan phyla in the fossil record (Marshall, 2006) and is followed by the ca. 470 Ma Great Ordovician Biodiversification Event (GOBE) which saw a rapid tripling of taxonomic diversity

and a major increase in ecological complexity (Sepkoski, 1981; Droser and Finnegan, 2003; Miller et al., 2004; Harper et al., 2006; Servais et al., 2009). These diversification events are temporally separated by an interval referred to as the Cambrian 'dead interval' (Miller et al., 2006).

The so-called 'dead interval', which spanned the early-middle Cambrian to the Early Ordovician, is an interval with relatively low morphological disparity (Foote, 1988), anomalously high genus-level extinction rates and contains at least four distinct extinction events: the Botomian, end-Marjumian, end-Steptoean, and end-Sunwaptan (cf. Bambach et al., 2004; Bambach, 2006). The ca. 510 Ma Botomian extinction also marks the onset of the longest 'metazoan reef gap' of the Phanerozoic, approximately 40 million years (Rowland and Shapiro, 2002; Kiessling, 2009). The later Cambrian Marjumian, Steptoean, and Sunwaptan extinctions are most evident in trilobite fauna. These abrupt extinctions occur in shallow marine shelf environments and are followed by stratigraphic intervals dominated by low diversity assemblages of deeper water and potentially low-oxygen tolerant species of olenid trilobites (Palmer, 1984; Taylor, 2006). The success of olenids in shallow environments has been used to argue for flooding of anoxic water onto the shallow shelf as a kill mechanism for the extinctions (Taylor, 2006 and refs. therein). Geochemical studies corroborate the model of expanded oceanic euxinia (anoxic waters containing H_2S) during these times (Saltzman et al., 2004; Hough et al., 2008; Hurtgen et al., 2010; Gill et al., 2011). These events occur during an interval suggested to have the highest concentrations of atmospheric CO_2

recorded during the Phanerozoic while the end of this interval marked by the onset of the GOBE follows a period of global cooling (Trotter et al., 2008).

Understanding the driving mechanisms behind these global environmental shifts is critical to understanding how they shaped biospheric evolution during this crucial interval of Earth history. These transitions occurred at a time of continental reorganization and widespread tectonic plate margin activity associated with the amalgamation of Gondwana during the late Neoproterozoic–Ordovician (Cawood and Buchan, 2007). Ocean–atmosphere chemistry and climate are influenced by a complex array of lithospheric and surface processes. On geological time scales the long-term carbon cycle and atmospheric CO_2 are regulated by tectonic processes and chemical weathering: the outgassing of CO_2 from volcanism and metamorphism ("tectonic outgassing") is the major source for CO_2; chemical weathering of silicate rocks is a major CO_2 sink (Supporting Material SM3.1) (Walker et al., 1981; Berner et al., 1983; Kump et al., 2000; Berner, 2004; West et al., 2005). Also, the burial of organic matter plays a significant role in CO_2 drawdown (France-Lanord and Derry, 1997; Galy et al., 2007). Thus, considering temporal variation in tectonic activity along plate margins is important when indentifying the drivers behind climate change in deep time. Here we argue the history of global plate tectonics exerted a principal control on the timing and trajectory of the early evolution of metazoans.

Utility of detrital zircon geochronology in paleotectonic studies

Zircon is a common accessory mineral in felsic-intermediate igneous rocks, and is physically resistant to sediment transport, reworking, abrasion, and metamorphism. Evaluation of age populations from U-Pb dating of individual detrital zircons from siliciclastic rocks provides two critical pieces of information: 1) the youngest zircon grains provide maximum age constraints for the depositional age of the strata from which they were extracted (i.e., the rock cannot be older than the youngest zircon), and 2) age populations of detrital zircons indicate the provenance and crustal composition of source–rock. Large populations of similar age detrital zircons represent voluminous igneous sources. The presence of large populations of first-cycle detrital zircons with ages close to depositional age of the host strata (referred to here as relatively 'young' zircons) require the exhumation and erosion of igneous bodies rapidly following crystallization. Large populations of relatively 'young' zircons are common along active continental margins, often with ages within less than 10 million years of the depositional age of the rock, whereas rifted and passive margins generally lack 'young' zircons (Cawood et al., 2012). To evaluate spatial and temporal variations in tectonic activity, specifically the spatial extent of active continental-arcs and subaerial volcanism, we present a compilation of new and published U-Pb detrital zircon age distributions from globally dispersed strata with depositional ages ranging from the Cryogenian to the Late Devonian (Fig. 3.1). We primarily focused on data reported from samples with independent

depositional age control to at least the geologic epoch, although less constrained samples were included if they were part of a dataset with otherwise generally well-constrained depositional ages and expanded the temporal and spatial coverage of this study. Age data are presented in two ways: 1) as regionally and temporally differentiated age probability plots, (Figs 3.2, 3.3) which allow for spatial evaluation of margin activity, and 2) as temporally differentiated age distributions with all regional data presented in 20Ma bins, normalized to remove bias due to uneven sampling and combined to assess overall global variation in continental-arc volcanism (Fig. 3.4) (See Supporting Material SM3.2 for details of normalization process). Data generated from strata that have problematic paleogeographies and/or poor depositional age constraints are treated separately and are presented in Supporting Material (SM3.3).

Neoproterozoic tectonics and the Cryogenian 'icehouse'

The youngest robust populations of zircons in Cryogenian strata are more than ~100 million years older than the depositional age of the rocks (Fig. 3.3 – IND, SCB, and WLA). Probability distributions from Ediacaran-age rocks of African-associated terranes (SAF, NAF, IRN, ISR, CAD, and IBR) are flooded with 'young' zircons that are absent in other terranes. In striking contrast with Neoproterozoic distributions, Cambrian age probability distributions of all non-Laurentian terranes contain large populations of 'young' detrital zircons with a mix of Ediacaran and Cambrian ages.

Prominent Cambrian age-peaks within ~20 million years of the depositional age of the rock are present in Baltica (BAL), South America (SAM) and all east Gondwanan terranes (ANT, AUS, IND, SCB, NCB, SBU), while the most prominent peaks of distributions from African associated terranes are of Ediacaran age. Overall, Cryogenian-aged zircons are minor components of most detrital populations. Zircon ages close to the initiation of the glacial interval are particularly spares; age frequencies increase towards the end of the glacial interval (Figs 3.2, 3.3, 3.4).

A major obstacle in understanding and modeling climate during the Cryogenian involves constraining variation in atmospheric CO_2 (e.g., Hyde et al., 2000; Donnadieu et al., 2004; Pierrehumber 2005, 2010; LeHir et al., 2008;). The notable low-abundance of zircon ages close to the onset of the Cryogenian glacial interval represents a reduction in global felsic-intermediate magmatism. Large Igneous Provinces (LIPS) are well known globally from ~850-750 Ma, whereas the ca. 720 Franklin igneous province is the only known LIP to occur between ~750 Ma and the early to middle Cambrian (Ernst and Buchan, 2002; Ernst et al., 2009). The paucity of detrital zircons of magmatic origin and global LIP activity near the onset of the Cryogenian glacial interval is evidence for a minimum in continental volcanism and implies a reduction in the volcanic flux of CO_2 to the atmosphere. Many factors have been suggest to have contributed to the generation of the Cryogenian "icehouse" including the continental albedo effect (Kirschvink, 1992; Evans, 2000) and mechanisms which drawdown CO_2 such as enhanced burial of organic matter (Hoffman et al., 1998), silicate weathering (Schrag et al., 2002), oceanic crust

alteration (Le Hir et al., 2008) and the weathering of LIP continental basalts (Goddéris et al., 2003). However, a reduction in volcanic CO_2 outgassing, as inferred from our detrital zircon compilation, would have played a critical role in pushing Earth climate into the Cryogenian icehouse state.

The progressive accumulation of CO_2 from volcanic emissions and limited weathering have long been the suggested as mechanisms to bring Earth out of its "icehouse" (Hoffman et al., 1998). The marked increase in terminal Cryogenian-Ediacaran age detrital zircons reported here requires a major increase in felsic and intermediate volcanism during this interval, particularly at the onset of the pan-African orogeny. The initiation of synchronous widespread tectonic outgassing would have caused rapid, rather than progressive, global warming. This warming, aided initially by slow chemical weathering rates due to ice cover on the continents and lower global temperatures, drove end-Cryogenian deglaciation.

Early Paleozoic tectonism, climate, and biodiversity: lessons from a Cenozoic analog

With the exception of Laurentia, all Cambrian strata contain a distinct peak of 'young' detrital zircons (Fig. 3.2) representing extensive magmatic arc exhumation during the Cambrian. In many cases this peak dominates the age distribution. The 'young' age-peaks remain broadly unchanged through Cambrian and Ordovician aged strata in most regions (Figs 3.3, 3.4) indicating that the major pulses of pluton

emplacement occurred in the Cambrian. The persistence of this age class into Ordovician sediments indicates a protracted interval of exhumation. This is consistent with thermochronologic data that suggest regional metamorphism continued along numerous Gondwanan orogens until the middle Ordovician ~480-470 Ma (Cawood and Buchan, 2007). Age distributions from Silurian and Devonian strata preserve Cambrian–Ediacaran age-peaks that are similar to the age distributions from older Paleozoic strata, but contain higher concentrations of older zircons (and younger Taconic-aged material in the case of Laurentia) than the Ordovician distributions. The observed homogeneity in zircon populations of Silurian–Devonian strata can be explained by a transition to mixed crustal sources of detritus no longer overwhelmed by the exhumation of Cambrian-age plutons. Exhumation ceased with the termination of Gondwanan convergence. To evaluate the relationship between these tectonic transitions and changes in the climate and surface environment, a comparison is drawn with the Cenozoic Indian-Eurasian collision and Himalayan orogeny.

The southern margin of Tibet maintained an Andean-type subduction system prior to the ~50 Ma continent-collision with India (Kapp et al, 2007; Royden et al., 2009). This system emplaced large Cretaceous-early Tertiary plutons along the margin (Yin and Harrison, 2000; Chiu et al., 2009). The transition from Andean-type subduction to continental collision terminated Tibetan arc-volcanism and initiated bedrock uplift and exhumation on the north Indian Himalayan margin (e.g., Yin and Harrison, 2000; Hodges, 2004; Yin, 2006). This interval is coincident with the onset

of long-term Cenozoic cooling following the Paleocene-Eocene Thermal Maximum (PETM) (e.g., Zachos et al., 2001). In addition to the cessation of arc-volcanism, chemical weathering of uplifted Himalayan-Tibetan silicate bedrock has been linked to post-PETM cooling (e.g., Raymo and Ruddiman, 1992), although organic matter burial in the various Himalayan sedimentary basins has been suggested to have played an even greater role in CO_2 sequestration and cooling (France-Lanord and Derry, 1997; Galy et al., 2007).

A Cenozoic–Cambrian analogy can be extended to the seawater strontium isotope record. The strontium isotope ratio ($^{87}Sr/^{86}Sr$) of seawater is dictated by relative amounts of riverine flux, which is enriched in the radiogenic ^{87}Sr due to weathering of old continental crust, and mantle-derived hydrothermal flux, which is depleted in ^{87}Sr. The intense weathering of ancient bedrock along the Himalayan margin has caused modern seawater $^{87}Sr/^{86}Sr$ to rise to the second highest value in Earth history (Palmer and Edmond, 1989; Edmond, 1992; Derry and France-Lanord, 1996), the $^{87}Sr/^{86}Sr$ values seen in the Cambrian being the highest (Shields and Veizer, 2002). High weathering rates in the Himalayan system result from the South Asian monsoon, which is a function of the geographic position of the orogen (Molnar et al., 2010). Considering the spatial extent of orogenic belts during the Cambrian, especially those in tropical regions of eastern Gondwana (Supporting Material SM3.4), one or more Himalayan-type systems likely existed throughout this interval and could have produced similarly high $^{87}Sr/^{86}Sr$ values in Cambrian seawater.

Following the Himalayan analogy, it is suggested here that tectonic outgassing associated with pan-African tectonic activity during the late Cryogenian-Ediacaran may have been the main factor in terminal-Cryogenian warming with the cumulative effects of "Greater Gondwanan" tectonism driving Earth into an early Paleozoic "hothouse". Cessation of arc-magmatism is recorded along both the internal sutures of Gondwana and the Indian-Asian, Ross Delamarian, and Pampean orogens of the "Greater Gondwanan" realm (Supporting Material SM3.4) around the late Cambrian-Early Ordovician, although regional metamorphism continued until ~480-470 Ma (e.g., Cawood and Buchan, 2007). This represents the transition from Andean-type subduction to Himalayan-type collisional zones along the internal Gondwanan sutures and regions of micro-continent accretion of the peri-Gondwanan realm. The cessation of metamorphism reflects a reduction in regional uplift and crustal exhumation that coincides with a sharp decline in seawater $^{87}Sr/^{86}Sr$ (Young et al., 2009) and an interval of rapid global cooling during at the onset of the GOBE (Trotter et al., 2008) (Fig. 3.6). The decline in $^{87}Sr/^{86}Sr$ may result from a combination of increased weathering of 'young' Cambrian plutons, as is evident from the detrital zircon record, and an overall reduction in exhumation and weathering of old crustal material. Furthermore, the widespread shutdown of the volcanic CO_2 flux followed by continuous silicate weathering and high sedimentation rates and burial of organic material along active margins would have been prime drivers for the observed cooling in the Ordovician.

An important observation is the apparent coupling between tectonism, climate and early metazoan biodiversity. The Cambrian 'explosion' paralleled the transition from the Cryogenian "icehouse" to a "hothouse" climate, and the subsequent radiation of the Paleozoic fauna that followed the return to cooler conditions during the Ordovician. Following the Cambrian 'explosion' overall taxonomic diversity remained relatively low throughout the so-called Cambrian 'dead interval' until the GOBE. Evidence for oxygen-deficiency and increased euxinia in the ocean throughout this interval has been reported from sedimentological and geochemical data (e.g., Zhuravlev and Wood, 1996; Hough et al., 2006; Hurtgen et al., 2009; Gill et al., 2011). Poor oceanic circulation during a greenhouse climate is a suggested mechanism for early Paleozoic oxygen deficiency (Saltzman, 2005) and global heterogeneity in the sulfur isotopic composition of Cambrian and Early to Middle Ordovician oceans supports this hypothesis (Gill et al., 2011; Thompson and Kah, 2012). The severe greenhouse conditions and oxygen-deficient oceans of the Cambrian favored morphotypes adapted to stressed-environments such as the lingulellid brachiopods and trilobites rich in thoracic segments—key components of the Cambrian Evolutionary Fauna (Sepkoski, 1981; Droser and Finnegan, 2003; Harper et al., 2006; Hughes, 2007). These conditions persisted until the major reduction in Gondwanan tectonism around the late Early Ordovician where subsequent global cooling improved the habitability of the ocean allowing the ecological and taxonomic diversification of the GOBE. Global cooling continued to the end-Ordovician glaciations and associated mass extinction (Kump et al., 1999;

Finnegan et al., 2011). Tectonic outgassing from the Late Ordovician Taconic orogeny has been suggested as a possible mechanism to alleviate those "icehouse" conditions (Kump et al., 1999), and the concentration of Late Ordovician-Silurian detrital zircons in Devonian strata of Laurentia support this hypothesis, although these climate changes were less dramatic than those observed in the late Neoproterozoic-early Paleozoic. Overall, early metazoan biodiversity appears to have responded to the major climatic shifts in the Neoproterozoic-Cambrian transition, with ecosystem expansion and taxonomic radiations occurring during transitional climatic phases and extinction intervals corresponding with climatic extremes. Thus climate, as influenced by major tectonic events, appears to have played an integral role in the mediating the evolutionary history of life on our planet.

Acknowledgments

I thank N. Hughes, B. Gill, P. Cawood, P. Myrow, P. Sadler, C. Reinhard, and T. Lyons for assistance with multiple aspects of this project. G. Gehrels, V. Valencia, and M. Ibanez-Mejia at the Arizona LaserChron Center are thanked for analytical assistance.

References

Bambach, R.K., 2006. Phanerozoic biodiversity mass extinctions. Annual Review of Earth and Planetary Sciences 34, 127-155.

Bambach, R.K., Knoll, A.H., Wang, S.C., 2004. Origination, extinction, and mass depletions of marine diversity. Paleobiology 30, 522-542.

Berner, R.A., 1990. Atmospheric Carbon-Dioxide Levels over Phanerozoic Time. Science 249, 1382-1386.

Berner, R.A., 2004. The Phanerozoic carbon cycle: CO2 and O2. Oxford University Press, New York.

Berner, R.A., 2006. GEOCARBSULF: A combined model for Phanerozoic atmospheric O-2 and CO2. Geochimica Et Cosmochimica Acta 70, 5653-5664.

Berner, R.A., Lasaga, A.C., Garrels, R.M., 1983. The Carbonate-Silicate Geochemical Cycle and Its Effect on Atmospheric Carbon-Dioxide over the Past 100 Million Years. American Journal of Science 283, 641-683.

Cawood, P.A., Buchan, C., 2007. Linking accretionary orogenesis with supercontinent assembly. Earth-Science Reviews 82, 217-256.

Cawood, P.A., Hawkesworth, C.J., Dhuime, B., in press. Detrital zircon record and tectonic setting. Geology.

Chiu, H.-Y., Chung, S.-L., Wu, F.-Y., Liu, D., Liang, Y.-H., Lin, I.-J., Iizuka, Y., Xie, L.-W., Wang, Y., 2009. Zircon U–Pb and Hf isotopic constraints from eastern Transhimalayan batholiths on the precollisional magmatic and tectonic evolution in southern Tibet. Tectonophysics 477, 3-19.

Condon, D., Zhu, M., Bowring, S., Wang, W., Yang, A., Jin, Y.-G., 2005. U-Pb ages from the Neoproterozoic Doushantuo Formation, China. Science 308, 95-98.

Derry, L.A., France-Lanord, C., 1996. Neogene Himalayan weathering history and river $^{87}Sr/^{86}Sr$: impact on the marine Sr record. Earth and Planetary Science Letters 142, 59-74.

Donnadieu, Y., Godderis, Y., Ramstein, G., Nedelec, A., Meert, J., 2004. A 'snowball Earth' climate triggered by continental break-up through changes in runoff. 428, 303-306.

Droser, M.L., Finnegan, S., 2003. The Ordovician Radiation: a follow-up to the Cambrian explosion? Integrative and Comparative Biology 43, 178-184.

Droser, M.L., Gehling, J.G., Jensen, S.R., 2006. Assemblage palaeoecology of the Ediacara biota: The unabridged edition? Paelaeogeography, Palaeoclimatology, Palaeoecology 232, 131-147.

Edmond, J.M., Palmer, M.R., Measures, C.I., Grant, B., Stallard, R.F., 1995. The fluvial geochemistry and denudation rate of the Guayana Shield in Venezuela, Colombia, and Brazil. Geochemica et Cosmochimica Acta 59, 3301-3325.

Ernst, R.E., Buchan, K.L., 2002. Maximum size and distribution in time and space of mantle plumes: evidence from large igneous provinces (vol 34, pg 309, 2002). Journal of Geodynamics 34, 711-714.

Ernst, R.E., Wingate, M.T.D., Buchan, K.L., Li, Z.X., 2008. Global record of 1600-700 Ma Large Igneous Provinces (LIPs): Implications for the reconstruction of the proposed Nuna (Columbia) and Rodinia supercontinents. Precambrian Research 160, 159-178.

Evans, D.A.D., 2000. Stratigraphic, geochronological, and paleomagnetic constraints upon the Neoproterozoic climatic paradox. American Journal of Science 300, 347-433.

Finnegan, S., Bergmann, K., Eiler, J.M., Jones, D.S., Fike, D.A., Eisenman, I., Hughes, N.C., Tripati, A.K.,

Fischer, W.W., 2011. The Magnitude and Duration of Late Ordovician-Early Silurian Glaciation. Science 331, 903-906.

Foote, M., 1988. Survivorship analysis of Cambrian and Ordovician trilobites. Paleobiology 14, 258-271.

FranceLanord, C., Derry, L.A., 1997. Organic carbon burial forcing of the carbon cycle from Himalayan erosion. Nature 390, 65-67.

Galy, V., France-Lanord, C., Beyssac, O., Faure, P., Kudrass, H., Palhol, F., 2007. Efficient organic carbon burial in the Bengal fan sustained by the Himalayan erosional system. Nature 450, 407-411.

Gill, B.C., Lyons, T.W., Young, S.A., Kump, L.R., Knoll, A.H., Saltzman, M.R., 2011. Geochemical evidence for widespread euxinia in the later Cambrian ocean. Nature (London) 469, 80-83.
Godderis, Y., Donnadieu, Y., Nedelec, B., Dupre, B., Dessert, C., Grard, A., Ramstein, G., Francois, L.M., 2003. The Sturtian 'snowball' glaciation: fire and ice. Earth and Planetary Science Letters 211, 1-12.

Harper, D.A.T., 2006. The Ordovician biodiversification: Setting an agenda for marine life. Palaeogeography Palaeoclimatology Palaeoecology 232, 148-166.

Hoffman, P.F., Kaufman, A.J., Halverson, G.P., Schrag, D.P., 1998. A Neoproterozoic snowball earth. Science 281, 1342-1346.

Hoffmann, K.H., Condon, D.J., Bowring, S.A., Crowley, J.L., 2004. U-Pb zircon date from the Neoproterozoic Ghaub Formation, Namibia: Constraints on Marinoan glaciation. Geology 32, 817-820.

Hough, M.L., Shields, G.A., Evins, L.Z., Strauss, H., Henderson, R.A., Mackenzie, S., 2006. A major sulphur isotope event at c.510 Ma: a possible anoxia-extinction-volcanism connection during the Early-Middle Cambrian transition? Terra Nova 18, 257-263.

Hughes, N.C., 2007. The evolution of trilobite body patterning. Annual Reviews of Earth and Planetary Sciences 35, 401-434.

Hurtgen, M.T., Halverson, G.P., Arthur, M.A., Hoffman, P.F., 2006. Sulfur cycling in the aftermath of a 635-Ma snowball glaciation: Evidence for a syn-glacial sulfidic deep ocean. Earth and Planetary Science Letters 245, 551-570.

Hyde, W.T., Crowley, T.J., Baum, S.K., Peltier, W.R., 2000. Neoproterozoic `snowball Earth' simulations with a coupled climate/ice-sheet model. Nature 405, 425-429.

Kapp, P., DeCelles, P.G., Gehrels, G.E., Heizier, M., Ding, L., 2007. Geological records of the Lhasa-Qiangtang and Indo-Asian collisions in the Nima area of central Tibet. Geological Society of America Bulletin 119, 917-932.

Kiessling, W., 2009. Geologic and Biologic Controls on the Evolution of Reefs. Annual Review of Ecology Evolution and Systematics 40, 173-192.

Kirschvink, J.L., 1992. Late Proterozoic low-lattitude global glaciation: the snowball Earth, in: Schopf, J.W., Klein, C. (Eds.), The Proterozoic Biosphere: A Multidisciplinary Study. Cambridge University Press, New York, pp. 51-52.

Kump, L.R., Arthur, M.A., Patzkowsky, M.E., Gibbs, M.T., Pinkus, D.S., Sheehan, P.M., 1999. A weathering hypothesis for glaciation at high atmospheric pCO(2) during the Late Ordovician. Palaeogeography Palaeoclimatology Palaeoecology 152, 173-187.

Kump, L.R., Brantley, S.L., Arthur, M.A., 2000. Chemical, weathering, atmospheric CO2, and climate. Annual Review of Earth and Planetary Sciences 28, 611-667.

Le Hir, G., Ramstein, G., Donnadieu, Y., Godderis, Y., 2008. Scenario for the evolution of atmospheric pCO2 during a snowball Earth. Geology 36, 47-50.

Love, G.D., Grosjean, E., Stalvies, C., Fike, D.A., Grotzinger, J.P., Bradley, A.S., Kelly, A.E., Bhatia, M., Meredith, W., Snape, C.E., Bowring, S.A., Condon, D.J., Summons, R.E., 2009. Fossil steroids record the appearance of Demospongiae during the Cryogenian period. Nature 457, 718-U715.

Macdonald, F.A., Schmitz, M.D., Crowley, J.L., Roots, C.F., Jones, D.S., Maloof, A.C., Strauss, J.V., Cohen, P.A., Johnston, D.T., Schrag, D.P., 2010. Calibrating the Cryogenian. Science 327, 1241-1243.

Maloof, A.C., Porter, S.M., Moore, J.L., Dudas, F.O., Bowring, S.A., Higgins, J.A., Fike, D.A., Eddy, M.P., 2010. The earliest Cambrian record of animals and ocean geochemical change. Geological Society of America Bulletin 122, 1731-1774.

Marshall, C.R., 2006. Explaining the Cambrian "explosion" of animals. Annual Review of Earth and Planetary Sciences 34, 355-384.

Miller, A.I., 2004. The Ordovician Radiation: toward a new global synthesis, in: Webby, B.D., Florentin, P., Droser, M.L., Percival, I.G. (Eds.), The Great Ordovician Biodiversification Event. Columbia University Press, New York, p. 473.

Miller, A.I., Bulinkski, K.V., Buick, D.P., Ferguson, C.A., Hendy, A.J.W., 2006. The Ordovician Radiation: A macroevolutionary crossroads. Geological Society of America Abstracts with Programs 38, 114.

Molnar, P., Boos, W.R., Battisti, D.S., 2010. Orographic controls on climate and paleoclimate of Asia: thermal and mechanical roles for the Tibetan Plateau. Annual Review of Earth and Planetary Sciences 38, 77-102.

Montañez, I.P., Oselger, D.A., Banner, J.L., Mack, L.E., Musgrove, M.L., 2000. Evolution of the Sr and C isotope composition of Cambrian oceans. GSA Today 10, 1-7.

Palmer, A.R., 1984. The biomere problem: Evolution of an idea. Journal of Paleontology 58, 599-611.

Palmer, M.R., Edmond, J.M., 1989. The strontium isotope budget of the modern ocean. Earth and Planetary Science Letters 92, 11-26.

Pierrehumbert, R.T., 2004. High levels of atmospheric carbon dioxide necessary for the termination of global glaciation. Nature 429, 646-649.

Pierrehumbert, R.T., Abbot, D.S., Voigt, A., Koll, D., 2011. Climate of the Neoproterozoic. Annual Review of Earth and Planetary Sciences, Vol 39 39, 417-460.

Raymo, M.E., Ruddiman, W.F., 1992. Tectonic Forcing of Late Cenozoic Climate. Nature 359, 117-122.

Rowland, S.M., Shapiro, R.S., 2002. Reef patterns and environmental influences in the Cambrian and earliest Ordovician, in: Kiessling, W., Flugel, E., Golonka, J. (Eds.), Phanerozoic Reef Patterns. Society of Sedimentary Geology, Tulsa, pp. 95-128.

Royer, D.L., Berner, R.A., Montanez, I.P., Tabor, N.J., Beerling, D.J., 2004. CO2 as a primary driver of Phanerozoic climate. GSA Today 14, 4-10.

Royer, D.L., Berner, R.A., Park, J., 2007. Climate sensitivity constrained by CO2 concentrations over the past 420 million years. Nature 446, 530-532.

Saltzman, M.R., 2005. Phosphorus, nitrogen, and the redox evolution of the Paleozoic oceans. Geology 33, 573-576.

Saltzman, M.R., Cowan, C.A., Runkel, A.C., Runnegar, B., Stewart, M.C., Palmer, A.R., 2004. The Late Cambrian SPICE (delta(13)c) event and the Sauk II-Sauk III regression: New evidence from Laurentian basins in Utah, Iowa, and Newfoundland. Journal of Sedimentary Research 74, 366-377.

Schrag, D.P., Berner, R.A., Hoffman, P.F., Halverson, G.P., 2002. On the initiation of a snowball Earth. Geochemistry Geophysics Geosystems 3.

Sepkoski, J.J., Bambach, R.K., Raup, D.M., Valentine, J.W., 1981. Phanerozoic Marine Diversity and the Fossil Record. Nature 293, 435-437.

Servais, T., Harper, D.A.T., Li, J., Munnecke, A., Owen, A.W., Sheehan, P.M., 2009. Understanding the Great Ordovician Biodiversification Event (GOBE): Influences of paleogeography, paleoclimate, or paleoecology? GSA Today 19, 4-10.

Shields, G., Veizer, J., 2002. Precambrian marine carbonate isotope database: Version 1.1. Geochemistry Geophysics Geosystems 3.

Taylor, J.F., 2006. History and status of the biomere concept. Memoirs of the Association of Australasian Palaeontologists 32, 247-265.

Thompson, C.K., Kah, L.C., 2012. Sulfur isotope evidence for widespread euxinia and a fluctuating oxycline in Early to Middle Ordovician greenhouse oceans. Palaeogeography Palaeoclimatology Palaeoecology 313, 189-214.

Trotter, J.A., Williams, I.S., Barnes, C.R., Lecuyer, C., Nicoll, R.S., 2008. Did cooling oceans trigger Ordovician biodiversification? Evidence from conodont thermometry. Science 321, 550-554.

Walker, J.C.G., Hays, P.B., Kasting, J.F., 1981. A Negative Feedback Mechanism for the Long-Term Stabilization of Earths Surface-Temperature. Journal of Geophysical Research-Oceans and Atmospheres 86, 9776-9782.

West, A.J., Galy, A., Bickle, M., 2005. Tectonic and climatic controls on silicate weathering. Earth and Planetary Science Letters 235, 211-228.

Xiao, S., Zhang, Y., Knoll, A.H., 1998. Three-dimensional preservation of algae and animal embroys in a Neoproterozoic phosphate. Nature 391, 553-558.

Yin, A., 2006. Cenozoic tectonic evolution of the Himalayan orogen as constrained by along-strike varaition in structural geometry, exhumation history, and foreland sedimentation. Earth Science Reviews 76, 1-131.

Yin, A., Harrison, T.M., 2000. Geologic evolution of the Himalayan-Tibetan orogen. Annual Reviews of Earth and Planetary Sciences 28, 211-280.

Young, S.A., Saltzman, M.R., Foland, K.A., Linder, J.S., Kump, L.R., 2009. A major drop in seawater (87)Sr/(86)Sr during the Middle Ordovician (Darriwilian): Links to volcanism and climate? Geology 37, 951-954.

Zachos, J., Pagani, M., Sloan, L., Thomas, E., Billups, K., 2001. Trends, rhythms, and aberrations in global climate 65 Ma to present. Science 292, 686-693.

Zhuravlev, A.Y., Wood, R.A., 1996. Anoxia as the cause of the mid-early Cambrian (Botomian) extinction event. Geology 24, 311-314.

Figures

Figure 3.1. Sample locality map. Open stars indicate samples used for temporal and regional differentiation. Closed stars indicate samples with poor paleogeographic constraints or lack of well-established depositional ages (Supporting Material

SM3.2). Open-star abbreviations: WLA, ELA, NLA = West, East, and North Laurentia, respectively; GRN = Greenland; BAL = Baltica; SAM = South America; SAF = South Africa; NAF = North Africa; ARB = Arabia; IRN = Iran; IBR = Iberia; CDM = Cadomia; ANT = Antarctica; AUS = Australia; IND = India; SCB = South China Block; NCB = North China Block; SBU = Sibumasu. Closed-star abbreviations = ALK = Alaska; AVW = Avalonia-West; AVE = Avalonia-East; SCT = Scotland; TAR = Tarim. References incl

Figure 3.2. Detrital zircon age distributions from Neoproterozoic and Cambrian age strata. Blue bar highlights 'glacial interval' from 715-635 Ma. See Fig. 3.1 for locality abbreviations. Age abbreviations: Ear = Early, Mid = Middle, Lt = Late, Neoptz = Neoproterozoic; Cambr = Cambrian. All Cryogenian samples include material that is at least Marinoan in age. Late Neoproterozoic samples include both Cryogenian and Ediacaran material. Data sources listed in Supporting Material (SM3.5).

Figure 3.3. Detrital zircon age distributions from Ordovician, Silurian, and Devonian age strata. Blue bar highlights 'glacial interval' from 715-635 Ma. See Fig. 3.1 for locality abbreviations. Age abbreviations: Ear = Early; Mid = Middle; Lt = Late; Ord = Ordovician; Devo = Devonian. All Cryogenian samples include material that is at least Marinoan in age. Late Neoproterozoic samples include both Cryogenian and Ediacaran material. Data sources listed in Supporting Material (SM3.5).

Figure 3.4. Normalized age distributions of combined global detrital zircon age data. Blue bar highlights 'glacial interval' from 715-635 Ma. Red dashed bars indicate Large Igneous Province activity (from Ernst and Buchan, 2002; Ernst et al., 2008).

Figure 3.5. Temporal composite of geochronologic, thermochronologic, and geochemical data related to metazoan marine biodiversity and mass extinctions (see Supporting Material SM3.6 for references.)

Figure 3.1

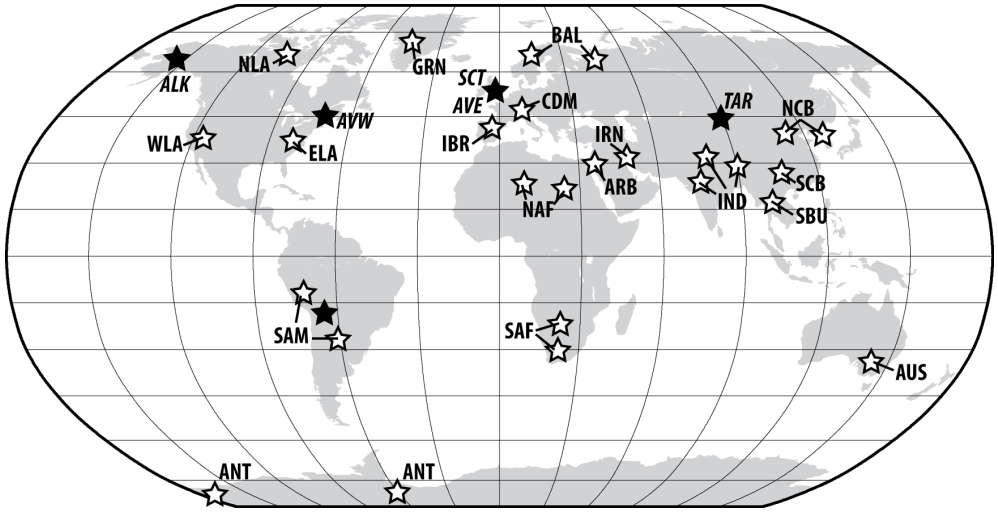
ALK
NLA
GRN
BAL
SCT
AVE
CDM
TAR
NCB
AVW
WLA
ELA
IBR
IRN
ARB
NAF
IND
SCB
SBU
SAM
SAF
AUS
ANT
ANT

Figure 3.2

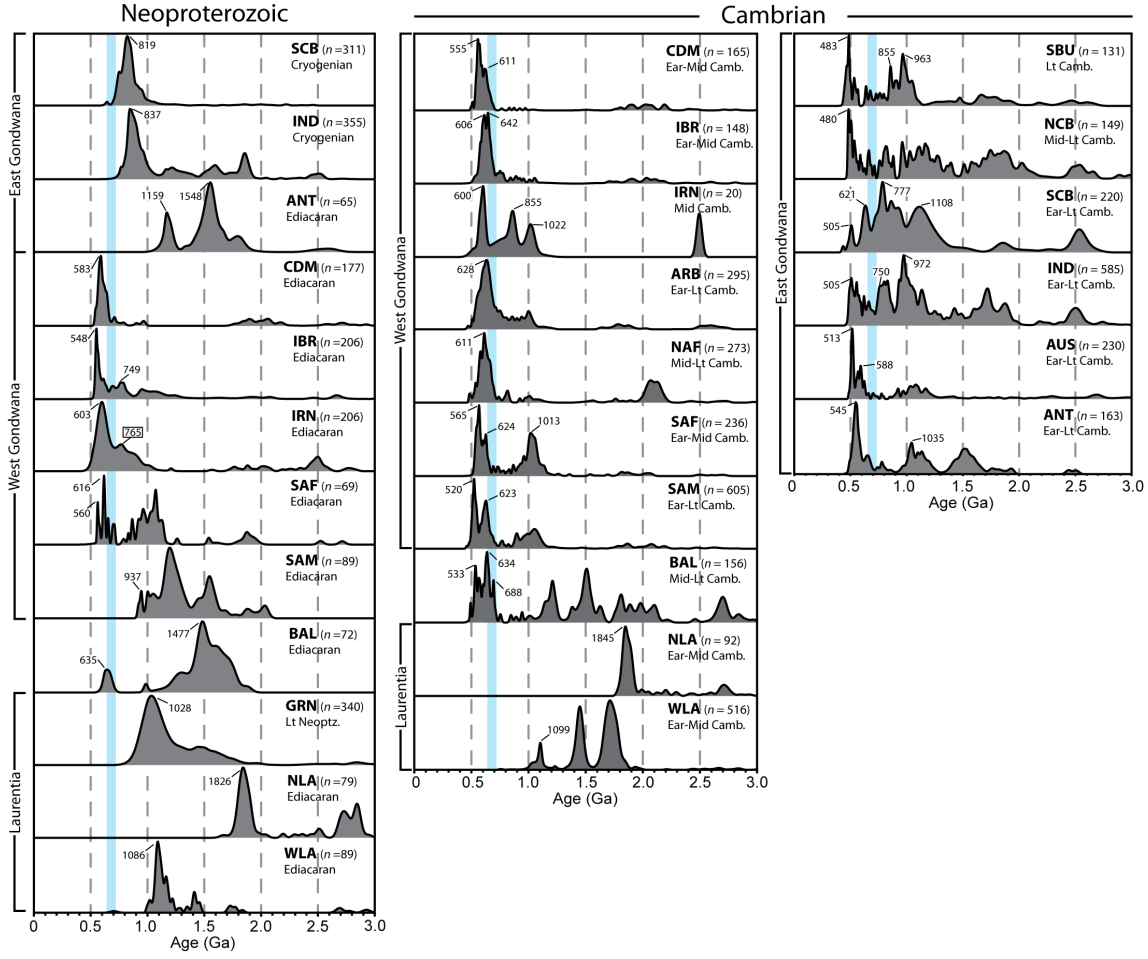
Neoproterozoic
Cambrian
East Gondwana
West Gondwana
Laurentia
SCB (n =311) Cryogenian
IND (n =355) Cryogenian
ANT (n =65) Ediacaran
CDM (n =177) Ediacaran
IBR (n =206) Ediacaran
IRN (n =206) Ediacaran
SAF (n =69) Ediacaran
SAM (n =89) Ediacaran
BAL (n =72) Ediacaran
GRN (n =340) Lt Neoptz.
NLA (n =79) Ediacaran
WLA (n =89) Ediacaran
CDM (n = 165) Ear-Mid Camb.
IBR (n = 148) Ear-Mid Camb.
IRN (n = 20) Mid Camb.
ARB (n = 295) Ear-Lt Camb.
NAF (n = 273) Mid-Lt Camb.
SAF (n = 236) Ear-Mid Camb.
SAM (n = 605) Ear-Lt Camb.
BAL (n = 156) Mid-Lt Camb.
NLA (n = 92) Ear-Mid Camb.
WLA (n = 516) Ear-Mid Camb.
SBU (n = 131) Lt Camb.
NCB (n = 149) Mid-Lt Camb.
SCB (n = 220) Ear-Lt Camb.
IND (n = 585) Ear-Lt Camb.
AUS (n = 230) Ear-Lt Camb.
ANT (n = 163) Ear-Lt Camb.
Age (Ga)

Figure 3.3

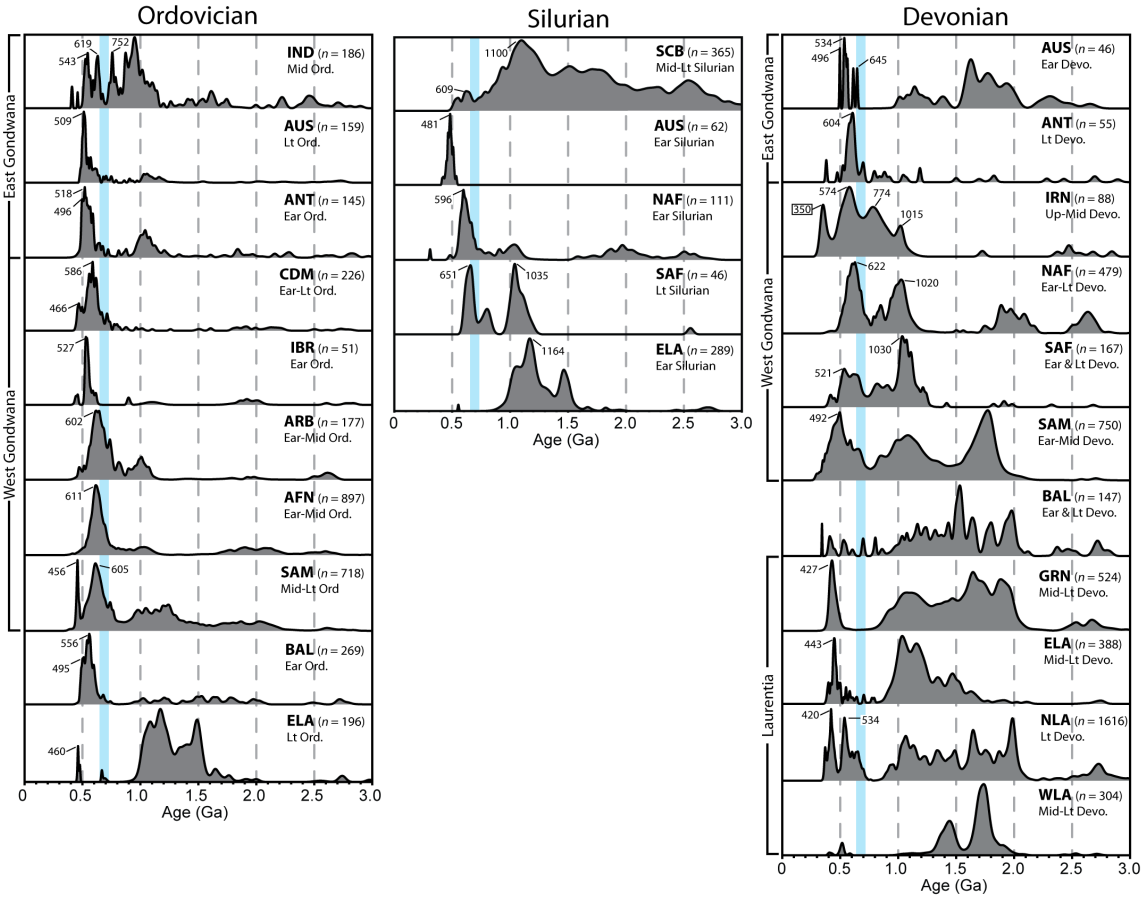
Ordovician
Silurian
Devonian
East Gondwana
West Gondwana
Laurentia
IND (n = 186) Mid Ord.
AUS (n = 159) Lt Ord.
ANT (n = 145) Ear Ord.
CDM (n = 226) Ear-Lt Ord.
IBR (n = 51) Ear Ord.
ARB (n = 177) Ear-Mid Ord.
AFN (n = 897) Ear-Mid Ord.
SAM (n = 718) Mid-Lt Ord
BAL (n = 269) Ear Ord.
ELA (n = 196) Lt Ord.
SCB (n = 365) Mid-Lt Silurian
AUS (n = 62) Ear Silurian
NAF (n = 111) Ear Silurian
SAF (n = 46) Lt Silurian
ELA (n = 289) Ear Silurian
AUS (n = 46) Ear Devo.
ANT (n = 55) Lt Devo.
IRN (n = 88) Up-Mid Devo.
NAF (n = 479) Ear-Lt Devo.
SAF (n = 167) Ear & Lt Devo.
SAM (n = 750) Ear-Mid Devo.
BAL (n = 147) Ear & Lt Devo.
GRN (n = 524) Mid-Lt Devo.
ELA (n = 388) Mid-Lt Devo.
NLA (n = 1616) Lt Devo.
WLA (n = 304) Mid-Lt Devo.
Age (Ga)

Figure 3.4

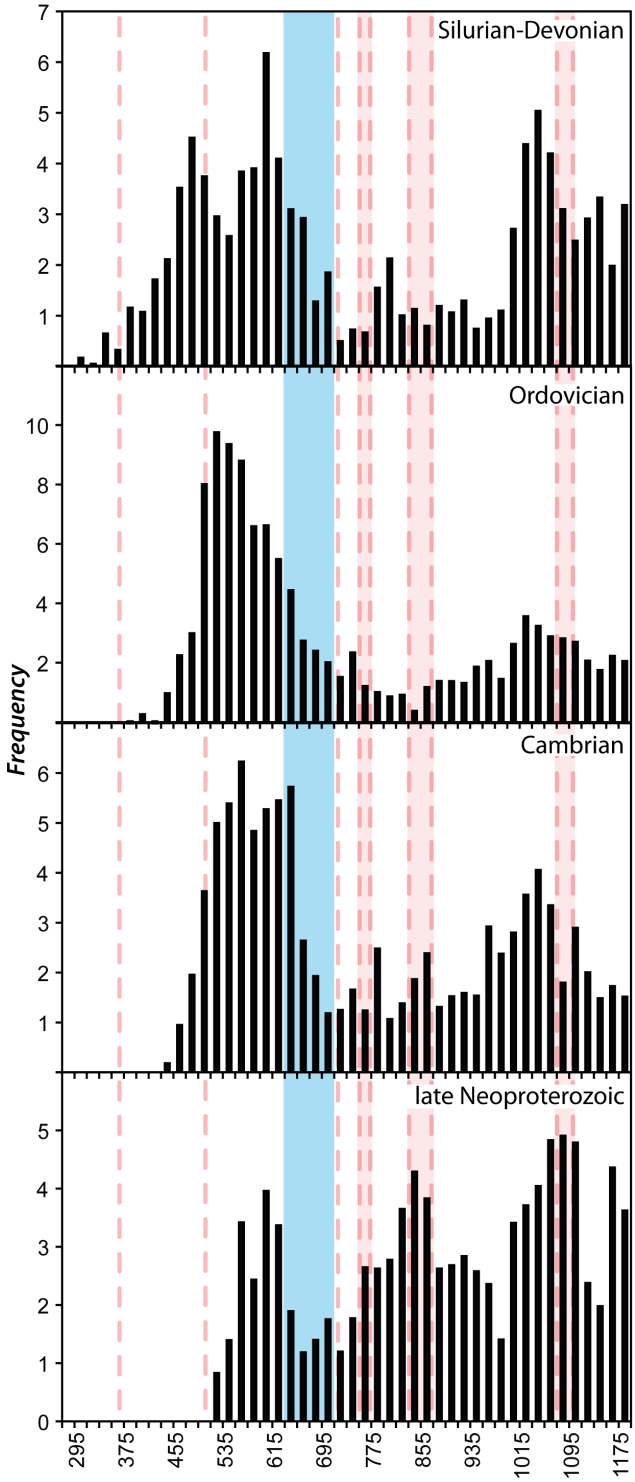
Silurian-Devonian
Ordovician
Cambrian
late Neoproterozoic
Frequency
295
375
455
535
615
695
775
855
935
1015
1095
1175

Figure 3.5

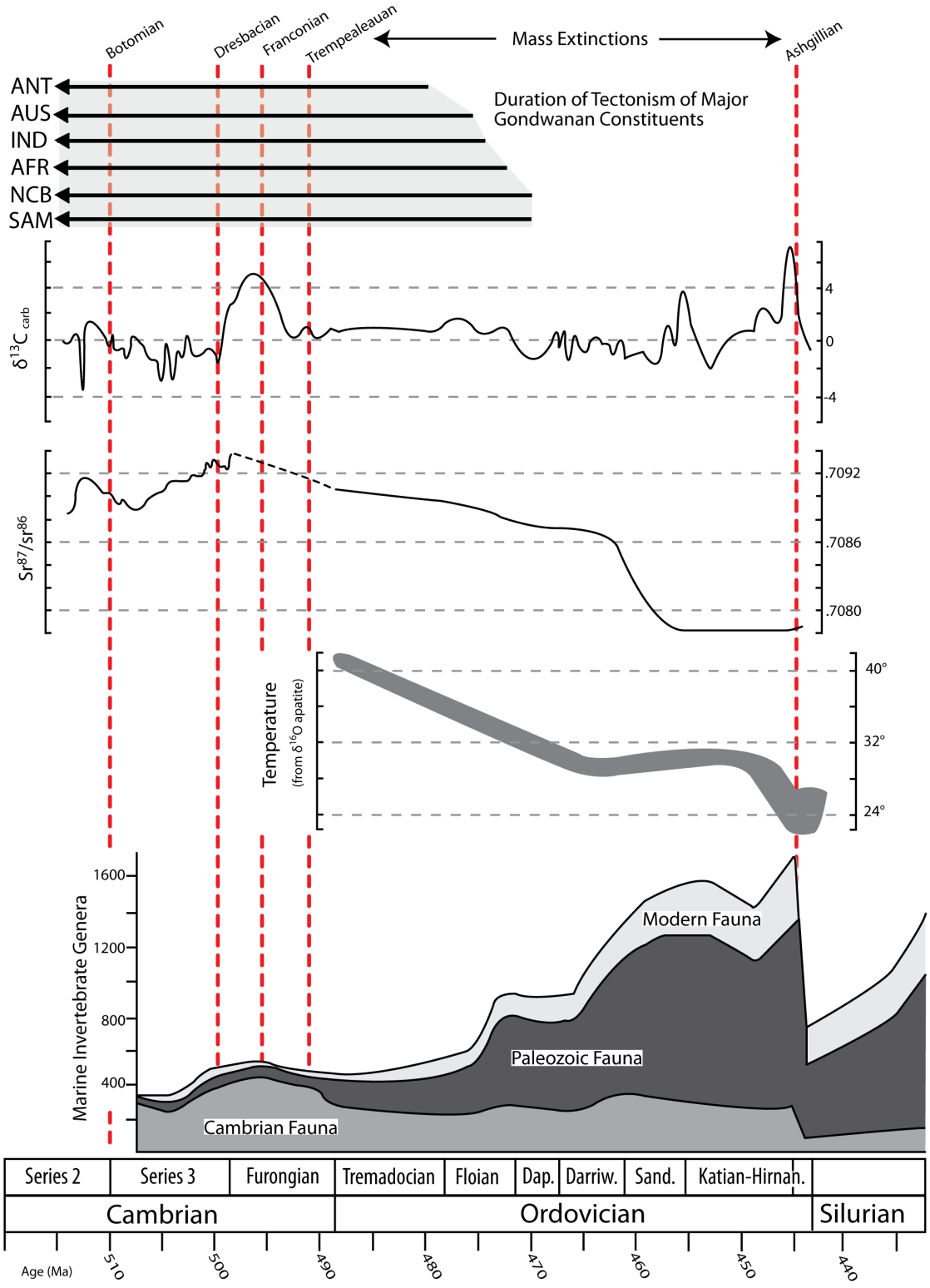
Botomian
Dresbacian
Franconian
Trempealeauan
Mass Extinctions
Ashgillian
ANT
AUS
IND
AFR
NCB
SAM
Duration of Tectonism of Major Gondwanan Constituents
δ13C carb
4
0
-4
Sr87/sr86
.7092
.7086
.7080
Temperature
(from δ16O apatite)
40°
32°
24°
Marine Invertebrate Genera
1600
1200
800
400
Modern Fauna
Paleozoic Fauna
Cambrian Fauna
Series 2
Series 3
Furongian
Tremadocian
Floian
Dap.
Darriw.
Sand.
Katian-Hirnan.
Cambrian
Ordovician
Silurian
Age (Ma)
510
500
490
480
470
460
450
440

Supporting Material

SM3.1. Simple schematic of the long-term carbon cycle (modified after Kump et al., 2000).

Figure SM3.1

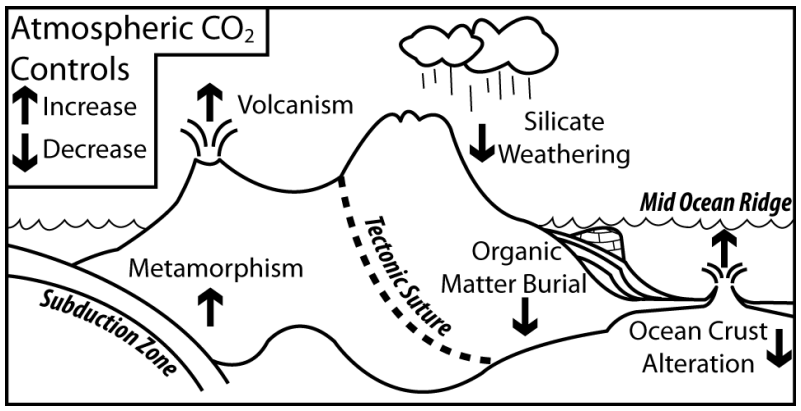

SM3.2. Normalization process for the global compilations. In an attempt to avoid biasing the global distributions towards regions with greater available zircon age data, all regions were normalized prior to inclusion in compilation. Normalization was accomplished by dividing all numerical age-dates into 20 million year age bins and converting the regional populations into percentages. Each region was then treated to have an equal number of age-dates (n = 100). Regions that were located in proximity along a continuous margin as part of the same terrane were normalized and combined prior to inclusion in the global complications, also to avoid biasing. i.e. samples close to one another were treated as one sample. The following regions were combined and treated as single regions in the global compilations: 1) the north African terranes (NAF, ABR, and IRN); 2) Cadomia and Iberia (CAD and IBR); 3)

western Laurentia and northern Laurentia (WLA and NLA); and 4) eastern Laurentian and Greenland (ELA and GRN).

SM3.3. Age probability distributions from poorly constrained siliciclastic rocks. These data are generally similar to data presented in the main text, with a low-abundance of zircons with ages around the onset of the Cryogenian glacial interval and large populations of Ediacaran to early Paleozoic age zircons. CAT = Cathaysia; TAR = Tarim; SAM = South America; SCT = Scotland; AVE = Avalonia-east; AVW = Avalonia-west; ALK = Alaska.

Figure SM3.3

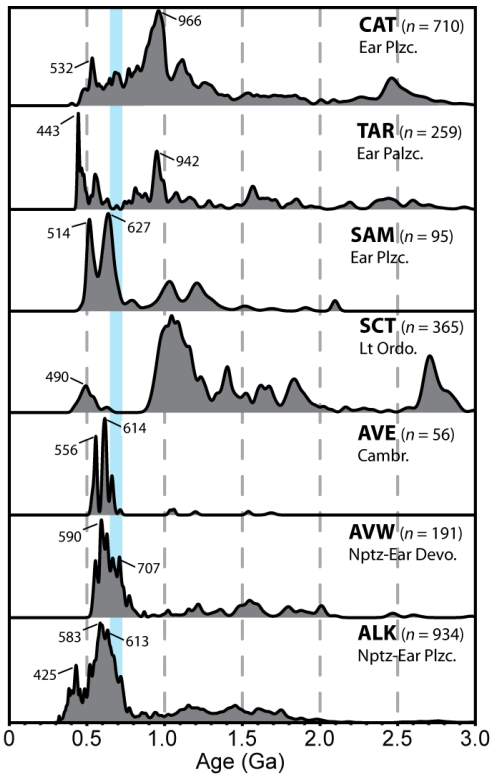

SM3.4. Simplified paleogeographic reconstruction of Gondwana during the Cambrian (modified after Cawood and Buchan, 2007).

Figure SM3.4

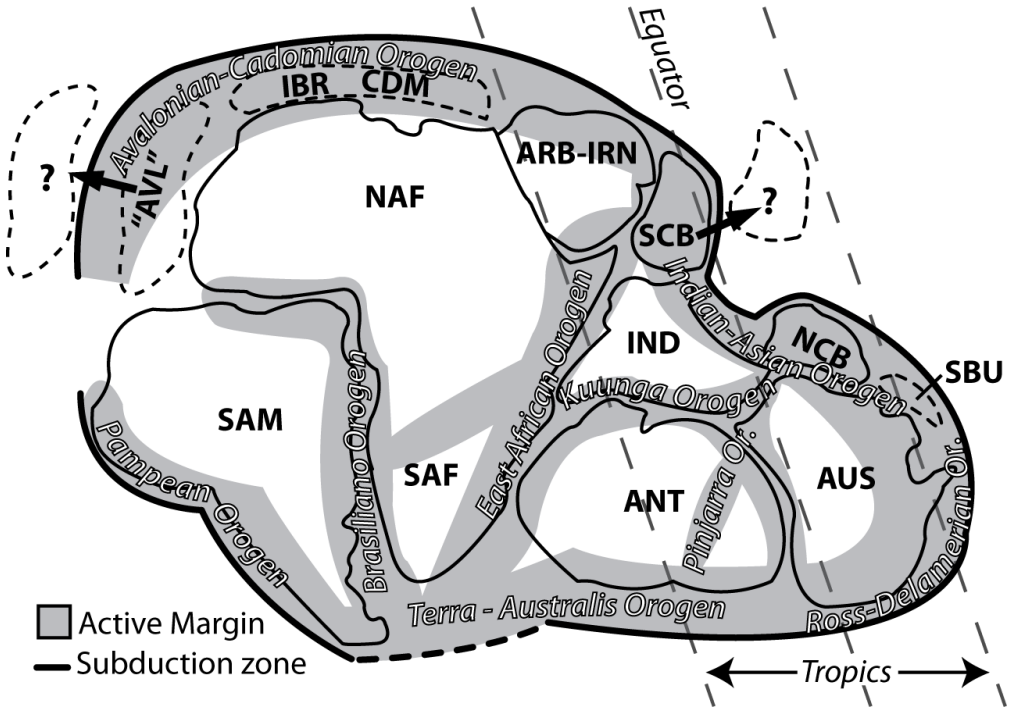

SM3.5. References for detrital zircon age distributions.

Adams, C.J., Miller, H., Acenolaza, F.G., Toselli, A.J., Griffin, W.L., 2011. The Pacific Gondwana margin in the late Neoproterozoic-early Paleozoic: Detrital zircon U-Pb ages from metasediments in northwest Argentina reveal their maximum age, provenance and tectonic setting. Gondwana Research 19, 71-83.

Amato, J.M., Toro, J., Miller, E.L., Gehrels, G.E., Farmer, G.L., Gottlieb, E.S., Till, A.B., 2009. Late Proterozoic-Paleozoic evolution of the Arctic Alaska-Chukotka terrane based on U-Pb igneous and detrital zircon ages: Implications for Neoproterozoic paleogeographic reconstructions. Geological Society of America Bulletin 121, 1219-1235.

Anfinson, O.A., Leier, A.L., Embry, A.F., Dewing, K., 2012. Detrital zircon geochronology and provenance of the Neoproterozoic to Late Devonian Franklinian Basin, Canadian Arctic Islands. Geological Society of America Bulletin 124, 415-430.

Bahlburg, H., Vervoort, J.D., DuFrane, S.A., 2010. Plate tectonic significance of Middle Cambrian and Ordovician siliciclastic rocks of the Bavarian Facies, Armorican Terrane Assemblage, Germany - U-Pb and Hf isotope evidence from detrital zircons. Gondwana Research 17, 223-235.

Bahlburg, H., Vervoort, J.D., DuFrane, S.A., Carlotto, V., Reimann, C., Cardenas, J., 2011. The U-Pb and Hf isotope evidence of detrital zircons of the Ordovician Ollantaytambo Formation, southern Peru, and the Ordovician provenance and paleogeography of southern Peru and northern Bolivia. Journal of South American Earth Sciences 32, 196-209.

Bingen, B., Griffin, W.L., Torsvik, T.H., Saeed, A., 2005. Timing of Late Neoproterozoic glaciation on Baltica constrained by detrital zircon geochronology in the Hedmark Group, south-east Norway. Terra Nova 17, 250-258.

Bingen, B., Jacobs, J., Viola, G., Henderson, I.H.C., Skar, O., Boyd, R., Thomas, R.J., Solli, A., Key, R.M., Daudi, E.X.F., 2009. Geochronology of the Precambrian crust in the Mozambique belt in NE Mozambique, and implications for Gondwana assembly. Precambrian Research 170, 231-255.

Blanco, G., Germs, G.J.B., Rajesh, H.M., Chemale, F., Dussin, I.A., Justino, D., 2011. Provenance and paleogeography of the Nama Group (Ediacaran to early Palaeozoic, Namibia): Petrography, geochemistry and U-Pb detrital zircon geochronology. Precambrian Research 187, 15-32.

Collo, G., Astini, R.A., Cawood, P.A., Buchan, C., Pimentel, M., 2009. U-Pb detrital zircon ages and Sm-Nd isotopic features in low-grade metasedimentary rocks of the Famatina belt: implications for late Neoproterozoic-early Palaeozoic evolution of the proto-Andean margin of Gondwana. Journal of the Geological Society 166, 303-319.

Fernandez-Suarez, J., Garcia, F.D., Jeffries, T.E., Arenas, R., Abati, J., 2003. Constraints on the provenance of the uppermost allochthonous terrane of the NW Iberian Massif: inferences from detrital zircon U-Pb ages. Terra Nova 15, 138-144.

Flowerdew, M.J., Millar, I.L., Curtis, M.L., Vaughan, A.P.M., Horstwood, M.S.A., Whitehouse, M.J., Fanning, C.M., 2007. Combined U-Pb geochronology and Hf isotope geochemistry of detrital zircons from early Paleozoic sedimentary rocks, Ellsworth-Whitmore Mountains block, Antarctica. Geological Society of America Bulletin 119, 275-288.

Fourie, P.H., Zimmermann, U., Beukes, N.J., Naidoo, T., Kobayashi, K., Kosler, J., Nakamura, E., Tait, J., Theron, J.N., 2011. Provenance and reconnaissance study of detrital zircons of the Palaeozoic Cape Supergroup in South Africa: revealing the interaction of the Kalahari and Rio de la Plata cratons. International Journal of Earth Sciences 100, 527-541.

Gehrels, G.E., Blakey, R., Karlstrom, K.E., Timmons, J.M., Dickinson, B., Pecha, M., 2011. Detrital zircon U-Pb geochronology of Paleozoic strata in the Grand Canyon, Arizona. Lithosphere 3, 183-200.

Goodge, J.W., Williams, I.S., Myrow, P.M., 2004. Provenance of Neoproterozoic and lower Paleozoic siliciclastic rocks of the central Ross Orogen, Antarctica: Detrital record of rift- to active-margin sedimentation. Geological Society of America Bulletin 116, 1253-1279.

Greenfield, J.E., Musgrave, R.J., Bruce, M.C., Gilmore, P.J., Mills, K.J., 2010. The Mount Wright Arc: A Cambrian subduction system developed on the continental margin of East Gondwana, Koonenberry Belt, eastern Australia. Gondwana Research 19, 650-669.

Hofmann, M., Linnemann, U., Rai, V., Becker, S., Gartner, A., Sagawe, A., 2011. The India and South China cratons at the margin of Rodinia - Synchronous Neoproterozoic magmatism revealed by LA-ICP-MS zircon analyses. Lithos 123, 176-187.

Horton, B.K., Hassanzadeh, J., Stockli, D.F., Axen, G.J., Gillis, R.J., Guest, B., Amini, A., Fakhari, M.D., Zamanzadeh, S.M., Grove, M., 2008. Detrital zircon provenance of Neoproterozoic to Cenozoic deposits in Iran; implications for chronostratigraphy and collisional tectonics. Tectonophysics 451, 97-122.

Hughes, N.C., Myrow, P.M., McKenzie, N.R., Harper, D.A.T., Bhargava, O.N., Tangri, S.K., Ghalley, K.S., Fanning, C.M., 2010. Cambrian rocks and faunas of the Wachi La, Black Mountains, Bhutan. Geological Magazine.

Kolodner, K., Avigad, D., McWilliams, M., Wooden, J.L., Weissbrod, T., Feinstein, S., 2006. Provenance of north Gondwana Cambrian-Ordovician sandstone: U-PbSHRIMP dating of detrital zircons from Israel and Jordan. Geological Magazine 143, 367-391.

Linnemann, U., Ouzegane, K., Drareni, A., Hofmann, M., Becker, S., Gartner, A., Sagawe, A., 2011. Sands of West Gondwana: An archive of secular magmatism and plate interactions - A case study from the Cambro-Ordovician section of the Tassili Ouan Ahaggar (Algerian Sahara) using U-Pb-LA-ICP-MS detrital zircon ages. Lithos 123, 188-203.

Linnemann, U., Pereira, F., Jeffries, T.E., Drost, K., Gerdes, A., 2008. The Cadomian Orogeny and the opening of the Rheic Ocean: The diacrony of geotectonic processes constrained by LA-ICP-MS U-Pb zircon dating (Ossa-Morena and Saxo-Thuringian Zones, Iberian and Bohemian Massifs). Tectonophysics 461, 21-43.

Lu, S., Zhao, G., Wang, H., Hao, G., 2008. Precambrian metamorphic basement and sedimentary cover of the North China Craton; a review. Precambrian Research 160, 77-93.
Ma, X.X., Shu, L.S., Santosh, M., Li, J.Y., 2012. Detrital zircon U-Pb geochronology and Hf

isotope data from Central Tianshan suggesting a link with the Tarim Block: Implications on Proterozoic supercontinent history. Precambrian Research 206, 1-16.

McKenzie, N.R., Hughes, N.C., Myrow, P.M., Choi, D.K., Park, T.Y., 2011. Trilobites and zircons link north China with the eastern Himalaya during the Cambrian. Geology 39, 591-594.

McKenzie, N.R., N.C., H., Myrow, P.M., Sharma, M., 2011. Correlation of Precambrian–Cambrian sedimentary successions across northern India and the utility of isotopic signatures of Himalayan lithotectonic zones. Earth and Planetary Science Letters 312, 471-483.

Meinhold, G., Morton, A.C., Fanning, C.M., Frei, D., Howard, J.P., Phillips, R.J., Strogen, D., Whitham, A.G., 2011. Evidence from detrital zircons for recycling of Mesoproterozoic and Neoproterozoic crust recorded in Paleozoic and Mesozoic sandstones of southern Libya. Earth and Planetary Science Letters 312, 164-175.

Miller, E.L., Kuznetsov, N., Soboleva, A., Udoratina, O., Grove, M.J., Gehrels, G., 2011. Baltica in the Cordillera? Geology 39, 791-794.

Miller, H., Adams, C., Acenolaza, F.G., Toselli, A.J., 2011. Evolution of exhumation and erosion in western West Gondwanaland as recorded by detrital zircons of late Neoproterozoic and Cambrian sedimentary rocks of NW and Central Argentina. International Journal of Earth Sciences 100, 619-629.

Miller, H., Adams, C., Acenolaza, F.G., Toselli, A.J., 2011. Evolution of exhumation and erosion in western West Gondwanaland as recorded by detrital zircons of late Neoproterozoic and Cambrian sedimentary rocks of NW and Central Argentina. International Journal of Earth Sciences 100, 619-629.

Murphy, J.B., Fernandez-Suarez, J., Jeffries, T.E., Strachan, R.A., 2004. U-Pb (LA-ICP-MS) dating of detrital zircons from Cambrian elastic rocks in Avalonia: erosion of a Neoproterozoic arc along the northern Gondwanan margin. Journal of the Geological Society 161, 243-254.

Myrow, P.M., Hughes, N.C., Goodge, J.W., Fanning, C.M., Williams, I.S., Peng, S.C., Bhargava, O.N., Parcha, S.K., Pogue, K.R., 2010. Extraordinary transport and mixing of sediment across Himalayan central Gondwana during the Cambrian-Ordovician. Geological Society of America Bulletin 122, 1660-1670.

Myrow, P.M., Hughes, N.C., Paulsen, T.S., Williams, I.S., Parcha, S.K., Thompson, K.R., Bowring, S.A., Peng, S.-C., Ahluwalia, A.D., 2003. Integrated tectonostratigraphic reconstruction of the Himalaya and implications for its tectonic reconstruction. Earth and Planetary Science Letters 212, 433-441.

Park, H., Barbeau, D.L., Rickenbaker, A., Bachmann-Krug, D., Gehrels, G., 2010. Application of Foreland Basin Detrital-Zircon Geochronology to the Reconstruction of the Southern and Central Appalachian Orogen. Journal of Geology 118, 23-44.

Reimann, C.R., Bahlburg, H., Kooijman, E., Berndt, J., Gerdes, A., Carlotto, V., Lopez, S., 2010. Geodynamic evolution of the early Paleozoic Western Gondwana margin 14 degrees-17 degrees S reflected by the detritus of the Devonian and Ordovician basins of southern Peru and northern Bolivia. Gondwana Research 18, 370-384.

Satkoski, A.M., Barr, S.M., Samson, S.D., 2010. Provenance of Late Neoproterozoic and Cambrian Sediments in Avalonia: Constraints from Detrital Zircon Ages and Sm-Nd Isotopic Compositions in Southern New Brunswick, Canada. Journal of Geology 118, 187-200.

Slama, J., Walderhaug, O., Fonneland, H., Kosler, J., Pedersen, R.B., 2011. Provenance of Neoproterozoic to upper Cretaceous sedimentary rocks, eastern Greenland: Implications for recognizing the sources of sediments in the Norwegian Sea. Sedimentary Geology 238, 254-267.

Squire, R.J., Campbell, I.H., Allen, C.M., Wilson, C.L., 2006. Did the Transgondwanan Supermountain trigger the explosive radiation of animals on Earth? . Earth and Planetary Science Letters 250, 116-133.

Stewart, J.H., Gehrels, G.E., Barth, A.P., Link, P.K., Christie-Blick, N., Wrucke, C.T., 2001. Detrital zircon provenance of Mesoproterozoic to Cambrian arenites in the western United States and northwestern Mexico. Geological Society of America Bulletin 113, 1343-1356.

Tagiri, M., Dunkley, D.J., Adachi, T., Hiroi, Y., Fanning, C.M., 2011. SHRIMP dating of magmatism in the Hitachi metamorphic terrane, Abukuma Belt, Japan: Evidence for a Cambrian volcanic arc. Island Arc 20, 259-279.

Waldron, J.W.F., Floyd, J.D., Simonetti, A., Heaman, L.M., 2008. Ancient Laurentian detrital zircon in the closing lapetus Ocean, Southern Uplands terrane, Scotland. Geology 36, 527-530.

Wang, Y.J., Zhang, F.F., Fan, W.M., Zhang, G.W., Chen, S.Y., Cawood, P.A., Zhang, A.M., 2010. Tectonic setting of the South China Block in the early Paleozoic: Resolving intracontinental and ocean closure models from detrital zircon U-Pb geochronology. Tectonics 29.

Yin, A., Dubey, C.S., Webb, A.A.G., Kelty, T.K., Grove, M., Gehrels, G.E., Burgess, W.P., 2010. Geologic correlation of the Himalayan orogen and Indian craton: Part 1. Structural geology, U-Pb zircon geochronology, and tectonic evolution of the Shillong Plateau and its neighboring regions in NE India. Geological Society of America Bulletin 122, 336-359.

SM3.6. References for Figure 3.5. Geochronology from compilations of Cawood & Buchan (2007) refs there in; Jacobs et al. (2008); Lu et al. (2008), Bingen et al. (2009); Greenfield et al. (2010) refs there in; Yin et al. (2010); Tagiri, et al., (2011). Carbon and strontium curves modified from Montanez et al. (2000); Shields et al., (2003); Young et al., (2009). Oxygen isotope data modified from Trotter et al., (2008). Biodiversity curve modified from Harper et al., (2006).

SM6 references that are not included in main text:

Bingen, B., Jacobs, J., Viola, G., Henderson, I.H.C., Skar, O., Boyd, R., Thomas, R.J., Solli, A., Key, R.M., Daudi, E.X.F., 2009. Geochronology of the Precambrian crust in the Mozambique belt in NE Mozambique, and implications for Gondwana assembly. Precambrian Research 170, 231-255.

Greenfield, J.E., Musgrave, R.J., Bruce, M.C., Gilmore, P.J., Mills, K.J., 2010. The Mount Wright Arc: A Cambrian subduction system developed on the continental margin of East Gondwana, Koonenberry Belt, eastern Australia. Gondwana Research 19, 650-669.

Lu, S., Zhao, G., Wang, H., Hao, G., 2008. Precambrian metamorphic basement and sedimentary cover of the North China Craton; a review. Precambrian Research 160, 77-93.

Tagiri, M., Dunkley, D.J., Adachi, T., Hiroi, Y., Fanning, C.M., 2011. SHRIMP dating of magmatism in the Hitachi metamorphic terrane, Abukuma Belt, Japan: Evidence for a Cambrian volcanic arc. Island Arc 20, 259-279.

Yin, A., Dubey, C.S., Webb, A.A.G., Kelty, T.K., Grove, M., Gehrels, G.E., Burgess, W.P., 2010. Geologic correlation of the Himalayan orogen and Indian craton: Part 1. Structural geology, U-Pb zircon geochronology, and tectonic evolution of the Shillong Plateau and its neighboring regions in NE India. Geological Society of America Bulletin 122, 336-359.

SM3.7. New detrital zircon data tables available in online supplement.